AND

NO. 5, MAY 1979

13 AUGUST 1979 (FOUO) 1 OF 2

JPRS L/8615

13 August 1979

USSR Report

METEOROLOGY AND HYDROLOGY

No. 5, May 1979

FBIS FOREIGN BROADCAST INFORMATION SERVICE

FOR OFFICIAL USE ONLY

APPROVED FOR RELEASE: 2007/02/08: CIA-RDP82-00850R000100080016-5

NOTE

JPRS publications contain information primarily from foreign newspapers, periodicals and books, but also from news agency transmissions and broadcasts. Materials from foreign-language sources are translated; those from English-language sources are transcribed or reprinted, with the original phrasing and other characteristics retained.

Headlines, editorial reports, and material enclosed in brackets [] are supplied by JPRS. Processing indicators such as [Text] or [Excerpt] in the first line of each item, or following the last line of a brief, indicate how the original information was processed. Where no processing indicator is given, the information was summarized or extracted.

Unfamiliar names rendered phonetically or transliterated are enclosed in parentheses. Words or names preceded by a question mark and enclosed in parentheses were not clear in the original but have been supplied as appropriate in context. Other unattributed parenthetical notes within the body of an item originate with the source. Times within items are as given by source.

The contents of this publication in no way represent the policies, views or attitudes of the U.S. Government.

For further information on report content call (703) 351-2938 (economic); 3468 (political, sociological, military); 2726 (life sciences); 2725 (physical sciences).

JPRS L/8615

13 August 1979

USSR REPORT

METEOROLOGY AND HYDROLOGY

No. 5, May 1979

Selected articles from the Russian-language journal METEOROLOGIYA I GIDROLOGIYA, Moscow.

CONTENTS PAGE

CONTENTS (Continued)

CONTENTS (Continued) Page

PUBLICATION DATA

English title	: METEOROLOGY AND HYDROLOGY No 5, May 79
Russian title	: METEOROLOGIYA I GIDROLOGIYA
Author (s)	: G. P. Kurbatkin, A. U. Karimov et al.
Editor (s)	: Ye. I. Tolstikov
Publishing House	: GIDROMETEOIZDAT
Place of Publication	: Moscow
Date of Publication	: 1979
Signed to press	: 20 Apr 79
Copies	: 3920
COPYRIGHT	: "Meteorologiya i gidrologiya," 1979

UDC 551.(509.313:589)

RESULTS OF USING INITIAL WIND DATA IN PRESSURE FIELD FORECASTING MODELS

Moscow METEOROLOGIYA I GIDROLOGIYA in Russian No 5, May 79 pp 5-15

[Article by Corresponding Member of the USSR Academy of Sciences G. P. Kurbatkin, and Candidates of Physical and Mathematical Sciences A. U. Karimov and V. N. Sinyayev, Computer Center of the Siberian Department of the USSR Academy of Sciences, Institute of Cybernetics, submitted for publication 18 Aug 78]

Abstract. Based on numerical experiments on two spectral hemispheric forecasting models a study is made of the possible use of initial wind data (GARP data) in pressure field forecasting problems. Comparative characteristics of the two models are presented. In addition, certain properties of the spectral solution to the linear balance equation are discussed, and methods are suggested for "improving" the solution to the given equation.

[Text] The main goal of this work is to verify the possible use of initial wind data in problems of forecasting the geopotential. The study was carried out according to the results of integrating two spectral hemispheric forecasting models.

One model (model II) uses untransformed equations in σ-coordinates [1]:

$$\frac{\partial u}{\partial t} = -\vec{v}\nabla u - \dot{\sigma}\frac{\partial u}{\partial \sigma} + \left(f - \frac{u}{a}\operatorname{ctg}\theta\right)v - \frac{1}{a\cos\theta}\left(\frac{\partial \Phi}{\partial \lambda} + RT\frac{\partial Z}{\partial \lambda}\right), \qquad (1)$$

$$\frac{\partial v}{\partial t} = -\vec{v}\nabla v - \dot{\sigma}\frac{\partial v}{\partial \sigma} - \left(f + \frac{u}{a}\operatorname{ctg}\theta\right)u - \frac{1}{a}\left(\frac{\partial \Phi}{\partial \theta} + RT\frac{\partial Z}{\partial \theta}\right), \qquad (2)$$

$$\frac{\partial T}{\partial t} = -\vec{v}\nabla T - \dot{\sigma}\frac{\partial T}{\partial \sigma} + \frac{RT}{c_p}\left(\frac{\dot{\sigma}}{\sigma} - \nabla\vec{v} - \tilde{A} + A\right), \qquad (3)$$

$$\frac{\partial Z}{\partial t} = -\widetilde{\nabla\vec{v}} - \tilde{A}, \qquad (4)$$

$$\frac{\partial \dot{\sigma}}{\partial \sigma} = -\nabla(\vec{v} - \tilde{\vec{v}}) - (A - \tilde{A}), \quad (5)$$

$$\frac{\partial \Phi}{\partial \sigma} = -\frac{RT}{\sigma}, \quad (6)$$

where $A = \vec{v}\nabla Z$, the symbol $(\sim)$ designates integration with respect to the entire mass of the atmosphere, $Z = \ln p_s$--value of the pressure logarithm on the earth's surface. The remaining designations are the generally accepted ones.

The boundary conditions with respect to σ were used in writing (1)-(6):

$$\dot{\sigma} = 0 \text{ with } \sigma = 1,$$
$$\dot{\sigma} = 0 \text{ with } \sigma = 0. \quad (7)$$

The solution to the system (1)-(6) with respect to the horizontal variables is sought for the hemisphere, assuming periodicity with respect to λ and the absence of streams through the equator: $\upsilon = 0$ with $\theta = 90°$. The distribution of the geopotential on the earth's surface is prescribed:

$$\Phi_s = g z_s, \quad z_s = z_s(\theta, \lambda).$$

The other model (model Φ') is a quasisolenoidal model in the isobaric coordinate system [2,3]:

$$\frac{\partial \nabla^2 \psi}{\partial t} + J(\psi, \nabla^2 \psi + f a^2) + \nabla(f \nabla \chi) = F_\Omega, \quad (8)$$

$$\frac{\partial \Phi_p}{\partial t} + J(\psi, \Phi_p) + \sigma(p)\,\omega = F_T, \quad (9)$$

$$\omega_p = -\nabla^2 \chi, \quad (10)$$

$$\nabla^2 \Phi = \nabla(f \nabla \psi), \quad (11)$$

$$T = -\frac{p}{R}\Phi_p. \quad (12)$$

T'e boundary conditions with respect to the vertical:

$$\omega = 0 \text{ with } p = 0,$$

$$\omega = \frac{p_0 g a^2}{RT}\left[\frac{1}{g}\left(\frac{\partial \Phi}{\partial t} + J(\psi, \Phi)\right) - J(\psi, \xi)\right], \quad p = p_0 = 1000 \text{ mbar}.$$

Here the following designations have been adopted:

$J(A,B)$--Jacobian,

χ--horizontal velocity potential,

$\omega = \frac{dp}{dt}$,

ξ--orography,

F_Ω and F_T--"nonadiabatic sources." Each of the functions F_Ω and F_T is presented in the form of a sum of two components:

$$F_\Omega(\theta, \lambda, p, t) = \tilde{F}_\Omega(\theta, \lambda, p, t) + F''_\Omega(\theta, \lambda, p, t),$$

$$F_T(\theta, \lambda, p, t) = \tilde{F}_T(\theta, \lambda, p, t) + F''_T(\theta, \lambda, p, t),$$

where F_Ω and F_T--mean climate values of the sources computed for each calendar day as multiple-year averages using system (8)-(12) as the diagnostic according to the technique stated in [2]. F''_Ω and F''_T--values of deviations in sources from their mean climate values. Here these functions are found from the solution to the inverse problem by statistical means [4]. The Adams-Beshfort method was used to integrate the quasisolenoidal model with respect to time.

Thus, in its main variant the quasisolenoidal model provides for consideration of the nonadiabatic factors in the form of mean climate sources and parametrized values for the deviations in sources from their mean climate values. Because of objective reasons (the absence of multiple-year data in the time interval from 4 to 9 November in which test forecasts were made) we were able to use only "December sources" computed as five-year averages for each day of December for 1964/1968, with additional averaging in the first 10 days of December.

It is natural that the competence of such an "approximation" requires empirical confirmation. At least by using the materials of the multiple-year synoptic analysis of the climate characteristics of these two months it was possible to draw a conclusion about the presence of significant differences. Thus, bearing the aforementioned in mind, it is necessary to approach an evaluation of the forecasting potentialities of the nonadiabatic model on the basis of the fulfilled calculations with a certain degree of caution. Within the framework of the quasisolenoidal model experiments were also carried out that permitted an evaluation of the effect of different methods for prescribing the initial data on the forecast quality.

Two-day forecasts by the untransformed model (model Π, variant Π_1) and the quasisolenoidal model (model Φ', variants Φ'_1, Φ'_2, Φ'_3) were computed for 4 initial dates 4,5,6 and 7 November 1969. We will briefly explain the content of the model variants. Variants Π_1 and Φ'_1 are adiabatic variants of models Π and Φ' respectively with the assignment at the initial moment, besides the geopotential the current functions from wind observations (GARP data).

Here the balance equation (11) in variant Φ_1' is used "in the less rigid" forecasting form:

$$\frac{\partial \nabla (f \nabla \psi)}{\partial t} = \frac{\partial \nabla^2 \Phi}{\partial t}.$$

In variant Φ_2' the current function is determined in all seasons including the initial from (11) (balance wind). Variant Φ_3' is the nonadiabatic variant of model Φ' in which the initial data are prescribed analogously to variant Φ_2'. The calculation results for the two models are presented in table 1. In addition, table 1 presents the absolute errors of the inertia forecast (model I. P). In our opinion the most important is the comparison of the results from integrating variants Π_1 and Φ_1' in which the initial data are identical (at the starting moment in both variants only the actual values of the current function and the geopotential are prescribed). The root-mean-square errors in both cases are approximately the same; in the untransformed model they are somewhat smaller, especially on the second day of integration. The correlation coefficients in variant Φ_1' are regularly greater for all four forecasting examples (the difference is most significant on the first day of integration for levels 700, 900 and 1000 mbar). This can be explained by the methodological difference in the temporal realization of the two models, and in particular, the methods of initialing (congruence).

In the quasisolenoidal model at all the temporal stages (including the starting moment in time) wind data obtained from the solution to the diagnostic equation (ω-equation) are used to approximate the divergent portion of the wind.

In variant Π_1 the first temporal step in integrating the eddy equation does not consider the main divergent term $\sim\omega_p$; for those levels where this component is significant, the approximation is very poor (which explains the low correlation coefficient on the lower levels on the first day of integration).

It is natural that methods are needed for the unfiltered model to attain a better initial congruence of the fields or acceleration of the adaptation processes. The proximity of the root-mean-square errors in variants Π_1 and Φ_1' for all four examples can be explained by the presence in the system of equations for model Π of an additional "divergent" degree of freedom governed by the forecasting equations for divergence, and in the case of the zero values of starting divergence this degree of freedom up to a certain moment plays the role of outlet of kinetic energy of the solenoidal movement (unique dissipative factor). A comparison of the forecasts from variants Φ_1' and Φ_2' of model Φ' shows that the use of the actual solenoidal wind (variant Φ_1') as the initial data significantly improves the quality of the forecasts. Introduction of nonadiabatic factors into the quasisolenoidal model (variant Φ_3') results in a noticeable improvement in the forecasts on

Table 1. Root-Mean-Square Errors, m(numerator) and Correlation Coefficients (denominator). November 1969

(a) Исходная дата	(b) Поверхность, мб / (c) Срок прогноза, сут: 300		500		700		900		1000		(d) Модель
	1	2	1	2	1	2	1	2	1	2	
4	90	140	64	94	48	73	46	67	43	67	I. P.
	76/0,73	115/0,71	54/0,69	83/0,68	47/0,68	71/0,58	50/0,42	63/0,60	61/0,37	75/0,58	$П_1$
	66/0,78	107/0,78	56/0,71	90/0,72	53/0,58	87/0,58	51/0,52	86/0,49	47/0,61	86/0,49	$Ф'_1$
	64/0,78	141/0,61	50/0,72	99/0,62	46/0,56	84/0,50	45/0,50	82/0,42	41/0,42	84/0,62	$Ф'_2$
	71/0,72	118/0,69	52/0,67	81/0,67	46/0,54	67/0,58	42/0,54	63/0,58	35/0,69	59/0,61	$Ф'_3$
5	98	133	66	97	50	80	48	78	48	80	I. P.
	74/0,70	119/0,60	53/0,66	87/0,59	46/0,59	74/0,56	43/0,51	61/0,68	55/0,69	71/0,61	$П_1$
	70/0,79	122/0,67	53/0,77	95/0,66	47/0,71	87/0,59	48/0,65	87/0,53	48/0,67	97/0,44	$Ф'_1$
	72/0,73	116/0,66	50/0,72	84/0,69	42/0,68	70/0,70	42/0,63	71/0,65	44/0,63	83/0,55	$Ф'_2$
	72/0,73	116/0,63	46/0,74	82/0,62	38/0,72	67/0,62	38/0,69	64/0,63	39/0.70	66/0,63	$Ф'_3$
6	106	166	73	113	58	87	56	83	58	89	I. P.
	79/0,72	118/0,75	57/0,71	32/0,74	49/0,63	73/0,63	52/0,47	69/0,60	65/0.46	83/0,58	$П_1$
	69/0,78	104/0,81	48/0,80	84/0,78	40/0,79	70/0,76	41/0,76	70/0,71	47/0,70	81/0,63	$Ф'_1$
	145/0,41	171/0,62	101/0,49	128/0,64	79/0,52	105/0,63	73/0,52	98/0,60	74/0,51	104/0,55	$Ф'_2$
	94/0,59	108/0,77	62/0,63	74/0,77	52/0,62	57/0,77	48/0,64	52/0.79	48/0,70	54/0;81	$Ф'_3$

[Continuation of table and key on next page]

(a) Исходная дата	(b) Поверхность, *мб* / (c) Срок прогноза, *сут*										(d) Модель
	300		500		700		900		1000		
	1	2	1	2	1	2	1	2	1	2	
7	109	161	62	104	50	74	48	68	52	73	I. P.
	76/0,78	108/0,78	53/0,70	81/0,70	48/0,52	66/0,56	52/0,29	60/0,52	66/0,26	72/0,53	Π_1
	70/0,80	103/0,81	54/0,71	82/0,72	47/0,59	72/0,60	46/0,58	74/0,53	48/0,61	83/0,51	Φ_1'
	82/0,72	134/0,77	60/0,65	106/0,66	52/0,56	90/0,53	49/0,55	88/0,44	50/0,60	104/0,43	Φ_2'
	80/0,74	121/0,71	50/0,71	76/0,70	66/0,71	56/0,67	33/0,74	51/0,68	35/0,77	56/0,69	Φ_3'
(e) Средние по четырем прогнозам для каждой модели	101	150	68	104	51	79	50	74	50	78	I. P.
	76/0,74	116/0,72	55/0,70	84/0,69	48/0,62	72/0,59	50/0,43	64/0,61	62/0,40	76/0,59	Π_1
	69/0,79	108/0,74	53/0,75	88/0,72	47/0,67	80/0,61	46/0,63	80/0,57	48/0,68	88/0,52	Φ_1'
	91/0,66	140/0,67	65/0,65	104/0,65	55/0,60	87/0,60	52/0,55	88/0,53	52/0,59	91/0,49	Φ_2'
	79/0,69	116/0,70	60/0,69	78/0,69	43/0,64	62/0,66	40/0,65	58/0,66	39/0,70	59/0,68	Φ_3'

Note. I.P.--inertia forecast, Π_1--untransformed model (solenoidal "actual" wind), Φ_1'--quasisolenoidal model (solenoidal "actual" wind), Φ_2'--quasisolenoidal model (solenoidal "balance" wind), Φ_3'--quasisolenoidal model (solenoidal "balance" wind, sources).

Key:
- a. Initial date
- b. Surface, mbar
- c. Period of forecast, day
- d. Model
- e. Mean for four forecasts for each model

the lower levels, although, as we have already indicated previously, for objective reasons the nonadiabatic sources in this model are introduced by a not quite correct method.

We will dwell in somewhat more detail on an analysis of the forecasts with respect to variants Φ_1' and Φ_2' with initial data for 6 November 1969. In this example the difference in the estimates of the variants is especially significant. Thus, if variant Φ_1' produces a relatively good forecast, the estimates for variant Φ'_2 are considerably worse. In order to reveal the reasons for such a drastic difference we conducted the following two experiments. In the first experiment the initial values of the zonal section of the current function were taken from the GARP data (analogously to variant Φ'_1) and remained in the calculation process unchanged, while the initial values of the nonzonal section were determined from the linear balance equation (variant Φ'_3), and further were forecasted. The obtained estimates were close to the estimates for variant Φ'_2, that is the differences in the zonal sections of the initial data for the current function in these two variants in the given case are not the reason for such a large discrepancy (judging from the proximity of the estimates, the differences in the zonal sections cannot be significant).

Consequently, another reason remains, the difference in the nonzonal sections of the current function fields in both variants. To all appearances, this is linked to the known fact that for certain synoptic situations the solution to the spectral balance equation for nonzonal current function harmonics (the current function is presented in a series with respect to the odd spherical harmonics, while the geopotential--the even) can prove to be incorrect in the sense of the convergence of the corresponding series. From the viewpoint of the correctness of using the series for the current function in solving the system of hydrodynamic equations the convergence must at least be on the order of $O(\frac{1}{n^2})$.

We previously made a special examination of this problem. In particular, we studied two approaches to the possibility of improving the solution for nonzonal sections. We will briefly explain the essence of these approaches. In the case of a symmetric geopotential field and antisymmetric current function field (in precisely this case the problem of correctness arises) the precise satisfying of the balance for the prescribed zonal wave number requires

$$\sum_{n=m}^{N} (\vec{f}_n^m \vec{\psi}^m)\, P_n^m(\theta) = \sum_{n=m}^{N} \Phi_n^m\, P_n^m(\theta), \qquad (13)$$

where $\vec{f}_n^m = (f^m_{n,\,n+1},\ f^m_{n,\,n-1})$ — known functions of wave numbers satisfying the following "boundary" conditions:

$$f^m_{m,\,m-1} = 0, \quad f^m_{m,\,N+1} = 0. \qquad (13a)$$

$\vec{\psi}^m = (\psi^m_{m+1}, \psi^m_{m+3}, \ldots, \psi^m_{N-1})$ — vector of expansion factors of current function for given zonal number m according to the associated Legendre polynomials.

Φ_n^m--expansion factor of geopotential field. We noted that the number of coefficients for the current function is a unit smaller than for the geopotential.

Equality (13) must be fulfilled for any θ. If we attempt to satisfy correlation (13) by equating the coefficients for the same Legendre functions then we will arrive at the following system of equations of relatively unknown $\vec{\psi}^m$;

$$(\vec{f}_n^m \vec{\psi}^m) = \Phi_n^m, \quad n = m, m+2, \ldots, N.$$

This system is redetermined in virtue of conditions (13a). It can be simultaneous only in that case where the geopotential coefficients satisfy the coupling condition of the type $\sum_{n=m}^{N} {}_2\, \alpha_n^m \Phi_n^m = 0$, where α_n^m--known coefficients.

This, of course, does not have a place in the general case of the independent analysis of the observed geopotential field. But this correlation can be viewed as the coupling condition in an "additional" objective analysis, i.e., the prescribed values of the coefficients of the geopotential field we can "correct" such that the coupling conditions are fulfilled. The corrected geopotential field (Φ_n^{*m}) is found from the condition for the functional minimum of the type

$$I = \int |L(\Phi - \Phi^*)|^2 \, ds + \nu \sum_{n=m}^{N} {}_2\, \alpha_n^m \Phi_m^{*n}, \qquad (14)$$

where L--scalar or vector linear operator, the integral is taken with respect to the surface of the hemisphere, ν--Lagrange multiplier, the variations in the functional are carried out with respect to Φ_n^{*m} and ν. This method and the results of its practical application are stated in publication [5]. It also gives an interpretation of the coupling condition for the final result of adaptation to the nondivergent movement of a certain dynamic linear system.

The second method is based on the search for generalized solutions for $\vec{\psi}^m$ of equation (13) that satisfy the functional minimum

$$I = \int \left\{ L \left[\sum_{n=m}^{N} {}_2 (\vec{f}_n^m \vec{\psi}^m) P_n^m(\theta) \, l^{im\lambda} - \sum_{n=m}^{N} {}_2\, \Phi_n^m P_n^m(\theta) \, l^{im\lambda} \right] \right\}^2 ds, \qquad (15)$$

where L, as in the first method, scalar or vector linear operator (in a particular case L=1), variations are carried out with respect to $\vec{\psi}^m$.

Three types of operators were tested:

$$L = 1, \quad L = \vec{\nabla}, \quad L = \nabla^2.$$

The three-point equations to determine $\vec{\varphi}^m$ that can be obtained by variation in the corresponding functionals, can be written as

$$(D\nabla^{-4}\ D\psi)_n^m = (D\nabla^{-2}\Phi)_n^m,$$

$$(D\nabla^{-2}D\psi)_n^m = (D\Phi)_n^m,$$

$$(D^2\psi)_n^m = (D\nabla^2\Phi)_n^m,$$

where $D(A) = \nabla(f\nabla A)$, ∇^{-2} and ∇^{-4} — operators inverse to ∇^2 and ∇^4 respectively. In solving any of the systems (16) it is necessary to always bear in mind that the number of harmonics for $\vec{\psi}^m (m \neq 0)$ is by one order lower than for $\vec{\Phi}^m$.

Table 2. Root-Mean-Square Error, m(numerator) and Correlation Coefficient (denominator). November 1969 ("corrected"geopotential)

(a) Исходная дата	(b) Поверхность, мб									
	300		500		700		900		1000	
	(c) Срок прогноза, сут									
	1	2	1	2	1	2	1	2	1	2
4	58/0,82	119/0,70	49/0,73	90/0,67	47/0,57	82/0,52	46/0,50	82/0,42	42/0,61	84/0,41
5	65/0,77	118 0,65	48/0,73	86/0,66	41/0,67	71/0,66	41/0,62	71/0,62	42/0,63	81/0,53
6	86/0,67	112/0,78	56/0,73	88/0,76	44/0,75	74/0,75	42/0,74	74/0,72	48/0,67	85/0,64
7	74/0,77	114/0,79	55/0,70	88/0,72	47/0,59	75/0,61	46/0,57	76/0,53	48/0,60	84/0,51
(d) Средние по четырем прогнозам	71/0,76	116/0,73	52/0,72	88/0,70	45/0,64	76/0,64	44/0,61	76/0,57	45/0,63	84/0,52

Key:
a. Initial date
b. Surface, mbar
c. Period of forecast, day
d. Mean for four forecasts

The mean statistical estimate (from 100 forecasts) of the effect on the quality of barotropic forecasts (500 mbar) of the described methods for determining the current function showed that the best result in both methods is produced by $L = \vec{\nabla}$. Here the first method (method of "correction") yields better estimates than the second. Bearing these results in mind we computed the forecasts with correction of $\vec{\Phi}^m (m \neq 0)$ for the given four examples. The estimates show (table 2) that the forecast is significantly improved for the initial date from 6 November 1969, for the remaining three examples it remained approximately on the same level as in model Φ_2', (i.e., when the current function correlations for ψ^m are found from the balance equation by the "classic" method of direct recursion).

Table 3. Spectrum of Kinetic Energy of Geostrophic Wind, Solenoidal "Balance" Uncorrected (numerator) and Corrected (denominator) Wind on Level 500 mbar for 6 November 1969

n	*m*							
	1	2	3	4	5	6	7	8
m	0,1	0,0	0,8	0,2	0,5	0,1	0,2	0,2
m+2	1,8	0,1	1,0	1,5	2,9	1,9	1,2	2,3
m+4	1,8	1,0	2,1	1,0	2,7	3,2	0,6	3,5
m+6	3,3	0.7	3,1	0,6	2,5	0,9	1,4	0,5
m+8	4,0	3,3	1,3	0,2	0,2	0,9	0,8	0,4
m+10	0,1	1,3	0,0	0,4	0,4	0,3	0,3	0,0
m+12	0,6	0,6	0,0	0,1	0,2	0,3	0,2	0,1
m+14	0,3	0,1	0,1	0,0	0,1	0,0	0,0	0,2
m+16	0,1	0,0	0,2	0,1	0,0	0,1	0,0	0,0
m+1	$\frac{0,2}{0,41}$	$\frac{0,0}{0,0}$	$\frac{3,5}{2,5}$	$\frac{1,0}{0,7}$	$\frac{3,4}{3,1}$	$\frac{0,5}{0,1}$	$\frac{1,5}{2,1}$	$\frac{1,9}{1,9}$
m+3	$\frac{2,6}{1,6}$	$\frac{0,1}{0,7}$	$\frac{0,2}{1,5}$	$\frac{1,6}{2,4}$	$\frac{9,0}{4,0}$	$\frac{8,9}{7,0}$	$\frac{1,0}{0,7}$	$\frac{4,7}{2,9}$
m+5	$\frac{3,4}{1,9}$	$\frac{1,7}{0,9}$	$\frac{0,1}{0,9}$	$\frac{2,1}{3,3}$	$\frac{2,9}{2,5}$	$\frac{8,8}{4,7}$	$\frac{3,1}{0,8}$	$\frac{15}{6,3}$
m+7	$\frac{1,0}{2,2}$	$\frac{5,4}{4,4}$	$\frac{6,9}{4,8}$	$\frac{0,2}{0,7}$	$\frac{8,6}{2,0}$	$\frac{2,0}{0,2}$	$\frac{0,6}{1,4}$	$\frac{7,2}{1,5}$
m+9	$\frac{3,4}{1,3}$	$\frac{1,5}{2,5}$	$\frac{5,8}{0,8}$	$\frac{0,2}{1,7}$	$\frac{6,5}{0,5}$	$\frac{5,0}{2,0}$	$\frac{2,2}{0,3}$	$\frac{6,2}{0,5}$
m+11	$\frac{5,0}{2,0}$	$\frac{1,6}{0,3}$	$\frac{5,0}{0,6}$	$\frac{0,6}{0,2}$	$\frac{12}{2,0}$	$\frac{4,5}{0,8}$	$\frac{1,9}{0,1}$	$\frac{6,0}{0,2}$
m+13	$\frac{3,8}{0,9}$	$\frac{4,6}{0,3}$	$\frac{5,8}{0,6}$	$\frac{0,3}{0,0}$	$\frac{9,7}{0,6}$	$\frac{22}{0,0}$	$\frac{3,6}{0,2}$	$\frac{4,4}{0,1}$
m+15	$\frac{1,5}{0,2}$	$\frac{3,4}{0,0}$	$\frac{6,0}{0,2}$	$\frac{0,2}{0,1}$	$\frac{10}{0,3}$	$\frac{1,6}{0,1}$	$\frac{3,0}{0,0}$	$\frac{7,9}{0,1}$
m+17	$\frac{1,7}{0,0}$	$\frac{4,0}{0,0}$	$\frac{8,9}{0,0}$	$\frac{0,7}{0,0}$	$\frac{8,4}{0,0}$	$\frac{3,1}{0,0}$	$\frac{3,3}{0,0}$	$\frac{7,5}{0,0}$

A certain idea about the nature of the differences in the solutions for the nonzonal current function fields found by the "classic" method and with the use of "correction" for the initial date for 6 November 1969 can be obtained from a comparison for level 500 mbar of the spectral distribution of kinetic energy of geostrophic wind (f=const=$10^{-4}s^{-1}$) and the corresponding spectrum of solenoidal wind energy. It is apparent from table 3 that in the spectrum of kinetic energy of the solenoidal wind for 6 November 1969 found by the "classic" method there are small scale components present that are considerable in size (in contrast to the spectrum of "geostrophic" energy for the given date). Here the"defect" in the solution is present. For the spectrum of energy computed using the "correction," such a sharp difference is not observed, and the convergence of the spectrum with respect to wave numbers is more uniform.

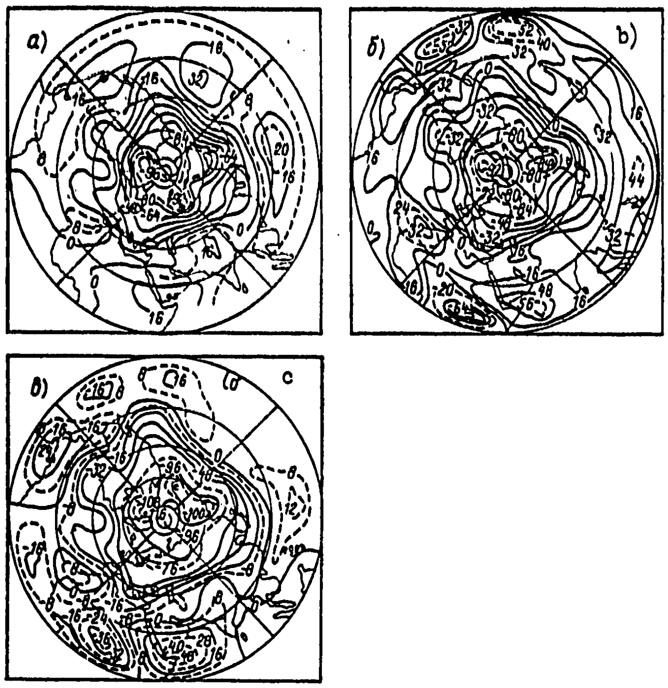

Figure 1. Initial Current Function Fields for 6 November 1969

Key:
- a. from GARP data
- b,c. computed from linear balance equation without "correction" and with "correction" of geopotential respectively.

The maps (fig 1) for 500 mbar level have been constructed for a graphic idea of the difference in the current function fields in three cases (actual field, field computed from the balance equation without correction, and field with correction). It is apparent from these maps that with respect to the indicated level the "defect" in the solution is the presence of small-scale components that is expressed in the very large gradients in the near-equatorial region in the current function field determined from the solution to the balance equation without preliminary correction of the geopotential. In the case of "correction" this defect is considerably smaller. In conclusion we note that the given problem can hardly be avoided in the spectral methods of solving the more common nonlinear balance equation since the "defect" in the solution can occur in determining the components of the zero order of approximation according to the Rossby number (corresponding to the linear equation).

Table 4. Root-Mean-Square Errors in Forecasts of Geopotential, m(numerator) and Correlation Coefficients (denominator) according to Full Model (Initial Wind Full). November 1969

(a) Исходная дата	(b) Поверхность, мб											
	100		300		500		700		900		1000	
	(c) Срок прогноза, сут											
	1	2	1	2	1	2	1	2	1	2	1	2
4	88/0,41	147/0,36	74/0,66	123/0,62	57/0,59	87/0,60	50/0,55	77/0,60	40/0,32	63/0,59	58/0,40	75/0,52
5	97/0,36	112/0,53	79/0,67	125/0,57	54/0,67	92/0,55	45/0,63	79/0,51	44/0,53	60/0,68	65/0,43	71/0,64
6	98/0,45	124/0,56	83/0,70	132/0,69	58/0,70	95/0,67	53/0,61	87/0,53	53/0,48	75/0,52	61/0,46	93/0,48
7	91/0,52	105/0,68	80/0,75	110/0,78	58/0,65	84/0,70	49/0,51	67/0,58	53/0,30	63/0,48	69/0,29	86/0,46

Key:
- a. Initial date
- b. Surface, mbar
- c. Period of forecast, day

Table 4 presents the results of forecasts for four initial dates according to the untransformed model, where the full wind is taken as the initial wind data (GARP data). By comparing the obtained estimates with the estimates according to variant Π_1 one can conclude that the full wind produces a poorer result than the "solenoidal."

It is natural that with respect to the four aforementioned examples it is impossible to speak of the objectivity of the analysis. But nevertheless analysis of the actual wind requires serious attention for its use in the hydrodynamic forecasting models.

For a graphic idea about the nature of the forecast from variants Π_1 and Φ_1 the isolines of the actual and forecasting geopotential fields at level 500 mbar for forecasts with initial period of 6 November 1969 have been derived on the graph plotter (fig 2).

Conclusion

Based on the conducted experiments the following conclusions can be drawn:

a) the technique of temporal integration of untransformed equations (including the problem of initial congruence) requires further methodological modification in order to improve the quality of the forecasts;

b) use of the actual solenoidal wind significantly improves the quality of the forecasts both with respect to the untransformed model, and the quasi-solenoidal;

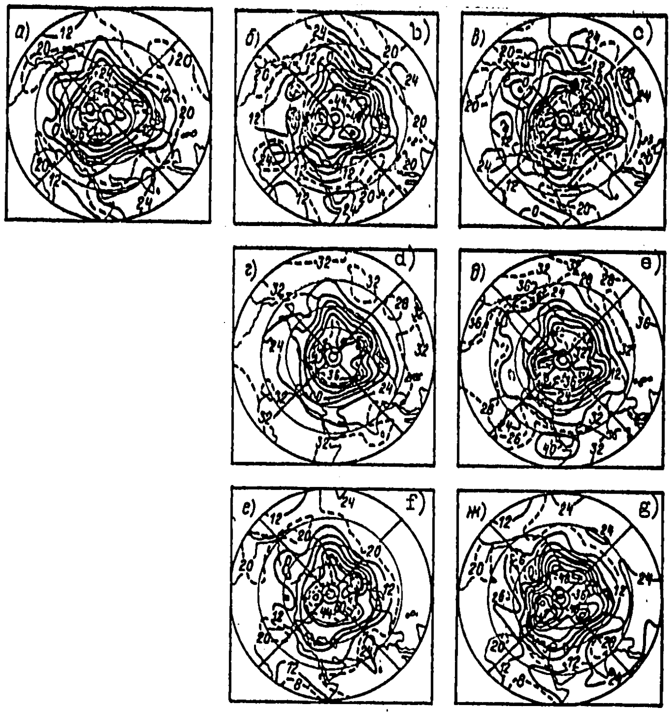

Figure 2. Actual and Forecasting Values AT_{500} (in Deviations from the Standard) for Forecasts with Initial Period for 6 November 1969

Key:

a,b,c. Actual values for 6,7,8 November 1969 respectively

d,e. Forecasts according to variant Π_1 on 7, 8 November 1969 respectively

f,g. Forecasts according to variant Φ_1' for 7,8 November 1969 respectively

c) use as the initial data for wind of the solenoidal section obtained from the solution to the spectral balance equation in certain cases can result in considerable errors (cases of incorrectness of the solution). The proposed method of "correction" of the geopotential of the initial data in these cases can be an effective means of improving the forecast quality.

It is evidently necessary to conduct more objective studies in the statistical sense; for this it is extremely useful to have a more extensive archive of data analogous to the given.

BIBLIOGRAPHY

1. Kurbatkin, G. P.; and Karimov, A. U. "Solution to Equations of Baroclinic Atmosphere Dynamics with the Help of Spherical Functions by the Semi-implicit Method of Integration with Respect to Time," "Ul'tradlinnyye volny i dolgosrochnyy prognoz pogody" [Ultralong Waves and Long-Term Weather Forecast], Novosibirsk, 1976.

2. Kurbatkin, G. P. "Certain Problems of Simulating Ultralong Atmospheric Waves," DOKLADY AN SSSR, Vol 192, No 4, 1970.

3. Kurbatkin, G. P.; Sinyayev, V. N.; and Yantsen, A. G. "Spectral Model of Long-Term Forecast with Mean-Climate Limitations," IZVESTIYA AN SSSR. FIZIKA ATMOSFERY I OKEANA, Vol 9, No 11, 1973.

4. Kurbatkin, G. P.; and Sinyayev, V. N. "Diagnostic Estimates of Turbulent Friction and Macroscale 'External' Heat Effect on General Atmospheric Circulation," IZVESTIYA AN SSSR. FIZIKA ATMOSFERY I OKEANA, Vol 8, No 12, 1972.

5. Kurbatkin, G. P.; Sinyayev, V. N.; and Eykher, M. Sh. "Accuracy of Diagnostic Description of Atmospheric Processes of Synoptic Scale with Respect to Time," "Ul'tradlinnyye volny i dolgosrochnyy prognoz pogody", Novosibirsk, 1976.

UDC 551.509.33

PREDICTABILITY IN LONG-RANGE WEATHER FORECASTING

Moscow METEOROLOGIYA I GIDROLOGIYA in Russian No 5, May 79 pp 16-21

[Article by Candidate of Physical and Mathematical Sciences G. V. Alekseyev, and Doctor of Physical and Mathematical Sciences Yu. V. Nikolayev, Arctic and Antarctic Scientific Research Institute, submitted for publication 10 July 1978]

Abstract. It is shown that synoptic-scale oscillations that are not completely excluded in averaging are one of the main sources of noise in averaged values of meteorological elements. Such noises are unpredictable, which places limitations on the possible justifiability of long-range meteorological forecasts. From data of 42 Northern Hemisphere stations it is calculated that the limit of justifiability of the air pressure mean monthly anomalies averages 70-75%, while that of the air temperature mean monthly anomalies averages 75-80%.

[Text] According to the definition given by A. S. Monin [3] the limit of predictability is a segment of time during which the forecasting error does not exceed the mean climate variations of predictable amounts. As Monin notes, the problem of determining the limits of predictability can be called the problem of predictability. The definition given above was presented in relation to an evaluation of the possible term of the forecast for individual synoptic processes with the help of general atmospheric circulation models.

Currently the problem of predictability arises more and more in the discussion of questions related to the long-range forecasts of weather and climate. Although there is not precise definition of long-range predictability, however, judging from a number of publications, for example [2], in the given case this problem is also linked to the possible term of the forecast. At the same time there are grounds to think that in forecasting long-period trends in weather and climate the problem of predictability has basic differences from the short-range predictability.

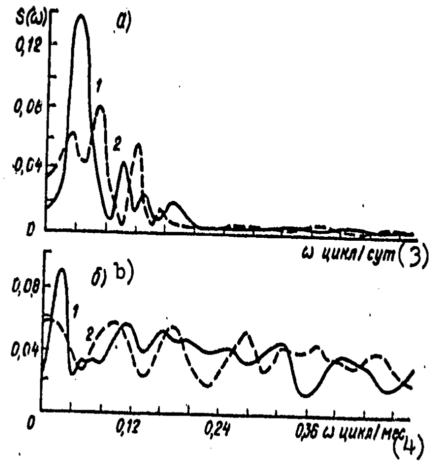

Figure 1. Spectra of Daily Average (a) and Monthly Average (b) Values of Air Pressure at Stations Leningrad (1) and London (2).

Key:
3. cycle/day
4. cycle/month

Numerical experiments on general atmospheric circulation models show that the predictability limit of individual synoptic processes is 2-3 weeks. In order to forecast weather for longer periods it is necessary to operate with averaged values of meteorological elements which is usually done in long-range weather forecasts of great term. In this respect it is necessary to note one important circumstance.

Spectral analysis of the averaged values of meteorological elements shows that a considerable part of their dispersion occurs in the high-frequency fluctuations that form the so-called meteorological noise. In particular, a relatively high level of noises is observed in a number of monthly average and seasonal average values of meteorological elements. Figure 1 as an example depicts the spectra of daily average and seasonal average air pressure values at the Leningrad and London stations. As is apparent from the figure, in the daily average values the main portion of the dispersion is concentrated in a relatively narrow band of frequencies. With monthly averaging dispersion "scatters" over the entire range of frequencies, as a result of which the spectra of monthly average air pressure values approach the spectra of a random process of the "white noise" type.

In relation to the fact that samplings of averaged amounts are a mixture of processes of different time scales the question arises whether all the sections of the spectrum of averaged values are potentially predictable. This question, posed in the publication of S. Ye. Leyts [2] is of basic importance. In fact, if certain components included in the spectrum of averaged values cannot be predicted, then this means that there exists a certain predictability limit that can be presented in the form of the ratio of dispersion of the predictable portion of the process (σ^2_p) to its summary dispersion (σ^2).

Evidently, each model or method of forecasting can have its predictability limit determined by their individual peculiarities. In our case of greatest importance is the evaluation of the predictability limit linked not to the peculiarities of a certain model, but the properties of the atmospheric processes. In examining the predictability problem from this viewpoint, it is first of all necessary to focus attention on the reason for the development of noises in a number of averaged values, since it is precisely their forecasting that produces the greatest difficulties.

One can hypothesize that one of the main sources of noise in a number of monthly average values is synoptic-scale oscillations that are not completely eliminated during averaging. The latter is equivalent to smoothing of the initial data by an equilibrium filter with samplings of smoothed values through the period of averaging. The effect of the filter's action on the temporal series can be expressed through the spectral characteristics

$$S_{\bar{x}}(\omega) = S_x(\omega)\, A^2(\omega), \qquad (1)$$

where $S_{\bar{x}}(\omega)$ and $S_x(\omega)$--spectra of initial and smoothed series, while $A^2(\omega)$--amplitude-frequency characteristic of filter that is the coefficient of attenuation of the component amplitude with frequency ω as a result of the smoothing of the initial series. For the equilibrium filter with weights $\frac{1}{T}$, where T--period of averaging, the amplitude-frequency characteristic looks like

$$A_T(\omega) = \frac{\sin \pi \omega T}{\pi \omega T}$$

The square of this function, besides the main maximum in the beginning of the coordinates has a number of diminishing maximums that are called the lateral bands of filter transmission.

It follows from an analysis of function $A(\omega)$ and correlation (1) that the spectrum of the smoothed series will contain residual energy on the periods smaller than the averaging interval T. Samplings of smoothed values through the averaging interval, according to the theorem of readings [3] make it possible to present in a number of averaged values only the oscillations with periods greater than 2T. The residual energy of oscillations with smaller periods will be connected in the spectrum of this series to periods greater than 2T.

During averaging for a month the oscillations with scales from 40 to 60 days maintain from 25 to 65% of the initial amplitude, while the synoptic oscillations with periods from 3 to 7 days--from 5 to 8%. All of these residual oscillations transfer to series of average monthly values, but with other frequencies, which are determined by the known aliasing error

$$f_k = 2\,kf_N \pm f, \quad k = 1, 2, \ldots, \qquad (2)$$

where $f_N = \frac{1}{2T}$ --boundary frequency of a number of averaged values,

f_k--frequencies greater than f_N whose residual energy transfers to a number of averaged values,

f--frequency of averaged series that receives the residual energy of oscillations with frequencies f_k.

According to formula (2) the most significant part of the residual oscillations with scales from 40 to 60 days, as well as the residual synoptic oscillations with periods 4,5 and 7 days are manifest in the series of monthly average values in the interval of scales from 2 to 5 months. In the spectral analysis of a number of monthly average data the effect of such type of noises is found in the form of a noticeable increase in the spectral density level at the high-frequency ends of the spectra.

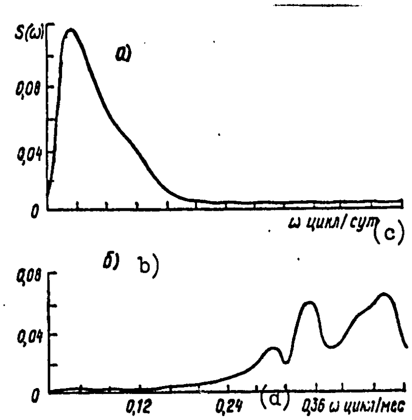

Figure 2. Spectrum of Simulated Series Imitating the Daily Average Values (a), and Spectrum of Series Imitating the Monthly Average Values (b).

Key:
c. cycle/day
d. cycle/month

The process of noise formation in the averaging of initial data can be reprodced by numerical modeling of the temporal series by the Monte Carlo method. Figure 2,a presents the spectrum of a series obtained with the help of band filtering of a sequence of uniformly distributed random values. By comparing figures 1,a and 2,a it is easy to reveal that the spectrum of the simulated series in its main features coincides with the spectra of daily average values of air pressure at the Leningrad and London stations. Figure 2,b presents the spectrum of a series formed by averaging the values imitating the daily average data. As is apparent from the figure, the effect of the emergence of noises during averaging due to the impossibility of completely excluding the short-period oscillations is manifest very strongly.

It has already been noted above that the predictability limit of individual synoptic processes averages 2 weeks. From here it follows that in the long-range weather forecasts of great term the noises created by such processes are practically unpredictable. Here the predictability limit determined by the ratio σ^2_{np}/σ^2 is linked not to the possible term of the long-range forecast, but to its justifiability. In fact, if in the forecast of averaged values only a certain part of their dispersion is potentially predictable, then regardless of the term of the forecast its justifiability cannot exceed a certain limit. It follows from this that the difference in the short-range predictability from the long-range consists of the fact that the first determines the term of the forecasts, while the second--their justifiability.

One can switch from the predictability limit σ^2_{np}/σ^2 to justifiability of the forecast based on the following considerations. We will present the averaged values of the predictable element x in the form

$$x = \eta + \xi,$$

where η--predictable part of the value x, and ξ --unpredictable noise. If it is assumed that the amount η is predicted without errors, then the justifiability of forecast P can be presented as

$$P = \text{Bep}\,\{|x - \eta| \leq \Delta\}.$$

The amount Δ is the permissible error of forecast x, equal to

$$\Delta = \lambda\sigma_x,$$

where λ-- a certain number that can be selected from the guide for verification of the justifiability of forecasts.

The expression given above for P can be rewritten as

$$P = \text{Bep}\,\{|\xi| \leq \lambda\beta\sigma_\xi\},$$

where

From here

$$P=\frac{2}{\sqrt{2\pi}}\int_0^{\lambda_3} e^{-\frac{t^2}{2}}\,dt.$$

By knowing the predictability limit $\sigma^2_{\text{np}}/\sigma^2$ it is easy to obtain the value and determine the justifiability of forecast P. Below are the values of justifiability P depending on the ratio $\sigma^2_{\text{np}}/\sigma^2$ with $\lambda=0.68$:

$\sigma^2_{\text{np}}/\sigma^2$	0,80	0,75	0,70	0,65	0,60	0,55	0,50
P	0,88	0,82	0,78	0,75	0,71	0,68	0,66

The predictability limit of averaged values can be evaluated with respect to their spectrum, and precisely:

$$\sigma^2_{\text{np}}/\sigma^2=\int_0^{\omega_n} S(\omega)\,d\omega,$$

where $S(\omega)$--normed spectral density of averaged values;
ω_n--threshold frequency that determines the border of noise spread.

As shown by the simulation results, for the monthly average data the boundary frequency corresponds to the period 3.5 months. On the basis of this, according to the spectra of the monthly average air pressure at the Leningrad and London stations the ratio and limit justifiability of the forecast were computed, which proved to be equal to 0.77 for Leningrad and 0.71 for London.

The relatively high level of noises at the aforementioned stations is not an exception. Analysis of the anomalies of the monthly average air pressure at 42 stations of the Northern Hemisphere shows that the ratio $\sigma^2_{\text{np}}/\sigma^2$ averages 0.30-0.40. Figure 3 depicts the map of limit justifiability of forecasting the monthly average air pressure anomalies with permissible error of the forecast equal to 0.68 σ. It is apparent on the figure that in individual regions this justifiability is very low and is 65-70%. The limit justifiability of the monthly average anomalies of air temperature is somewhat higher and equals on the average 75-80%.

Naturally, the limit justifiability of the forecast can be increased by increasing the permissible forecasting error. In this respect the question arises of the optimal correlation between the limit justifiability of the forecast and its permissible error that requires special examination.

The cited data provide the foundation for the belief that the justifiability of the methods for forecasting the monthly average air pressure and temperature anomalies approaches its theoretical limit. However, this circumstance does not provide the grounds for pessimistic conclusions. Although the actual noise is unpredictable, some of its parameters can be predicted

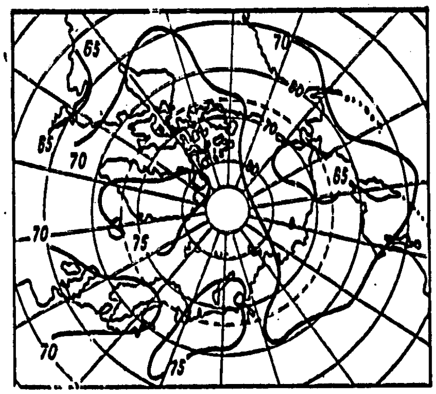

Figure 3. Map of Limit Justifiability (%) of Forecasting Monthly Average Anomalies of Air Pressure with Permissible Forecasting Error Equal to 0.68 σ.

apparently with success. In particu , one of these parameters is the noise amplitude. Changes in amplitude in time have a significantly greater time scale as compared to the period of oscillations of high-frequency fluctuations. This makes it possible to link the time changes of noise amplitude to the long-periods of the atmospheric circulation processes.

On the other hand, the noise amplitude characterizes the stability of the atmospheric processes, and its forecasting can be of definite importance for the users. In this way one of the possible means of further developing long-range weather forecasts of great term consists of solving the problem of parametrization of noises.

BIBLIOGRAPHY

1. Goldman, S. "Teoriya informatsii" [Theory of Information], Moscow, IL, 1957, 446 p.

2. Leyts, S. Ye. "Formulation of a Statistical-Dynamic Model of Climate and the Statistical Limitations of its Predictability," "Fizicheskiye osnovy teorii klimata i ego modelirovaniye" [Physical Foundations of the Climate Theory and its Modeling], Leningrad, Gidrometeoizdat, 1977, 270 p.

3. Monin, A. S. "Prognoz pogody kak zadacha fiziki" [Weather Forecasting as a Problem of Physics], Moscow, Nauka, 1969, 184 p.

UDC 551.(582.2+584.5)

FEATURES OF THE METEOROLOGICAL PATTERN OF A LARGE CITY*

Moscow METEOROLOGIYA I GIDROLOGIYA in Russian No 5, May 79 pp 22-27

[Article by Professor L. T. Matveyev, Leningrad Hydrometeorological Institute, submitted for publication 26 Oct 78]

Abstract. Observational data have been used to obtain the statistical characteristics of the air temperature differences (ΔT) between a large city and its environs. For the first time the differential and integral distribution functions for the ΔT difference are constructed; it follows from their analysis that the greatest contribution to the formation of a "heat island" is made by urban air pollution that significantly reduces heat losses by means of effective radiation. The role of the additional amount of heat released by industrial enterprises, transportation and dwellings is insignificant. In large cities the rise in temperature is already so considerable that it affects the conditions of fog formation. Contrary to existing opinion, the probability of fog formation in a large city is 2-3 times lower than in its environs. This important conclusion is confirmed also on the basis of an analysis of the statistical characteristics of the meteorological visibility range.

[Text] The problem of the change in the atmospheric pattern under the influence of human production activity in the last decades has attracted more and more intensive attention of the scientists, engineers and economists. This problem has been covered extensively in the literature. From the surveys we will name here [k,2,4]. The most important changes are noted in the air basin pattern of large cities. These changes are spread several tens (or the first hundreds) of kilometers along the horizontal, and several hundreds of meters along the vertical, and thus must be grouped with the class of mesometeorological changes. Despite the large number of studies there still remain many unanswered questions.

* The main content of the reports at the Leningrad Hydrometeorological Institute conference (1976) and the International Symposium on Meteorological Aspects of Atmospheric Pollution (1977).

The goal of this article is to reveal by analysis of observational materials certain laws governing the formation of the meteorological pattern of a large city.

Air temperature. Many researchers have established that the urban air temperature (T_{rop}) is above the air temperature in its environs (T_{okp}). The mean values of the difference

$$\Delta T = T_{rop} - T_{okp}$$

most often for large cities are 1-2°C. However, until now there has not been a detailed statistical analysis of the ΔT difference. In filling this gap we analyzed the observations (for eight periods) of air temperature in Leningrad (Hydrometeorological Observatory) and in several points (Voyeykovo, Volkhov, Sosnovo, Belogorka) 80-100 km from the center of Leningrad (Voyeykovo is an exception since it is located roughly 20 km from the center of Leningrad). The mean (multiple-year) values of ΔT difference fluctuate (for different points) between 0.9 and 1.2°C in winter, and between 1.0 and 1.3°C in summer. The ΔT difference rises with time. Thus, from observations for the five-year period 1970-1974 the mean ΔT values were between 1.5 and 2.0°C in winter, and between 1.1 and 1.6°C in summer.

The changes in ΔT difference during the day are important. The mean ΔT values for 5 years at different times of the day are given in table 1. Here the point is indicated for which the mean (for winter and summer) ΔT difference is determined between the air temperature in Leningrad and in the given point. In the last two columns of table 1 the ΔT differences are given between the air temperature in Leningrad and the temperature averaged for all four points in the environs.

According to the data of table 1 the greatest ΔT difference values are attained at night and in the morning hours, while the smallest--during the day. Since the industrial enterprises, heating systems, and especially transportation emit heat, of course, considerably more during the day than at night, then it follows from the findings that the decisive role in the formation of a "heat island" in the city is played not by that additional heat released by the industrial enterprises and transportation, but by other factors (among the latter the reduction in effective radiation in the city under the influence of pollutants is especially important).

The analyzed data mass (the samplings include 17,366 ΔT differences in winter and 14, 720 in summer were used to construct the empirical functions for ΔT distribution (tables 2 and 3).

The probability density (differential distribution function) reaches the maximum (modal value) equal to 33.9% in winter and 25.6% in summer in the interval 0-1°C and 1-2°C respectively. The ΔT extremes are contained in winter between 16 and -9°C(at the intervals 15-16°C and -9- -8°C there are 3 and 6 cases respectively), in summer between 11 and -11°C (at the intervals 10-11°C and -11- -10°C there are 2 cases each). The distribution function

Table 1. Daily Course of Mean ΔT°C Difference Values, 1970-1974

(a) Время, ч	(b) Воейково		(c) Сосново		(d) Белогорка		(e) Волхов		(f) Все пункты	
	(g) зима	(h) лето	(g) зима	(h) лето	(g) зима	(h) лето	(g) зима	(h) лето	(g) зима	(h) лето
00	1,3	1,6	1,2	2,7	2,0	2,5	2,0	2,2	1,5	2,2
03	1,2	1,9	1,1	3,0	2,0	3,1	1,9	2,7	1,5	2,7
06	1,4	1,6	0,9	2,4	1,9	2,8	2,1	2,0	1,5	2,2
09	1,4	0,8	1,2	0,7	1,9	1,2	2,2	0,6	1,0	0,8
12	1,2	0,7	1,0	0,7	1,5	0,5	1,7	0,1	1,3	0,5
15	1,1	0,5	0,8	0,8	1,0	0,3	1,4	0,1	1,0	0,4
18	1,3	0,9	1,1	0,7	1,5	0,2	1,6	0,3	1,4	0,5
21	1,5	1,5	1,2	1,3	2,0	0,8	2,0	1,0	1,6	1,1

Key:
a. Time, h
b. Voyeykovo
c. Sosnovo
d. Belogorka
e. Volkhov
f. All points
g. Winter
h. Summer

Table 2. Probability Density (P%) of ΔT Difference

Δ T°C	(a) Зима	(b) Лето	Δ T°C	(a) Зима	(b) Лето	Δ T°C	(a) Зима	(b) Лето	Δ T°C	(a) Зима	(b) Лето
−7÷−6	0,0	0,1	−3÷−2	1,2	1,7	1÷2	23,4	25,6	6÷7	1,2	1,2
−6÷−5	0,2	0,1	−2÷−1	2,5	5,2	2÷3	10,5	15,7	7÷8	1,0	0,5
−5÷−4	0,3	0,3	−1÷0	12,0	11,9	3÷4	6,0	8,3	8÷9	0,5	0,2
−4÷−3	0,8	0,7	0÷1	33,9	22,0	4÷5	3,6	4,2	9÷10	0,3	0,1
						5÷6	2,2	1,2	10÷11	0,1	0,0

Key: a. Winter b. Summer

Table 3. Integral Function $F(\Delta T \geq X)$ of Distribution (%) of ΔT Difference

Δ X°C	(a) Зима	(b) Лето	Δ X°C	(a) Зима	(b) Лето	Δ X°C	(a) Зима	(b) Лето	Δ X°C	(a) Зима	(b) Лето
12	0,1	0,0	7	2,1	0,8	2	25,5	32,4	−3	98,6	98,8
11	0,2	0,0	6	3,3	2,0	1	48,9	58,0	−4	99,4	99,5
10	0,3	0,0	5	5,5	4,2	0	82,9	80,0	−5	99,7	99,8
9	0,6	0,1	4	9,1	8,4	−1	94,9	91,9	−6	99,9	99,9
8	1,1	0,3	3	15,0	16,7	−2	97,4	97,1			

Key: a. Winter b. Summer

has also been constructed for the data referring to different observational periods. The analysis showed that in summer at 03.00 the probability density reaches the maximum (equal to 22.5%) in the interval 2-3°C, in the daytime hours (09.00, 12.00 and 15.00)--in the interval 0-1°C, and in the evening

(18.00, 21.00 and 00.00) and morning (06.00)--in the interval 1-2°C, i.e., the ΔT distribution also indicates that at night larger ΔT differences are observed than during the day.

The mean ΔT values for the samplings used to compile tables 2 and 3 equal 1.33°C in winter and 1.40°C in summer, the dispersion equal 3.87 (°C)^2 in winter and 3.68 (°C)^2 in summer.

According to the data of table 3, the city is warmer than its environs ($\Delta T \geq 0$°C) in 82.9% of the cases in winter and in 80.0% of the cases in summer. Large positive ΔT values ($\Delta T \geq 4$°C and especially $\Delta T \geq 7$°C) are observed considerably more often in winter than in summer.

Analysis of the functions $F(\Delta T \geq X)$ constructed from the observational data for individual periods indicated that at night positive ΔT are found more often than during the day. Thus, in summer at 00.00 and 0.300 the $F(\Delta T \geq 0$°C) values equal 92.7 and 94.5%, while at 13.00, 15.00 and 18.00 these values equal 67.8, 64.1 and 67.0% respectively.

A comparison of ΔT for individual points shows that for Voyeykovo, Sosnovo and Belogorka the $F(\Delta T \geq 0$°C) values are roughly the same (in summer 79-85%), while Leningrad is warmer than Volkhov (the point is larger, and apparently, more polluted) in a smaller number of cases (in summer in 73.2%).

Information about ΔT with a varying cloud cover is important. According to observational data in summer (June-August) for 1970-1974 the mean values of air temperature differences ($\Delta T = T_{л} - T_{c}$) in Leningrad and Sosnovo are:

Amount of lower cloud cover, points	0-2	3-8	9-10
Night (21.00-06.00)	2.8	2.0	1.4
Day (09.00-18.00)	0.8	0.6	1.2
Days	2.0	1.1	1.3
Number of cases (for days)	1492	399	381

According to these data, at night with an increase in the cloud cover the ΔT difference is reduced, and at night the transition from slightly cloudy weather to overcast is accompanied by a rise in ΔT.

Visibility and fog. The most important value is the range of visibility (everywhere we have in mind the meteorological visibility range S_m linked to the linear index of radiation attenuation a by the correlation $S_m = 3.5/a$). According to the observational data for winter of a five-year period (1970-1974, December was taken for 1969-1973) the following probabilities were obtained (P) for visibility range not exceeding 10 km ($S_m \leq 10$ km):

	Leningrad	Voyeykovo	Volkhov	Sosnovo	Belogorka
n	2457	1657	744	1284	1383
P%	68.2	45.9	20.7	35.6	38.2

According to these data, the reduced visibility in a large city is observed considerably more often (in the given example, in 68% of the cases) than in the environs of the city (in Sosnovo--in 36%, in Belogorka--in 38%, and in Volkhov--21% of the cases), which is governed by the effect of pollutants. This conclusion agrees with the data of previously fulfilled studies [3].

Table 4. Density of Probabilities (%) of Visibility Range (Sampling Volume for Each Point--3608). Winter 1970-1974

	(1) Интервал $S_м$, км					
	<1	1—2	2—6	6—10	10—20	>20
Ленинград (2)	1,4	2,1	22,9	41,8	15,0	16,8
Воейково (3)	2,8	2,5	19,4	21,2	20,8	33,3
Волхов (4)	1,5	0,5	4,1	14,6	32,7	46,7
Сосново (5)	4,7	3,4	8,5	19,0	22,9	41,5
Белогорка (6)	3,5	2,7	10,3	21,7	31,8	29,9

Key:
1. Interval S_m, km
2. Leningrad
3. Voyeykovo
4. Volkhov
5. Sosnovo
6. Belogorka

Analysis of table 4 shows that in Leningrad the exacerbated visibility conditions are mainly created as a consequence of the weak and moderate haze (S_m=6-10 km and S_m=2-6 km): in these intervals the recurrence of S_m in the city is roughly 2 times greater than in its environs. The probability of thick haze (S_m=1-2 km) is roughly the same in Leningrad and its environs. The results on the probability of the visibility range not exceeding 1 km ($S_m \leq 1$ km) proved to be unexpected. In many articles, the educational and monograph literature it is indicated that in the city the visibility range is significantly lower than in the suburbs. The data of table 4 refute this assertion in relation to the poor visibility. In fact the probability of $S_m \leq 1$ km in Leningrad is 1.4%, and in its environs this probability is 2-3 times greater (in Sosnovo--4.7%, in Belogorka--3.5%, in Voyeykovo--2.8%). Since the visibility range $S_m \leq 1$ km is mainly governed by the appearance of fog (snowstorms and snowfalls also make a certain contribution) then we turned to the data on the recurrence of fogs (table 4) not only in the winter period (1970-1974), but also during all the seasons of the two five-year periods (1965-1969 and 1970-1974).

The data of table 5 contradict the extant opinion according to which in the large cities the conditions for fog formation supposedly are more favorable than in the rural locality.

In actuality, in Leningrad the fogs are formed 2-3 times less often than in the suburbs (in small populated areas). This is also indicated by the data on the total duration of fog t* for winter 1970-1974 and the probability (P) of its observation:

	Leningrad	Voyeykovo	Volkhov	Sosnovo	Belogorka
t*, h	115	319	117	443	265
P%	1.1	3.0	1.1	4.1	2.4

Table 5. Number of Days with Fog

(1) Период наблюдений	(2) Ленинград	(3) Воейково	(4) Волхов	(5) Сосново	(6) Белогорка
1965—1969 гг. (7) (все сезоны)	80	104	206	142	191
1970—1974 гг. (7) (все сезоны)	74	265	120	206	238
1970—1974 гг. (зима) (8)	24	51	26	51	45

Key:

1. Period of observations
2. Leningrad
3. Voyeykovo
4. Volkhov
5. Sosnovo
6. Belogorka
7. all seasons
8. winter

Atmospheric pollution of the city, of course, promotes exacerbation of visibility and fog formation. However the difference in temperatures ΔT between the city and environs has a stronger effect on fog formation. In fact, when the state of saturation is attained (f_{okp} =100%) in the environs the relative humidity f_{rop} in the city with different T_{okp} and ΔT adopts the following values:

$T_{окр}$ °C	−20	−10	0	10
with $\Delta T=1°$C, %	92	92	93	94
with $\Delta T=2°$C, %	84	85	87	88

From the data given in tables 4 and 5 another conclusion follows: the visibility range is decisively affected by the particles of pollutants on which moisture has settled (otherwise in the city the probability of visibility S_m < 1 km would be greater than in the environs). Since the urban conditions for the beginning of condensation due to ΔT are less favorable than in the environs, then the recurrence of visibility S_m < 1 km and fog in the city is lower than in the suburbs.

Since the conclusion on the significantly lower probability of fog in a large city has been formulated (as far as we know) for the first time, then we also turn to the climate data. The mean (for the year) number of days with fog, according to multiple-year data, in Leningrad and its environs are:

Leningrad (Hydrometeorological Observatory)	-29	Toksovo	-67
Leningrad (Nevskaya)	-39	Lodeynoye pole	-52

Voyeykovo	-64	Volosovo	-68
Petrc'krepost'	-46	Lisiy Nos	-21
Vyborg	-47	Lomonosov	-25

According to these data, the recurrence of fog in Leningrad is roughly 2 times lower than in the environs. The exceptions are Lisiy Nos and Lomonosov, located on the northern and southern shores of the Gulf of Finland where the fog recurrence is somewhat even lower than in Leningrad. But these data do not only not contradict, but even support the advanced viewpoint on the role of ΔT in the formation of fog. In fact, the temperature difference between Leningrad and Lomonosov averages for the year only 0.2°C, while in October-January, when fog is mainly formed this difference is even negative (apparently, the warming effect of the Gulf of Finland has an influence). It is quite natural that such differences ΔT cannot have a significant effect on the recurrence of fog, therefore the difference in the number of fogs in Leningrad and its environs under these conditions is governed only by stronger air pollution of a large city (for this reason the number of days with fog in Leningrad was somewhat greater than in Lomonosov and Lisiy Nos).

The conclusion about the dominant effect of the ΔT difference on the formation of fog also follows from the data on the mean (for the year) number of days with fog in Moscow and its environs:

Moscow (Hydrometeorological Observatory)	Moscow (Exhibition of Achievements of the National Economy of the USSR)
20	26

Klin	Dimitrov	Zagorsk	Kashira
36	37	46	49

In Moscow and Leningrad the mean differences ΔT exceed 1°C and here, thus, the effect of this difference on the reduction in relative humidity and fog recurrence is perceptible. Moreover, these cities are less polluted than a number of other cities. Analysis of the data given in the "Klimaticneskiye spravochniki SSSR"[Climate References of the USSR] has shown that for the majority of the large cities in our country (except Moscow and Leningrad) the mean values of the ΔT difference do not exceed several tens of degrees (in Minsk the mean ΔT value for the year is 0.2°C, in Kuybyshev 0.3°C, in Kiev and Tashkent 0.4°C, in Sverdlovsk 0.5°C, and so forth).

Since such ΔT differences reduce only insignificantly the relative humidity (in the city as compared to the environs), then no perceptible difference is observed in the recurrence of fog in the city and its environs for the majority of regions of the Soviet Union. Moreover, under the influence of pollution (which, of course, makes its contribution to impaired visibility) the fog recurrence in a number of cities is greater than in the environs (for the year the number of days with fog in Minsk is 67, in Negoreloye--55, and in Radishkovichi--46).

The experimental data that were given above and briefly analyzed make it possible to pinpoint a number of ideas about the peculiarities and laws governing the formation of the meteorological pattern of a large city.

BIBLIOGRAPHY

1. Adamenko, V. N. "Klimat bol'shikh gorodov (obzor)" [Climate of Large Cities. (Survey)], Obninsk, VNIIGMI-MTsD, 1975, 70 p.

2. Berlyand, M. Ye., and Kondrat'yev, K. Ya. "Goroda i klimat planety" [Cities and Climate of the Planet], Gidrometeoizdat, 1972, 39 p.

3. Dovgyallo, Ye. N. "Horizontal Transparency in Cities and Industrial Centers" TRUDY GGO, No 279, 1972, pp 154-170.

4. "Klimat Moskvy (osobennosti klimata bol'shogo goroda)" [Climate of Moscow (Peculiarities of the Climate of a Large City], edited by A. A. Dmitriyev and N. N. Bessonov. Gidrometeoizdat, 1974, 320 p.

UDC 551.510.522

STRUCTURE OF THE BAROCLINIC EKMAN PLANETARY BOUNDARY LAYER

Moscow METEOROLOGIYA I GIDROLOGIYA in Russian No 5, May 79 pp 28-34

[Article by Professor S. Panchev and D. Atanasov, Sofia University, Bulgaria, submitted for publication 14 Jul 78]

Abstract. A model of the planetary boundary layer over a thermally heterogeneous underlying surface is examined. The obtained formulas are asymptotically transformed into the classic Ekamn solution on the condition that the underlying surface temperature is constant. The problem can be viewed as the first approximation in solving the problem of the joint effects of turbulence, baroclinicity, and the underlying surface relief.

[Text] Introduction

The planetary boundary layer [PBL] over the thermally heterogeneous underlying surface ($\nabla T_0 \neq 0$) also is heterogeneous ($\nabla T \neq 0$). Here $T_0 = T(x,y)$ is the temperature of the earth's surface that is considered flat, $T = T(x,y,z)$ is the atmospheric temperature at altitude z, $\nabla = (\partial/\partial x, \partial/\partial y, 0)$ is the nabla (grad)--operator. It is said that in this case the PBL is baroclinic. If there is no other reason for heterogeneity, then with altitude $\nabla T \rightarrow 0$ and the PBL asymptotically approaches the barotropic free atmosphere ($\nabla T_\infty = 0$, where $T_\infty = T(x, y, \infty) = \text{const}$). The barotropicity is essentially reached at the upper boundary of the so-called thermal boundary layer, on the order of dynamic altitude (1-2 km). The general case, when $T_\infty = T(x,y)$ is of undoubted importance.

Thermal heterogeneity of the earth's surface can be created by the presence of large cities, reservoirs, islands in the ocean, steppe or desert regions, and so forth. The baroclinicity will be manifest especially strongly at the boundaries of these regions where ∇T_0 has large values.

It is very necessary to consider baroclinicity in the PBL dynamics problems. Baroclinicity has a significant effect on wind distribution in this layer, which is apparent, for example, from the velocity hodographs constructed by Wiin-Nielsen [4].

There are many publications covering this question. They are mainly based on the similarity theory [5]. We will solve this problem in the classic formulation as was done in [2-4], with certain refinements. They will permit a more complete interpretation of the findings.

Approximation of Baroclinicity and Turbulence

Our goal was to study the joint effect of baroclinicity and turbulence on wind in the PBL. Here we will consider that:

A. The temperature field has been prescribed;
B. The turbulence coefficient has been assigned;
C. The quasistatic equation is fulfilled;
D. The underlying surface is flat.

Condition C permits us to write

$$p(x, y, z) = p_0(x, y) \exp\left(-\frac{g}{R}\int_0^z \frac{dz'}{T(x, y, z')}\right). \quad (1)$$

From here we find the link between the gradients:

$$\nabla p = \frac{p}{p_0} \nabla p_0 + \frac{gp}{R}\int_0^z \frac{1}{T^2} \nabla T\, dz'. \quad (2)$$

From this gradient we compute the geostrophic wind:

$$\vec{v}_g = \frac{RT}{lp} \vec{k} \times \nabla p = \frac{T}{T_0}\vec{v}_g^0 + \frac{gT}{l}\int_0^z \frac{1}{T^2} \vec{k} \times \nabla T\, dz', \quad (3)$$

where, according to (2), $(\nabla p)_0 = \nabla p_0$,

$$\vec{v}_g^0 = \frac{RT_0}{lp_0}\vec{k} \times \nabla p_0 \quad (4)$$

--surface geostrophic wind,

$$\vec{k} = (0, 0, 1),$$

l--Coriolis parameter.

We assume, as usual, that

$$T(x, y, t) = T_0(x, y) - \gamma z, \quad \gamma = \text{const}. \quad (5)$$

By substituting (5) into (3), and by using (4) we obtain without any simplifications

$$\vec{v}_g = \vec{v}_g^0 + \vec{v}_\tau' z, \quad \vec{v}_\tau' = -\frac{\gamma R}{lp_0} \vec{k} \times \nabla p_0 + \frac{g}{lT_0} \vec{k} \times \nabla T_0, \quad (6)$$

i.e., the formula that is usually assigned a priori [3,4], but with the "expanded" thermal wind $\vec{v}_T'$. The linear relationship $\vec{v}_g(z)$ is the simplest and most convenient for solving the motion equations in the PBL [3,4], however, the unrestricted rise in $\vec{v}_g$ with altitude is its shortcoming. It does not agree with the idea on the asymptotic transition of the baroclinic PBL to the barotropic free atmosphere ($\nabla T_\infty = 0$).

In order to satisfy the latter requirement we assume

$$T(x, y, z) = T_\infty - \theta(x, y)\, e^{-mz},$$
$$\theta(x, y) = T_\infty - T_0(x, y), \quad m = \text{const.} \tag{7}$$

Analogously to the previous, by substituting (7) into (3) we obtain

$$\vec{v}_g = \vec{v}_g^{\infty} - \vec{v}_T\, e^{-mz}, \tag{8}$$

$$\vec{v}_T = \frac{R\theta}{lp_0} \vec{k} \times \nabla p_0 + \frac{g}{mlT_0} \vec{k} \times \nabla T_0, \tag{9}$$

$$\vec{v}_g^{\infty} = \vec{v}_g^0 + \vec{v}_T = \frac{RT_\infty}{lp_0} \vec{k} \times \nabla p_0 + \frac{g}{mlT_0} \vec{k} \times \nabla T_0, \tag{10}$$

where $\vec{v}_T$, evidently has the meaning of a full thermal wind, while the parameter m determines the speed of attenuation in ∇T with altitude; to a certain measure it characterizes baroclinicity. The formula of the exponential type (8) for $\vec{v}_a$ was proposed in [2].

More complex approximations than (7) can be tested, however this hardly makes sense. Of main importance are the temperature drop $\theta = T_\infty - T_0$ and altitude $z_m = 1/m$ at which $T \approx T_\infty$ is realized, and not the specific profile T(z). In addition as we will see below (8) guarantees a simple solution to the PBL motion equations. Therefore we will pass to the question of approximation of turbulence.

In the Ekman model its unique characteristic is the coefficient of vertical turbulent exchange K. Generally speaking, K=K(x,y,z). We will examine two examples:

$$\overline{K}^{(x,y,z)}_{(x,y,z)} = K = \text{const}, \tag{11}$$

$$\overline{K}^{(z)}_{(x,y,z)} = K(x, y), \tag{12}$$

where the characteristic at the top designates averaging with respect to the noted variables.

One can indicate, at least two examples on which the coefficient K(x,y) must depende: drop in velocity $c_g^\infty = |\vec{v}_g^\infty|$ on the boundaries of the PBL and l.

From the considerations of dimensions

$$K(x, y) = \delta c_g^{\infty 2}/l, \qquad (13)$$

where $|\vec{v}_g^\infty|$ is defined by formula (10). The expression of type (13) was previously proposed by Gandin [1] for the barotropic PBL with empirical constant $\delta = 6.25 \cdot 10^{-6}$. He showed that in the computation of the vertical velocity w from the conservation equation based on the Ekman solution with variable K(x,y) an additional term appears on the order of the main. One can assume that in the baroclinic PBL this effect will be even more significant, the more so since the substitution of (10) into (3) links K to all the previous characteristics of the problem, including baroclinicity. By averaging (13) with respect to region (x,y) in accordance with (11) we obtain K=const. Analogous considerations of dimensions in application to the true coefficient K(x,y,z) result in

$$K(x, y, z) = \delta \frac{c_g^{\infty 2}}{l} f\left(\frac{zl}{c_g^\infty}\right),$$

where $f(\eta)$ is the dimensionless function.

Wind Field in Baroclinic PBL

The motion equations of a horizontally heterogeneous PBL look like

$$\frac{\partial}{\partial z} K \frac{\partial \vec{v}}{\partial z} - l\vec{k} \times (\vec{v} - \vec{v}_g) = \frac{\partial \vec{v}}{\partial t} + (\vec{v} \cdot \nabla)\, \vec{v} - K' \nabla^2 \vec{v}, \qquad (14)$$

where K'--coefficient of horizontal macroturbulent exchange. We note that in this respect we solve the problem of the PBL structure for synoptic-scale movements.

As the zero approximation we assume with regard for (11) and (12) that

$$K \frac{\partial^2 \vec{v}}{\partial z^2} - l\vec{k} \times \vec{v} = - l\vec{k} \times \vec{v}_g \qquad (15)$$

with the classic boundary conditions

$$|\vec{v}| = 0, \quad z = 0; \quad \vec{v} \to \vec{v}_g, \quad z \to \infty. \qquad (16)$$

The horizontal heterogeneity enters the problem through $\vec{v}_g(x,y,z)$ and K(x,y). Then by the method of successive approximations one can take into consideration advection $(\vec{v} \cdot \nabla)\vec{v}$ and lateral friction $K' \nabla^2 \vec{v}$.

By omitting the intermediate computations we obtain the solution to the problem (15)-(16) for the case of linear approximation (6) in the form [4]

$$\vec{v} = \vec{v}_g^0 + \vec{v}_\tau' z - \vec{v}_g^0 e^{-az} \cos az + \vec{k} \times \vec{v}_g^0 e^{-az} \sin az \qquad (17)$$

and for the exponential approximation (8) in the form

$$\vec{v} = \vec{v}_g^\infty + (-\vec{v}_g^\infty + r\vec{v}_\tau - q\vec{k} \times \vec{v}_\tau) e^{-az} \cos az +$$

$$+ (\vec{k} \times \vec{v}_g^\infty - q\vec{v}_\tau - r\vec{k} \times \vec{v}_\tau) e^{-az} \sin az +$$

$$+ (-r\vec{v}_\tau + q\vec{k} \times \vec{v}_\tau) e^{-mz}, \qquad (18)$$

where

$$a = \sqrt{\frac{l}{2K}}, \quad r = \frac{4}{4+s^4}, \quad q = \frac{2s^2}{4+s^4}, \quad s = \frac{m}{a}. \qquad (19)$$

With K=const a,s,r and q also will be constants. Since the value a determines the altitude of the Ekman PBL ($z_g = \pi/a$), according to the terms of the m parameter in (8) one can assume that $m \sim a$. In [2] it was directly considered that m=a(s=1). Then r=4/5, q=2/5. In extreme cases it is permissible (although only theoretically) for m<<a or m>>a. Consequently, $q, r \to 0$ with $s \to \infty$, and $r \to 1$ and $q = O(s^2/2)$ with $s \to 0$.

By having solutions (17) or (18) one can compute

$$D(x, y, z) = \nabla \cdot \vec{v} = u_x + v_y, \qquad (20)$$

$$\Omega(x, y, z) = \vec{k} \cdot (\nabla \times \vec{v}) = (\nabla \times \vec{v})_3 = v_x - u_y, \qquad (21)$$

$$w(x, y, z) = -\int_0^z D(x, y, z')\, dz'. \qquad (22)$$

The latter expression follows from equation $D + w_z = 0$ and the condition $w(x,y,0) = 0$. We write out the result only for the second solution (18):

$$D(x, y, z) = -F_2 \Omega_g^\infty + F_4 (\nabla \cdot \vec{v}_\tau) + F_5 (\nabla \times \vec{v}_\tau)_3 + (\nabla K \cdot \vec{U}_{08}) +$$

$$+ (\nabla K \times \vec{U}_{10})_3, \qquad (23)$$

$$\Omega(x, y, z) = (1 - F_1)\,\Omega_g^\infty - F_5(\nabla\cdot\vec v_T) + F_4(\nabla\times\vec v_T)_3 - (\nabla K\cdot\vec U_{79}) +$$

$$+ (\nabla K\times\vec U_{68})_3, \tag{24}$$

$$w(x, y, z) = -\overline{F}_2\,\Omega_g^\infty + \overline{F}_4(\nabla\cdot\vec v_T) + \overline{F}_5(\nabla\times\vec v_T)_3 + (\nabla K\cdot\vec{\overline{U}}_{68}) +$$

$$+ (\nabla K\times\vec{\overline{U}}_{79})_3, \tag{25}$$

where

$$\vec U_{\alpha\beta} = F_\alpha\vec v_g^\infty + F_\beta\vec v_T, \quad \vec{\overline{U}}_{\alpha\beta} = \overline{F}_\alpha\vec v_g^\infty + \overline{F}_\beta\vec v_T, \quad \vec v_g^\infty = \vec v_g^0 + \vec v_T. \tag{26}$$

Functions $F_4, F_5, \ldots, F_9$, in view of their awkwardness are not written out; they are easy to obtain, considering that $F_3 = e^{-az}$; $F_1 = F_3\cos az$; $F_2 = F_3\sin az$.

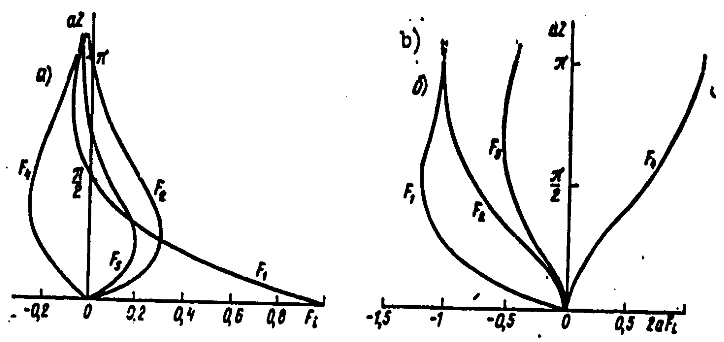

Figure 1. Dependence of Functions F_i(a) and $\overline{F}_i$(b) on z.

Based on these general formulas one can carry out diverse analyses. We will limit ourselves to the simplest case where K=const(∇K=0) and m=a, i.e., r=4/5, q=2/5. The course of curves $F_i(z)$, i=1,2,3,4, and 2a $\overline{F}_i$, i=2,4,5 is shown in fig 1. In formulas (23)-(25) in this case only the first 3 components remain.

On the other hand, by using (9)and (10) we obtain

$$\Omega_g^\infty = (\nabla\times\vec v_g^\infty)_3 = \frac{RT_\infty}{l}\nabla^2(\ln p_0) + \frac{g}{ml}\nabla^2(\ln T_0), \tag{27}$$

$$D_T = (\nabla\cdot\vec v_T) = \frac{R}{lp_0}(\nabla T_0\times\nabla p_0)_3 = \frac{R}{lp_0}\{T_0, p_0\}. \tag{28}$$

$$\Omega_\tau = (\nabla \times \vec{v}_\tau)_3 = -\frac{R}{lp_0}(\nabla T_0 \cdot \nabla p_0) + \frac{R\theta}{l}\nabla^2(\ln p_0) +$$

$$+\frac{g}{ml}\nabla^2(\ln T_0), \qquad (29)$$

where $\theta = T_\infty - T_0,\ m = a,$

$$\nabla^2(\ln A) = \frac{1}{A^2}[A\nabla^2 A - (\nabla A)^2]. \qquad (30)$$

Consequently,

$$D(x, y, z) = -F_2\Omega_g^\infty + F_4 D_\tau + F_5\Omega_\tau,$$

$$\Omega(x, y, z) = (1 - F_1)\Omega_g^\infty - F_5 D_\tau + F_4\Omega_\tau,$$

$$w(x, y, z) = -\overline{F}_2\Omega_g^\infty + \overline{F}_4 D_\tau + \overline{F}_5\Omega_\tau. \qquad (31)$$

Usually $A\nabla^2 A \gg (\nabla A)^2,\ A = p_0,\ T_0$. In fact, according to Yudin's known table on the characteristic values of meteorological elements and their derivatives we have (in SI units): $p_0 \sim 10^5$ N/m^2 (10^3 mbar), $\nabla p_0 \sim 10^{-3}$, $\nabla^2 p_0 \sim 10^{-9}$, $T_0 \sim 3\cdot10^2$°C, $\nabla T_0 \sim 7\cdot10^{-6}$, $\nabla^2 T_0 \sim 2\cdot10^{-11}$. Then $(\nabla A)^2$ is 2 orders smaller than $A\nabla^2 A$. Therefore one can write that

$$\nabla^2(\ln A) \approx A^{-1}\nabla^2 A. \qquad (32)$$

However in principle such situations are also permissible where $A\nabla^2 A \sim (\nabla A)^2$, $A = p_0, T_0$, so that separately or together

$$\nabla^2(\ln T_0) \approx 0 \quad \text{and} \quad \nabla^2(\ln p_0) \approx 0. \qquad (33)$$

In this special case $\Omega_g^\infty \approx 0$, while

$$\left.\begin{matrix} D(x, y, z) \\ \Omega(x, y, z) \\ w(x, y, z) \end{matrix}\right\} \approx \frac{R|\nabla T_0||\nabla p_0|}{lp_0}\left\{\begin{matrix} F_4\sin\alpha - F_5\cos\alpha \\ -(F_5\sin\alpha + F_4\cos\alpha) \\ \overline{F}_4\sin\alpha - \overline{F}_5\cos\alpha, \end{matrix}\right. \qquad (34)$$

where α is the angle between vectors ∇T_0 and ∇p_0.

Generally it is necessary to combine (31) with (27)-(29). Thus, D, Ω, and w are expressed as linear combinations of the type

$$f(x, y, z) = a_f\nabla^2 p_0 + b_f\nabla^2 T_0 + c_f(\nabla p_0)^2 + d_f(\nabla T_0)^2 + e_f(\nabla T_0 \times$$

$$\times \nabla p_0)_3 + h_f(\nabla T_0 \cdot \nabla p_0) \qquad (35)$$

with known coefficients $a_f, \ldots, h_f$, where $f = D, \Omega$ or w. Such a presentation makes it possible, by prescribing the configuration of the surface pressure fields $p_0(x,y)$ and temperature $T_0(x,y)$ to study the contribution of each term to (35). For example, in the case of a hot or cold "island" $\nabla^2 T_0 < 0$ or $\nabla^2 T_0 > 0$ respectively. On the synoptic background ($\nabla^2 p_0 > 0$--cyclone or $\nabla^2 p_0 < 0$--anticyclone) effects of baroclinicity can be manifest (components with coefficients e_f and h_j), and so forth.

As an example we will write out explicitly the formula for $w(x, y, \infty)$ (practically coinciding with $w(x,y,z_a)$, where $z_a = \pi/a$--PBL altitude. Bearing in mind that $\bar{F}_3^\infty = -1/2\, a$, $\bar{F}_4^\infty = 3/5\, a$, $\bar{F}_5^\infty = -1.5\, a$, we obtain

$$w(x, y, \infty) = \frac{1}{2a}\left[\frac{RT_\infty}{l}\left(1 - \frac{2}{5}\frac{\theta}{T_\infty}\right)\nabla^2(\ln p_0) + \frac{3}{5}\frac{g}{al}\nabla^2(\ln T_0) + \frac{R|\nabla T_0||\nabla p_0|}{5\, l p_0}(3\sin\alpha - 2\cos\alpha)\right]. \qquad (36)$$

However, $\theta \ll T_\infty$, so that formula (36) can be somewhat simplified. Another simplification is obtained with $\mathrm{tg}\,\alpha = 2/3$ ($\alpha \approx 34°$) when the latter term becomes equal to zero. And without this, however, it is usually two orders smaller than the first two, and it can be ignored.

Conclusion

Publications [2-4] have a priori assigned the thermal wind $\vec{V}_T$. We obtained it (formulas (6) and (8)-(10)) based on the static equation (1) according to the prescribed temperature field. Thus, the link between (9) $\vec{V}_T$ and a number of characteristics of the problem has been "expanded." This made it possible in the final analysis to find such links also for divergence D, eddy --Ω, and vertical velocity w. The Ekman problem was solved in the first approximation (15) and with condition (16), i.e., the simplest variant with regard for baroclinicity. The main result of the work is the formulas (27)-(31) or (35) that are easily interpreted. Further refinement can be carried out by introducing instead of (16) more correct boundary conditions [3,4].

This work is a stage in the solution to the more general problem of the joint effect of turbulence, baroclinicity and relief on the PBL structure.

BIBLIOGRAPHY

1. Gandin, L. S.; and Dubov, A. S. "Chislennyye metody kratkosrochnogo prognoza pogody" [Numerical Methods of Short-Term Weather Forecasting], Leningrad, Gidrometeoizdat, 1968, 427 p.

2. Mahrt, L. I.; and Schwerdtfeger, W. "Ekman Spiral for Exponential Thermal Wind," BOUND LAYER METEOROL, No 1, 1970.

3. Venkatesh, S.; and Csanady, G. T. "A Baroclinic Planetary Boundary Layer Model and Its Application to the Wangara Data," BOUND LAYER METEOROL , No 5, 1974.

4. Wiin-Nielsen, A. "Vorticity, Divergence, and Vertical Velocity in a Baroclinic Boundary Layer with A Linear Variation of the Geostrophic Wind," BOUND LAYER METEOROL., No 6, 1974.

5. Wippermann, F. "The Planetary Boundary Layer of the Atmosphere," Offenbach a., Moscow, 1973.

UDC 551.509.32

PROBLEM OF NUMERICAL FORECASTING OF THE ALTITUDE AND TEMPERATURE OF THE TROPOPAUSE

Moscow METEOROLOGIYA I GIDROLOGIYA in Russian No 5, May 79 pp 35-40

[Article by B. T. Kurbanov, Institute of Mathematics of the Uzbek SSR Academy of Sciences, Main Geophysical Observatory, submitted for publication 21 Dec 78]

Abstract. A technique is suggested for determining changes in altitude and temperature of the tropopause from data on changes in altitudes of isobaric surfaces adjacent to the tropopause, above and below it.

Evaluations of the calculated changes in tropopause altitude and temperature are given from data on actual altitude changes in the isobaric surface.

The proposed technique is tested on forecasting material. When the forecast of isobaric surface altitudes is satisfactory the forecast of tropopause temperature and altitude has forecasting significance.

[Text] In publication [4] L. V. Rukhovets proposed a formula for determining the change in tropopause altitude, considering that temperature and pressure at the tropopause are constant, while the vertical temperature gradient undergoes an interruption.

We will designate the tropopause altitude by H_{tp}, and the interruption in the function during the transition through the tropopause by $[f]$. In these designations the formula for the change in tropopause altitude looks like

$$\frac{\partial H_{\tau p}}{\partial t} = -\frac{\left[\frac{\partial T}{\partial t}\right]}{\left[\frac{\partial T}{\partial z}\right]} = \frac{\left[\frac{\partial T}{\partial t}\right]}{[\gamma]}, \qquad (1)$$

where T--temperature,

$\gamma = -\frac{\partial T}{\partial z}$ — vertical temperature gradient.

Thus, by forecasting the temperature in the troposphere and stratosphere, for example, with the help of a numerical model it becomes possible to forecast the tropopause altitude. If in (1) the temperature is expressed through the geopotential from the static equation, then it becomes possible to forecast the tropopause altitude on the basis of forecasting the baric field. In this case formula (1) adopts the appearance

$$\frac{\partial H_{\text{tp}}}{\partial t} = -\frac{gp}{R}\frac{\left[\frac{\partial^2 H}{\partial t\,\partial p}\right]}{[\gamma]}. \qquad (2)$$

By knowing the pressure change (geopotential) in the layers adjacent above and below the tropopause, as well as the temperature change with altitude in these layers, one can compute the tropopause altitude change. In the first approximation the amount $[\gamma]$ can be considered constant and equal to the difference in the standard vertical temperature gradients in the troposphere and stratosphere.

For the practical application of formula (2) it is necessary in some way to approximate the derivatives with respect to the vertical, for example, with the help of finite differences. Another way is to use the statistical approximation formula (2). For this purpose we present the change in tropopause altitude by the change in pressure (geopotential) in the form

$$\frac{\partial H_{\text{tp}}}{\partial t} = C_0 + \sum_{i=1}^{k} C_i \frac{\partial H_i}{\partial t} \qquad (3)$$

or

$$\Delta H_{\text{tp}} = C_0 + \sum_{i=1}^{k} C_i \Delta H_i, \qquad (4)$$

where the symbol Δ designates the change in a certain time interval. The unknown coefficients C_i can be determined by the method of least squares.

For this purpose record radiosonde data for 1974-1975 were used for the Leningrad station for the four main periods for the summer and winter seasons, and for the two main periods for the spring and fall seasons.

Preliminary analysis of the radiosonde data indicated that the tropopause most often (about 80% of the total number of cases) is located between the levels 300 and 200 mbar (here and further by tropopause we will mean the altitude of the lower boundary of the tropopause determined at stations [2]). Further calculations were made precisely for this case.

The C_i coefficients were defined for each season and for different time intervals (for 6-, 12- and 24-hour changes in the tropopause level) from two samplings referring to 1974 and 1975.

At first the coefficients C_i were defined from data for one year, and then a calculation was made of the changes in tropopause level both from the data for this same year (dependent sampling), and from the data for another year (independent sampling). Then the actual and calculated changes in tropopause level were compared with each other, the correlation coefficients r were defined, and the relative error and the error in determining the sign of change in ρ according to the formula

$$\rho = \frac{n_+ - n_-}{n_+ + n_-}. \qquad (5)$$

Here n_+--number of coincidences,
n_- --number of noncoincidences in the sign of physical and calculated changes in the tropopause level.

Further analysis showed that the best results are obtained in an examination of the diurnal changes in the tropopause level. Column A of table 1 presents evaluations of the calculated diurnal changes in tropopause altitude according to the dependent (i.e., that used to compute the corresponding coefficients of the regression equation) and independent samplings for each season. Here N--number of cases used for the calculations. In these

Table 1. Evaluations of Calculated Diurnal Changes in Tropopause Altitude from Data on Change in Surface Altitudes 500, 300, 200 and 100 mbar

(a) Сезон, год (выборка)	N	A			B Б		
		r	ρ	ε	r	ρ	ε
(b) Лето 1974 (зависимая) (f)	223	0,89	0,65	0,46	0,88	0,70	0,47
(b) Лето 1975 (независимая) (g)	238	0,84	0,60	0,57	0.83	0,56	0,58
(c) Зима 1974 (зависимая) (f)	131	0,86	0,68	0,51	0,83	0,63	0,55
(c) Зима 1975 (независимая) (g)	186	0,72	0,58	0,69	0,73	0,54	0,66
(d) Осень 1974 (зависимая) (f)	98	0,87	0,57	0,52	0,87	0,61	0,53
(d) Осень 1975 (независимая) (g)	95	0,78	0,50	0,64	0,76	0,45	0,66
(e) Весна 1974 (зависимая) (f)	89	0,81	0,62	0,54	0,76	0,60	0,62
(e) Весна 1975 (независимая) (g)	114	0,69	0,47	0,72	0,68	0,51	0,73

Key:
a. Season, year (sampling)
b. Summer
c. Winter
d. Fall
e. Spring
f. Dependent
g. Independent

calculations the diurnal geopotential changes were considered for four isobaric surfaces: 100, 200, 300 and 500 mbar. Thus, in this case we are using the value of geopotential changes on two levels located above the tropopause, and on two located below it. This makes it possible to obtain satisfactory approximation of the derivatives with respect to the vertical included in (2). Analysis shows that the results of calculating the tropopause altitude are in satisfactory agreement with the observational data.

The transition from the dependent sampling to the independent does not result in a significant exacerbation of the evaluations.

Since the forecasting of altitude 100 mbar is linked currently to certain difficulties it is important to evaluate how much the results are altered if level 100 mbar is not considered in the calculations. The corresponding evaluations are given in column B of table 1. A comparison of the data in table 1 shows that exclusion of the 100 mbar level practically does not impair the evaluations of the calculated tropopause altitude.

In order to improve the analysis of the regression equation coefficients as a consequence of increasing the volume of the sampling, these coefficients for each season were computed from data for 2 years (1974-1975). The results of calculating these coefficients are given in table 2. Here C_1--coefficient with ΔH_{500}, C_2--with ΔH_{300} and C_3--with ΔH_{200}. This same table also gives evaluations of the calculated diurnal changes in tropopause altitude from dependent samplings, as well as from independent samplings, whereby as the latter samplings were taken for the "opposite" seasons (summer-winter, spring-fall).

Table 2. Results of Calculated Diurnal Changes in Tropopause Altitude from Data for 1974-1975

(1) Сезон (выборка)	N	C_0	C_1	C_2	C_3	r	ρ	ε
(2) Лето (зависимая) (6)	461	−0,42	−7,90	18,47	−7,06	0,86	0,62	0,52
(3) Зима (независимая) (7)	317	—	—	—	—	0,78	0,57	0,63
(3) Зима (зависимая) (6)	317	−0,50	−9,51	18,16	−7,27	0,79	0,54	0,60
(2) Лето (независимая) (7)	461	—	—	—	—	0,85	0,62	0,55
(5) Осень (зависимая) (6)	193	−1,18	−7,32	15,77	−5,81	0,83	0,58	0,58
(4) Весна (независимая) (7)	203	—	—	—	—	0,71	0,55	0,68
(4) Весна (зависимая) (6)	203	−0,89	−6,58	13,65	−2,63	0,72	0,54	0,67
(5) Осень (независимая) (7)	193	—	—	—	—	0,82	0,58	0,64

Key:
1. Season (sampling)
2. Summer
3. Winter
4. Spring
5. Fall
6. Dependent
7. Independent

We will now switch to the question of forecasting the tropopause temperature.

We will present the tropopause temperature changes in the form

$$\Delta T_{\text{тр}} = C_0 + \sum_{i=1}^{k} C_i \Delta H_i. \qquad (6)$$

Also, as in the case with the change in tropopause altitude, the coefficients C_i were determined from the data for one year of any season. Then the diurnal temperature changes in the troposphere were computed both from data for this year (dependent sampling), and from data for another year (independent sampling) of the same season. The results from comparing the actual diurnal temperature changes in the tropopause computed from the diurnal changes in altitudes of the isobaric surfaces 300 and 200 mbar are given in column A of table 3.

Table 3. Evaluations of Calculated Diurnal Temperature Changes in the Tropopause from Data on Changes in Altitudes of Surfaces 300 and 200 mbar (A), 500, 300 and 200 mbar (B), 500, 300, 200 and 100 mbar (C)

(1) Сезон, год (выборка)	N	A			Б B			В C		
		r	ρ	ε	r	ρ	ε	r	ρ	ε
(2) Лето 1974 (зависимая) (6)	223	0,87	0,62	0,49	0,88	0,67	0,48	0,88	0,68	0,48
(2) Лето 1975 (независимая) (7)	238	0,80	0,55	0,60	0,82	0,60	0,58	0,82	0,60	0,58
(3) Зима 1974 (зависимая) (6)	128	0,94	0,73	0,35	0,95	0,75	0,33	0,95	0,77	0,32
(3) Зима 1975 (независимая) (7)	182	0,89	0,75	0,46	0,90	0,77	0,43	0,89	0,70	0,46
(4) Осень 1974 (зависимая) (6)	95	0,89	0,64	0,46	0,90	0,68	0,44	0,91	0,62	0,44
(4) Осень 1975 (независимая) (7)	94	0,86	0,55	0,54	0,88	0,64	0,48	0,89	0,64	0,46
(5) Весна 1974 (зависимая) (6)	89	0,85	0,64	0,52	0,87	0,75	0,49	0,89	0,75	0,46
(5) Весна 1975 (независимая) (7)	112	0,84	0,62	0,57	0,84	0,62	0,58	0,83	0,61	0,58

Key:

1. Season, year (sampling)
2. Summer
3. Winter
4. Fall
5. Spring
6. Dependent
7. Independent

We will attempt to refine formula (6) by increasing the number of levels examined near the tropopause. In column B of table 3 evaluations are given from formula (6) using the diurnal changes in geopotential at levels 500, 300 and 200 mbar; column C gives the analogous evaluations using the data at levels 500, 300, 200 and 100 mbar.

Comparison of the results given in table 3 indicates that addition of the data for the 500 mbar level to the data for levels 300 and 200 mbar somewhat improves the evaluations of the calculated diurnal tropopause temperature changes. This has an especially noticeable effect on the evaluation of ρ. The addition of the data from the 100 mbar level does not result on the average in an improvement in the evaluations. Therefore, appparently, the variant based on the use of data on changes in the surface altitudes 500, 300 and 200 mbar should be considered the optimal.

In order to improve the analysis of the regression equation coefficients by increasing the volume of the sampling these coefficients were computed from the data for both years. The results of the calculations of these

Table 4. Results of Calculated Diurnal Tropopause Temperature Changes from Data for 1974-1975

(1) Сезон (выборка)	N	C_0	C_1	C_2	C_3	r	ρ	ε
(2) Лето (зависимая) (6)	451	0,06	0,315	−1,364	0,984	0,85	0,64	0,52
(3) Зима (независимая) (7)	310	—	—	—	—	0,85	0,64	0,52
(3) Зима (зависимая) (6)	310	0,13	0,218	−1,368	1,082	0,93	0,75	0,38
(2) Лето (независимая) (7)	461	—	—	—	—	0,92	0,75	0,38
(5) Осень (зависимая) (6)	180	0,00	0,336	−1,258	0,865	0,89	0,69	0,45
(4) Весна (независимая) (7)	201	—	—	—	—	0,88	0,66	0,46
(4) Весна (зависимая) (6)	201	0,08	0,202	−1,188	0,896	0,85	0,67	0,53
(5) Осень (независимая) (7)	89	—	—	—	—	0,85	6,67	0,54

Key:
1. Season (sampling)
2. Summer
3. Winter
4. Spring
5. Fall
6. Dependent
7. Independent

Table 5. Evaluations of Forecasts of Isobaric Surface Altitudes, Tropopause Altitude and Temperature

(1) Сезон	(2) Поверхность	N	r	ρ	ε
(3) Лето	H_{500}	21	0,74	0,24	0,82
	H_{300}		0,80	0,33	0,76
	H_{200}		0,76	0,24	0,67
	$H_{тр}$		0,63	0,33	0,88
	$T_{тр}$		0,58	0,33	0,93
(4) Зима	H_{500}	12	0,72	0,33	0,81
	H_{300}		0,78	0,50	0,94
	H_{200}		0,60	0,00	1,41
	$H_{тр}$		0,27	0,33	1,31
	$T_{тр}$		0,57	0,33	0,80
(5) Осень	H_{500}	11	0,24	0,27	1,34
	H_{300}		0,74	0,27	0,90
	H_{200}		0,80	0,46	0,96
	$H_{тр}$		0,59	0,46	0,80
	$T_{тр}$		0,32	−0,09	0,95

Key:
1. Season
2. Surface
3. Summer
4. Winter
5. Fall

coefficients from the data on changes in altitudes of surfaces 500, 300 and 200 mbar are given in table 4. This same table gives the evaluations for calculated diurnal tropopause temperature changes according to dependent samplings, as well as independent samplings, whereby samplings for the "opposite" seasons are used as the latter.

Analysis of the results given in table 4 shows that the coefficients of the regression equations computed from data for any season "work" well in the other seasons as well. Apparently, for practical use it is sufficient to compute the coefficients only for any one season or to use coefficients computed from data for all four seasons together with those in question.

All the results given above were based on actual diurnal changes in the isobaric surface altitudes. It was important to evaluate the possibility of using the proposed technique on the forecasting material. As the forecasting model to determine diurnal changes in the isobaric surface altitudes 200, 300 and 500 mbar a six-level model developed in the Main Geophysical Observatory and efficiently employed in the Northwest UGMS [Administration of Hydrometeorological Service] was used [1,3]. With the help of this model forecasts were obtained for the altitudes of the indicated isobaric surfaces for the Leningrad station from data for 1974-1975 (for summer--21 forecasts, for winter--12 forecasts, for fall--11 forecasts). From these forecasting data with the use of the corresponding coefficients of the regression equations given in tables 2 and 4 forecasts were obtained for the tropopause altitude and temperature for the Leningrad station.

The results of the evaluations of forecasts AT_{500}, AT_{300} and AT_{200}, and the forecasts of tropopause altitude and temperature according to the suggested technique are given in table 5.

The evaluations given in table 5 show that the forecast of altitude and temperature of the tropopause according to the proposed technique have forecasting significance when the forecasting of the altitude of the isobaric surfaces is satisfactory.

BIBLIOGRAPHY

1. Bushkova, T. A., et al. "Description of the Scheme for a Numerical Analysis and Forecasting Efficiently Used in the Northwest UGMS," TRUDY GGO, No 353, 1975.

2. "Kod dlya peredachi dannykh vertikal'nogo zondirovaniya atmosfery" [Code for the Transmission of Data of Vertical Sounding of the Atmosphere] KN-04, Leningrad, Gidrometeoizdat, 1971.

3. Rukhovets, L. V. "Multiple-level Forecasting Model for the Geopotential Field Based on a Small Number of Parameters," TRUDY GGO, No 151,1964.

4. Rukhovets, L. V. "Reasons for the Change in Tropopause Altitude," TRUDY GGO, No 124, 1962.

UDC 551.574.12:661.185

EFFECT OF SURFACE-ACTIVE SUBSTANCES ON DROPLET GROWTH AND EVAPORATION

Moscow METEOROLOGIYA I GIDROLOGIYA in Russian No 5, May 79 pp 41-48

[Article by Candidates of Physical and Mathematical Sciences V. A. Borzilov, and N. V. Klepikova, V. M. Merkulovich, Institute of Experimental Meteorology, submitted for publication 11 Jul 78]

Abstract. The linear dependence of the water vapor condensation coefficient on the degree of filling of a monolayer of surface-active substance is suggested. It is demonstrated that such simulation makes it possible to explain the experimental data on evaporation of a passivated droplet.

[Text] One of the possible methods for actively affecting the microstructure of clouds and fog is the use of surface-active substancse (SAS), in particular cetyl alcohol (CA) in order to retard the condensation growth (evaporation) of droplets. Initially the effect of SAS on the processes of evaporation and condensation were studied for flat water surfaces, and only after publication [9] where it was suggested that SAS be used to passivate the nuclei of condensation, was an active investigation begun of the effect of SAS on the rate of growth or evaporation of individual droplets or their collectives [1-8, 10, 11, 13, 18, 19].

Publication [6] has suggested, and subsequent works have developed a model for the effect of SAS on the indicated processes. Briefly this model can be formulated as follows. The SAS molecules are adsorbed on the water surface and form a monomolecular film that prevents the penetration of water molecules from vapor into liquid and vice versa. Until the degree of filling of the monolayer exceeds a certain threshold value, the presence of the SAS does not affect the velocity of the phase transitions. Assume $z=\Gamma/\Gamma_0$ is the degree of filling of the monolayer (Γ --surface concentration of adsorbed SAS molecules, Γ_0--maximum possible surface concentration). Then the coefficient of vapor condensation on the surface modified by SAS, $\alpha_1(z)$ is linked to the degree of filling of the monolayer by the correlation

$$\alpha_1(z)=\begin{cases}\alpha_w \text{ with } z<z_n\\ \alpha_a \text{ with } z\geqslant z_n,\end{cases} \quad (1)$$

where α_w--condensation coefficient for clean water.

In this same work,based on experimental data [16] the value z_n=0.976 was found, and in publications [8,13] it was determined that α_a=3.5·10^{-5} for CA. Such simulation of the relationship $\alpha_1(z)$ makes it possible to describe the experimentally observed [8] fairly drastic change in the droplet evaporation rate with z close to a unit. From (1) is also follows that there are critical conditions for the amount of oversaturation of water vapor and density of SAS vapor in which passivation of the growth of cloud droplets is possible [1, 3, 11].

In our opinion, the introduction of the spasmodic behavior of $\alpha_1(z)$ has little substantiation from the physical viewpoint. In this work another approach is suggested for considering the effect of SAS on the rate of growth (evaporation) of droplets to explain the extant experimental material, without resorting to postulation of a jump in the condensation coefficient. At the same time it will be shown that the possibility exists for a noticeable passivation of small drops with any values of z. Recommendations will also be given for the conducting of the corresponding experimental studies. In addition, requirements will be formulated for the experiments to determine the ratio of rates of adsorption and desorption on which the kinetics of the SAS monolayer formation on the droplet surface significantly depends.

1. We will examine the stationary problem of evaporation from a flat water surface in the presence of an SAS monolayer with degree of filling z. The stream of water vapor j from surface S is determined by the expression

$$j=\beta S(C-C_\infty), \quad (2)$$

where C, C_∞--concentration of water vapor at surface and far from it respectively, β--coefficient of mass transfer determined by the geometry of the problem. On the other hand, based on the kinetic considerations [15] the stream of vapor can be written in the form

$$j=-\frac{1}{4}V_TS\left\{\alpha_w\left[(1-z)+ze^{-\frac{U_a}{kT}}\right]C-\left[(1-z)e^{-\frac{U}{kT}}+ze^{-\frac{U+U_a}{kT}}\right]C_0\right\}, \quad (3)$$

where V --thermal velocity of water molecule,
k--Boltzmann constant,
T--absolute temperature,
U--energy of water molecule bond with water surface,
U_a--work of transition of water molecule through monolayer,

C_0--concentration of water molecules in liquid phase.*

By exluding C from (2) and (3) we find that

$$j = \frac{C_s - C_\infty}{\frac{1}{\beta S} + \frac{4}{V_T S \alpha_2(z)}}, \qquad (4)$$

where $C_s = C_0 e^{-\frac{U}{kT}} \cdot \frac{1}{\alpha_w}$ --concentration of saturated water vapor above the flat surface of clean water.

The following designation is introduced into formula (4)

$$\alpha_2(z) = \alpha_w (1 - z) + \alpha_a z, \quad \alpha_a = \alpha_w e^{-\frac{U_a}{kT}}. \qquad (5)$$

In physical meaning the amount $\alpha^2(z)$ introduced by formula (5) is a condensation coefficient of water vapor on water surface covered with a monolayer of SAS with degree of filling z. In contrast to the condensation coefficient determined by expression (1) the introduced coefficient $\alpha^2(z)$ is a linear function of z. Actually this means that the exchange of molecules through the surface S(1-z) occurs with condensation coefficient α_w, while through surface Sz--with coefficient α_a. Such a description is to a certain degree a model, therefore relationship $\alpha_2(z)$ in form (5) can serve only as the first approximation.

It would seem that the proposed linear relationship $\alpha_2(z)$ must contradict the experimental data of Barnes and La Mer [16]. This work measured the dependence of r--resistance of the monolayer to evaporation--on the amount of surface pressure of the monolayer F. A characteristic feature of the relationship r(F) is the presence of bend. Precisely as a consequence of this fact B. V. Deryagin and Yu. S. Kurgin [6] proposed modeling $\alpha_1(z)$ in the form of (1).

Under the experimental conditions of Barnes and La Mer the resistance of the monolayer to evaporation is linked to the coefficients α_w and $\alpha_i(z)$ by the correlation (i=1,2)

$$r_i(z) = \frac{4}{V_T}\left(\frac{1}{\alpha_i(z)} - \frac{1}{\alpha_w}\right). \qquad (6)$$

By substituting (1) and (5) in correlation (6) we obtain

---

*Generally speaking, in front of the right side of expression (3) the coefficient $\varkappa$ should stand which alters from 1 to 2 during the transition from the diffuse pattern of evaporation to the kinetic. For simplicity we will consider that $\varkappa$=1.

$$r_1(z) = \begin{cases} 0 & \text{with } z < z_n \\ \frac{4}{V_T}\left(\frac{1}{a_a} - \frac{1}{a_w}\right) & \text{with } z \geq z_n \end{cases}, \quad (7)$$

$$r_2(z) = \frac{4}{V_T}\left(\frac{1}{a_a} - \frac{1}{a_w}\right)\frac{z}{\frac{a_w}{a_a} + \left(1 - \frac{a_w}{a_a}\right)z}. \quad (8)$$

From correlations (7) and (8) it follows that

$$r_1(1) = r_2(1) = \frac{4}{V_T}\left(\frac{1}{a_a} - \frac{1}{a_w}\right) \equiv r_m. \quad (9)$$

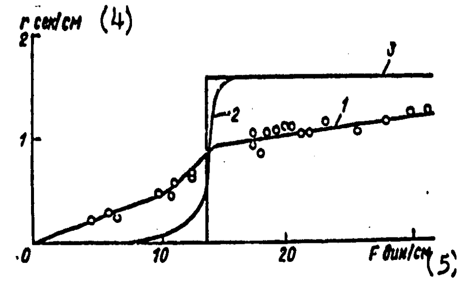

Figure 1. Dependence of Resistance of Evaporation Monolayer on Surface Pressure

Key:
1. experimental data [16]
2. $r_2(F)$
3. $r_1(F)$
4. sec/cm
5. dyne/cm

The amount r determines the maximum resistance of the monolayer to evaporation. For the calculations we will assume that the distribution of water molecules with respect to velocities is subject to the Maxwell distribution. This apparently is a rough assumption, however its denial would result in the need to solve the kinetic equation. This means that the theoretical value of r_m can differ from the experimentally observed maximum value of resistance of the monolayer.

For comparison of $r_1(z)$ and $r_2(z)$ with the experimental data [16] it is necessary to establish a link between z and F. For this purpose we will use the results of publication [17] which measured the dependence of F on σ--areas for one molecule of CA in the monolayer ($z = \frac{\sigma_0}{\sigma}$, σ_0--minimum possible value of σ). From the form of functions $r_1(z)$, $r_2(z)$ and $F(\sigma)$ ($\frac{dF}{d\sigma} < 0$; $\frac{d^2F}{d\sigma^2} > 0$) it follows that the relationship $r_1(F)$ has the appearance of a "step" (interruption of the first type), while $r_2(F)$--monotonically increasing function with bend. The possible experimental errors in determining $F(\sigma)$ and σ_0 result in a modification of curves $r_1(F)$ and $r_2(F)$. At the same time the change in the amount σ_0 shifts the point of rupture in the relationship $r_1(F)$ and the bending point in curve $r_2(F)$. The function $r_1(F)$ is not sensitive to the type of relationship $F(\sigma)$, while the curve $r_2(F)$ becomes more gently sloping in the region of the bend with a growth in $\left|\frac{dF}{d\sigma}\right|$.

Figure 1 depicts the functions $r_1(F)$ and $r_2(F)$ (σ_0=20.5 Å² [6]). It is apparent on figure 1 that function $r_1(F)$ differs insignificantly from $r_2(F)$. Consequently, the relationship $r(F)$ has low sensitivity to the type of function $\alpha_1(z)$, and the results of the experiment [11] cannot serve as the basis for the selection of relationship $\alpha_1(z)$.

2. In the case of growth (evaporation) in a droplet the coefficient of mass transfer equals $\beta = D/R$ (D--coefficient of molecular diffusion of water vapor, R--radius of drop). By using correlation (4) we obtain an expression for the rate of growth of a single droplet [14]

$$\dot{R}(R, z) = \frac{D\delta}{R + \lambda/\alpha_l(z)}, \tag{10}$$

where δ--oversaturation of water vapor, $\lambda = 4D/V_T$.

In a number of publications [1,8,13] an experimental study was made of the change with time in the size of a droplet passivated by SAS. Thus, in [8] a 300 μ droplet was kept for a certain time in CA vapors. Then it was evaporated with constant incomplete saturation. The experiments showed that at first the radius of the drop with time was altered according to the law $\frac{dR^2}{dt}$ = const, and then $\frac{dR}{dt}$ =const. From the viewpoint of the model proposed in publication [6] (formula (1)), such behavior of the droplet radius with time is explained by the fact that at first the CA monolayer has the degree of filling $z<z_\Pi$. With a reduction in the droplet surface the degree of filling is increased, and at that moment when z becomes equal to z_Π the condensation coefficient $\alpha_1(z)$ is reduced in a jump. Since $\frac{\lambda}{\alpha_a} \gg R \gg \frac{\lambda}{\alpha_w}$, then a sharp transition occurs from the diffusion pattern of evaporation to the kinetic.

We will examine these experimental data from the viewpoint of the proposed model. It follows from formulas (5) and (10) that evaporation will occur in a kinetic pattern if

$$(1 - z) \ll \left(\frac{\lambda}{\alpha_a R} - 1\right) \Big/ \left(\frac{\alpha_w}{\alpha_a} - 1\right) = \frac{\lambda}{\alpha_a R}\left(1 + O\left(\frac{\alpha_a}{\alpha_w}\right) + O\left(\frac{\alpha_a R}{\lambda}\right)\right). \tag{11}$$

If $R \gg \frac{\lambda}{\alpha_w}$, then the effect of the monolayer on evaporation (growth) of the droplet is important only with high degrees of filling. However, if

$R \sim \frac{\lambda}{\alpha_w}$ $\left(\frac{\lambda}{\alpha_w} \approx 0.12\right.$ µm with $\alpha_W = 1$ and $\frac{\lambda}{\alpha_W} = 3.3$ µm with $\alpha_W = 0.036$) then the monolayer will have a noticeable influence on the rate of condensation growth (evaporation) of drops with arbitrary degrees of filling. Assume that $f(R, z) = \dot{R}(R, z)/\dot{R}(R, 0)$. Then, if the condensation coefficient $\alpha_1(z)$ is determined by formula (1), then

$$f_1(R, z) = \begin{cases} 1 & \text{with } z < z_n \\ \dfrac{1+\frac{\lambda}{\lambda_n R}}{1+\frac{\lambda}{\alpha_w R}} & \text{with } z \geq z_n \end{cases} \qquad (12)$$

In the suggested approach (formula (5))

$$f_2(R, z) = \frac{1+\frac{\lambda}{\alpha_2(z) R}}{1+\frac{\lambda}{\alpha_w R}}. \qquad (12')$$

Figure 2 illustrates the relationships $f_1(z)$ and $f_2(z)$ for different R. As is apparent from the figure, for large R these relationships converge. However, if $R \sim \frac{\lambda}{\alpha_W}$, then the behavior of functions (12) and (12') varies.

Thus, the effect of SAS monolayers on the condensation growth (evaporation) of drops in the proposed model practically does not differ from the model of B. V. Deryagin and Yu. S. Kurgin [5] with $R \gg \frac{\lambda}{\alpha_W}$. But with $R \sim \frac{\lambda}{\alpha_W}$ redetermination of the dependence of the condensation coefficients on the degree of filling results in a significantly different result. This circumstance is extremely important from the viewpoint of using SAS in order to actively influence the microstructure of clouds and fog, since condensation (evaporation) of the vapor is a decisive mechanism in the formation of drop spectra in the region where the drop radii do not exceed 20-30 µm. And for active effects in order to prevent radiation fog the most important region of droplet sizes is the region from tens of fractions of a micrometer to micrometers.

This same circumstance (difference in the behavior of $f_1(R,z)$ and $f_2(R,z)$ with $R \sim \frac{\lambda}{\alpha_W}$ and z far from 1) can be used to experimentally verify the proposed model. For this studies should be made that are analogous to those described in publication [13]. But here it is necessary to either significantly (to seconds) reduce the time for preliminarily keeping the droplet in the CA vapors, or keep the droplet in a low density of CA vapors since according to the results of publication [8] the characteristic time for monolayer formation on the micron droplet is on the order of 10 seconds with saturated CA vapors.

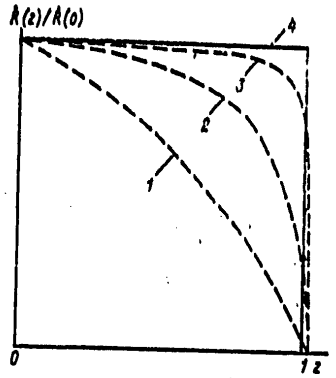

Figure 2. Dependence of $\dot{R}(z)/\dot{R}(0)$ on Degree of Filling of Monolayer

Key:

1,2,3. $f_2(R,z)$ ($R=0.1\mu$, 1μ, 10μ respectively, $\alpha_w=1$)
4. $f_2(R,z)$

It should be noted that in publication [12] a reduction in the rate of evaporation of small droplets with low degrees of filling of the monolayer of isoamyl alcohol was experimentally observed. This fact can be viewed as direct experimental confirmation of the proposed model.

Due to the fact that in this model it is suggested that the threshold degree of filling not be introduced the question arises of critical oversaturation. By definition [6, 11] the critical oversaturation is that maximum oversaturation of water vapors at which the surface of the droplet grows such that CA adsorption guarantees the existence of a monolayer with degree of filling z_n.

As was already mentioned, if $R \gg \frac{\lambda}{\alpha_w}$ then the transition from the diffusion pattern of evaporation (growth) of droplets to the kinetic occurs in a narrow region of change in z $\left(z \in \left(1, 1 - \frac{\lambda}{\alpha_w R}\right)\right)$, which permits a certain analog z_n to be introduced, and as a consequence of this, critical oversaturation. But with $R \sim \frac{\lambda}{\alpha_w}$ such an analog cannot be introduced and the concept of critical oversaturation loses meaning.

3. For the mathematical modeling of the SAS effect on droplet growth it is necessary to know the constants that determine the kinetics of SAS monolayer formation on the surface of a water droplet. One of these constants is ℓ--the ratio of adsorption and desorption. In order to determine this amount publication [8] used the link between the degree of filling of a monolayer and the time for holding in the CA vapors

$$z - \frac{\varepsilon}{1+\varepsilon} \ln |1 - (1+\varepsilon) z| = \frac{t}{t_0} (1+\varepsilon),$$

$$\varepsilon = \frac{1}{l \rho_v}, \quad t_0 = \frac{D' \rho_v}{\delta \rho_c R}, \qquad (13)$$

where ρ_v --density of CA vapors in space,
D'--coefficient of molecular diffusion of CA vapors,
ρ_c--density of condensed CA,
δ--thickness of adsorption monolayer.

The correlation (13) is correct on the condition that $R \gg \frac{4D'}{V_T'}$ (V_T' --thermal velocity of CA molecules). From the experimental data in publication [8] the z values were computed depending on the time for holding in the CA vapors. Then parameter l was selected such that the obtained z values would best be described by correlation [19]. It is evident that the relative change in the degree of filling of the monolayer $\Delta z/z$ is linked to the relative $\Delta l/l$ by the correlation

$$\frac{\Delta z}{z} = \frac{l}{z} \frac{\partial z}{\partial l} \frac{\Delta l}{l}. \qquad (14)$$

At the same time if $A \equiv \frac{l}{z} \frac{\partial z}{\partial l} \ll 1$, then, first, the relationship $z(t)$ has low sensitivity to changes in l, and second, the experimental errors in determining z result in great relative errors in determining l. It follows from correlation (13) that

$$A(\omega, \varepsilon) = \frac{\varepsilon}{(1+\varepsilon)(\varepsilon+\omega)} \left[\varepsilon - \omega + (1-\omega) \frac{\ln \omega}{\omega - 1}\right],$$

$$\omega = 1 - \frac{z}{z_*}, \quad z_* = \frac{1}{1+\varepsilon}, \qquad (15)$$

where z_*--maximum possible degree of monolayer filling with the given density of CA vapors.

It can be shown that the function $A(\omega, \varepsilon)$ with fixed ε has the maximum at point ω_0, whereby

$$A(\omega_0, \varepsilon) = \frac{(1-\omega_0)(\varepsilon+\omega_0)\varepsilon}{(1+\varepsilon)(\varepsilon+\omega_0^2)}. \qquad (16)$$

The value ω_0 is defined by the transcendental equation

$$\frac{\ln \omega_0}{1-\omega_0} - 1 = \frac{(\omega_0 - 1)(\omega_0 \varepsilon - \omega_0 - 2\varepsilon)}{(\varepsilon+\omega_0^2)(1-\varepsilon)}. \qquad (17)$$

Here $A(\omega_0, \varepsilon) > \frac{\varepsilon}{1+\varepsilon}$ in the region of $\omega_0 \in \left(0, \frac{1-\varepsilon}{2\varepsilon}\right)$. With $\omega_0 \in \left(\frac{1-\varepsilon}{2\varepsilon}, 1\right)$ $A(\omega_0, \varepsilon)$ monotonically drops from $\frac{\varepsilon}{1+\varepsilon}$ to zero. The maximum error $\Delta l/l$ in determining l is reached with the maximum value of A. It follows from formula (16) that $A(\omega_0, \varepsilon) \leqslant A_0$, where

$$A_0 = \frac{\sqrt{\varepsilon}(1+\varepsilon)}{2(1+\varepsilon)-4\sqrt{\varepsilon}}. \tag{18}$$

The experimental relationships z(t) in [8] were obtained with $\rho_{v_1} = 1.4 \cdot 10^{-10}$ g/cm³ and $\rho_{v_2} = 1.4 \cdot 10^{-11}$ g/cm³. If $l \sim 10^{12}$, then $A_0(\rho_{v_1}) \approx 0.05$ and $A_0(\rho_{v_2}) \approx 0.25$. Consequently, in the first case the relative error in determining l is roughly 20 times greater than the error in determining z, and in the second case--4 times.

It should be noted that these evaluations are correct only in a narrow range of change in z where both components in the left side of correlation (13) have comparable values. Outside this region $A(\omega, \varepsilon)$ a fortiori is smaller than A_0. This means that for a more precise determination of l it is necessary, first, to have many experimental values of z in the region where

$$z \sim -\frac{\varepsilon}{1+\varepsilon} \ln|1-(1+\varepsilon)z|, \tag{19}$$

and second, the experiments should be carried out by keeping the droplet in CA vapors with low density in order for ε to be the largest possible.

Publication [8] has found experimentally that with $\rho_v = 1.4 \cdot 10^{-12}$, $7 \cdot 10^{-12}$, $1.4 \cdot 10^{-11}$ g/cm³ the value of z_* that did not grow with a further increase in the degree of adsorption equals respectively 0.46; 0.76 and 0.88. Since

$$l = \frac{1}{\rho_v} \frac{z_*}{1-z_*}, \tag{20}$$

then we obtain $l = 0.6 \cdot 10^{12}$; $0.45 \cdot 10^{12}$; $0.52 \cdot 10^{12}$. This means that the amount l (for which the value $0.8 \cdot 10^{12}$ is adopted on the basis of these experiments) needs refinement.

In conclusion the authors express their gratitude to A. S. Stepanov for useful discussions.

BIBLIOGRAPHY

1. Bakhanova, R. A., et al. "Study of the Conditions Determining the Passivating Action of Surface-Active Substances on the Hygroscopic Nuclei of Condensation," "Trudy V Vsesoyuznogo meteorologicheskogo s"yezda"

[Proceedings of Fifth All-Union Meteorological Congress], Vol 4, Moscow Gidrometeoizdat, 1973, pp. 146-164.

2. Deryagin, B. V.,; Bakanov, S. P.; and Kurgin, Yu. S. "Effect of Monolayers on Droplet Evaporation," DOKLADY AN SSSR, Vol 135, No 6, 1960, pp 1417-1420.

3. Deryagin, B. V.; and Kurgin, Yu. S. "Nonstationary Evaporation of Droplet Covered with Adsorption Layer," DOKLADY AN SSSR, Vol 155, No 3, 1964, pp 644-646.

4. Deryagin, B. V.; and Kurgin, Yu. S. "Study of Passivating Action of Cetyl Alcohol Vapors on Condensation Growth of Fog Droplets," DOKLADY AN SSSR, Vol 192, No 3, 1970, pp 1067-1070.

5. Deryagin, B. V.; and Kurgin, Yu. S. "Theory of Passivation of Growth of Aqueous Fog Droplets," FIZIKA AERODISPERSNYKH SISTEM, No 4, 1971, pp 21-32.

6. Deryagin, B. V.; and Kurgin, Yu. S. "Theory of Passivation of Condensation Growth of Fog Droplets by Cetyl Alcohol Vapors," KOLLOIDNYY ZHURNAL, Vol 34, No 1, 1972, pp 36-42.

7. Deryagin, B. V.; and Kurgin, Yu. S. "Question of the Pasivation of Condensation Growth of Large Drops," DOKLADY AN SSSR, Vol 216, No 5, 1974, pp 1087-1090.

8. Deryagin, B. V.; Fedoseyev, V. A.; and Rozentsvayg, L. A. "Study of the Adsorption of Cetyl Alcohol Vapors and its Effect on Evaporation of Water Droplets," DOKLADY AN SSSR, Vol 167, No 3, 1966, pp 617-620.

9. Izmaylova, G. I.; Prokhorov, P. S.; and Deryagin, B. V. "Possibility of Surface Activation and Passivation of Nuclei in Condensation of Water Vapors," KOLLOIDNYY ZHURNAL, Vol 19, No 5, 1957, pp 556-561.

10. Leonov, L. F., et al. "Passivation of Nuclei of Sodium Chloride Condensation by Cetyl Alcohol Vapors," FIZIKA AERODISPERSNYKH SISTEM, No 5, 1971, p 7-11.

11. Leonov, L. F.; Prokhorov, P. S.; and Malikov, B. A. "Conditions for Preserving the Screening Action of Monolayers of Surface-Active Substances on Water Droplets Growing in an Oversaturated Medium," KOLLOIDNYY ZHURNAL, Vol 39, No 3, 1977, pp 460-465.

12. Leonov, L. F.; and Prokhorov, P. S. "Effect of Surface-Active Substances on Evaporation of Small Water Droplets," IZVESTIYA AN SSSR. SERIYA KHIMICHESKAYA, No 4, 1967, pp 735-742.

13. Rozentsvayg, L. A.; Deryagin, B. V.; Fedoseyev, V. A. "Effect of Monolayer of Cetyl Alcohol on Condensation Growth of Droplets of Aqueous Solutions," DOKLADY AN SSSR, Vol 176, No 3, 1967, pp 635-638.

14. Sedunov, Yu. S. "Fizika obrazovaniya zhidkokapel'noy fazy v atmosfere" [Physics of Formation of Liquid Drop Phase in the Atmosphere], Leningrad, Gidrometeoizdat, 1972, 207 p.

15. Frenkel', Ya. I. "Statisticheskaya fizika" [Statistical Physics], Moscow-Leningrad, Izd-vo AN SSSR, 1948, 760 p.

16. Barnes, G. T.; and La Mer, V. K. "The Evaporation Resistances of Monolayers of Long-Chain Acids and Alcohols and their Mixtures. Retardation of Evaporation by Monolayers: Transport Processes," ed. by La Mer, 1962, A. P. N. W. L.

17. Miller, X. H.; and Bavly-Lus, A. "Some Physical Properties of Monolayers and Their Relation to Evaporation Retardation," IBID, pp 158-165.

18. Podsimek, J.; and Saad, A. N. "Retardation of Condensation Nuclei Growth by Surfactant," J GEOPHYS RES, Vol 80, No 24, 1975, pp 3386-3392.

19. Warner, J.; and Warne W. G. "The Effect of Surface Films in Retarding the Growth of Condensation of Cloud Nuclei and Their Use in Fog Suppression," J APPL METEOROL, Vol 9, No 4, 1970, pp 639-650.

UDC 551.576.2(267)

SPECTRAL ANALYSIS OF CLOUD COVER OVER INDIAN OCEAN BASIN

Moscow METEOROLOGIYA I GIDROLOGIYA in Russian No 5, May 79 pp 49-56

[Article by A. V. Kislov, and Candidate of Geographical Sciences Ye. K. Semenov, Moscow State University, submitted for publication 2 Jun 78]

Abstract. The application of a spectral analysis to the time series of cloud cover of five-degree squares over the Indian Ocean basin made it possible to ascertain that fluctuations of two scales are characteristic: synoptic lasting 3-6 days, and global lasting 14-21 days. It was established that fluctuations in the synoptic scale cloud cover are linked to tropical cyclogenesis, while the global fluctuations are linked to the activity of processes in the ITCZ and polar front. With the help of cross-spectral analysis it was ascertained that large-scale cloud cover pulsations (14-21 days) occur simultaneously over the entire territory encompassed by monsoon circulation.

[Text] The Indian Ocean basin is one of the most important and unique regions of the earth in the meteorological respect. Here the general planetary circulation processes are actively influenced by the unique distribution of land and sea, resulting in the emergence of specific large-scale processes in the atmosphere and ocean. First of all this is the monsoon, a large-scale disturbance in the tropical atmosphere. Similar phenomena are known also in other regions of the Tropics, but nowhere do they attain such intensity and coverage.

The investigation of the Indian Ocean tropicl zone has a number of difficulties since the network of stations is arranged only on the coast and on infrequent islands, and is lacking over extensive regions. The observations made during expenditions on scientific research ships are occasional and cover a limited territory. Practically the only source of global meteorological information is the distribution of the cloud cover obtained from meteorological earth satellites that we have used in this work. Spectral analysis was selected as the research method.

The region of the Indian Ocean tropics was divided into five-degree squares (from 30 to 110° e.l. and from 30° s.l. to 30° n.l.). For each square for each day the cloud cover was found (in fractions of a unit). This amount was determined visually from the data of television images of clouds obtained from the ESSA-9 satellites [7,8]. These television images were obtained at different times for the territory since the satellite trajectories are such that over each point on the earth's surface the satellite is at the local noon. Thus, in the studied region the points that are the extreme in longitude always differ by 4 h. But since we used the data with discreteness of 1 day, this discrepancy could be ignored, and it could be considered that the information is synchronous over the entire territory. It was necessary to reveal the accuracy with which the cloud cover is determined in the five-degree squares, and to determine whether large systematic errors develop due to the visual processing. For this purpose the same material was processed by different individuals and the findings of each were compared. It was found that the error is roughly 15% so that the recovery of information with accuracy to 0.1 is justified.

It should be noted that on the television photographs presented in catalogues [7,8] only significant cloud formations are visible that are linked to large-scale processes. Thin clouds of the tradewind type are not noticeable; in this case the impression of cloudless conditions is created. Thus, from the very beginning a certain "filtering out" of the cloud cover that is not associated with disturbances occurs.

For each five-degree square series were obtained of 180 numbers each for the warm (from 1 April to 31 September 1971) and cold (from 1 October 1971 to 29 March 1972) periods. We had a total of 384 series of 180 numbers each, that is about 70,000 numbers.

In order to study the processes whose duration fluctutated from several days to a month it was necessary to filter out the low-frequency oscillations. This also permits an improvement in the evaluation of the obtained statistical characteristics. A cosine-filter was used to filter out oscillations with periods (T) exceeding 52 days. But since the filter is not ideal, it introduces certain distortions into the processes whose periods are close to 52 days. Therefore we will only examine oscillations with $T < 30$ days; it is natural to take the short-wave boundary of the spectrum as equal to 2 days. After filtering we obtained series in which the summer (or winter) months are completely included, while the spring and fall are also partially covered. The algorithm for the calculated functions of spectral density and the cross-spectrum is based on the iteration process of computing the Fourier coefficients of even and odd components of this series (Kula-T'yuka method). The simplest realization of this method is obtained when the number of terms in the series is a power of the number 2 [3]. In our case the length of the series is $128=2^7$.

Such worksusing the spectral analysis of time series of the cloud cover are very labor intensive, therefore there are few of them [11, 12] The Pacific Ocean tropics were selected as the region of study in order to exclude as much as possible the influence of continents on the atmospheric processes. One of the authors fulfilled analogous work for the Atlantic Ocean tropics [1].

Analysis of the spectral density function computed for each five-degree square made it possible to reveal that the most characteristic, first, are cloud cover oscillations with period from 14 to 21 days, second, a considerable part of the dispersion occurs also in the range from 3 to 6 days. The separation of the processes only into two classes is justified also because the existence in the atmosphere of processes with very close frequencies is not very likely. Publications [11, 12] have attempted to isolate several harmonics in the spectrum, but they did not succeed in making any physical interpretation of them.

According to the data of a number of researchers [9,10] in the period of the Indian monsoon quasiperiodically (with a period of about 2 weeks) changes occur in the intensity of the Tibetan and South Indian Ocean anticyclones, the monsoon trough over Hindustan, the meridional tropospheric jet stream, and others. The fluctuations we found in the cloud cover with T=14-21 days are undoubtedly linked to these fluctuations in the entire system of monsoon circulation. Following the classification proposed by A. S. Monin [4] we will further call the fluctuations with T=14-21 days global, while it is natural to group the processes with T=3-6 days with the so-called synoptic-scale atmospheric processes.

As the amount characterizing the intensity of the occurring processes dispersion was selected that occurs in the frequency interval corresponding to the synoptic (D_c) and global (D_r) processes. The calculations showed that these are amounts of one order, while together they exhaust 90-95% of the total dispersion. Figure 1 presents maps of D_r and D_c for the warm and cold periods.

Thus, the application of the spectral analysis methods to an investigation of general atmospheric circulation disturbances (such as monsoons for example) that are manifest in the large-scale variability in the cloud cover makes it possible to approach from a new viewpoint the question of the mechanism for the actual monsoon and its place in the general atmospheric circulation.

Analysis of the dispersion maps for global and synoptic scale atmospheric processes is made separately for the periods of the summer and winter monsoons.

In summer of the Northern Hemisphere over the Indian Ocean basin three regions of the maximum activity of global-scale atmospheric processes are clearly isolated (fig 1,a). The most significant region occupies almost all of Hindustan, separating here into two regions: northern--with the maximum along 20-25° n.l, and southern with maximum along 6-12° n.l. The separation of the maximum values of D_r into two centers is a reflection of the seasonal dynamics of monsoon development. Thus, in April 1971 in the premonsoon period the cloud accumulations in the northern branch of the ITCZ were concentrated over the southern water areas of the Arabian Sea and the extreme south of Hindustan. In the middle of May (15th-20th) an outbreak of the monsoon was observed, that is the rapid advance of the cloud systems of the northern ITCZ branch to the north of India. From June to

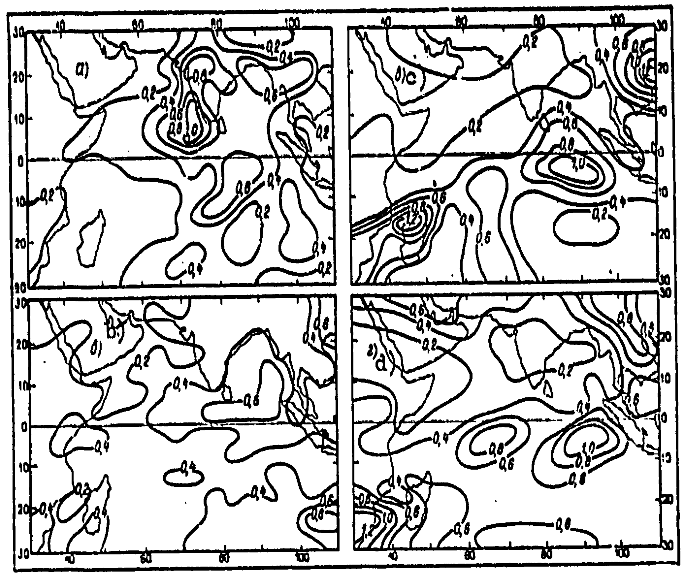

Figure 1. Distribution of Cloud Cover Dispersion in Summer (a,b) and Winter (c,d) of the Northern Hemisphere in Intervals of Fluctuations with Periods of 14-21 Days (a,b) and 3-6 Days (c,d)

August a so-called active monsoon period was established. In fall, in September, just as rapid a retreat of the monsoon from the foot of the Himalayas to the south of Hindustan and the Bay of Bengal took place. Thus, an undoubted coincidence was observed between the regions of localization of the maximum values of D_r with the mean position of the cloud cover of ITCZ in the summer and transitional seasons determined by one of the authors [6]. Here the southern center of the maximum D_r values reflects the activation of processes on the northern ITCZ branch in the premonsoon period and in the period of monsoon retreat, while the northern maximum is a consequence of the activity of the processes at the height of the monsoon.

The second region of large D_r values stretches along the northern water area of the Bay of Bengal, through northern Indochina to the coast of the East China Sea. The Indochinese section of the cloud cover in the northern ITCZ branch occurs precisely over these regions in the summer monsoon period [5].

The separation of the northern ITCZ branch into the Hindustan and Indochinese sections, apparently, is not characteristic merely for the summer monsoon of 1971. As a rule, in the northern summer the most intensive cloud formation occurs precisely in two regions: first, in the eastern section of the

Arabian Sea and in northern Hindustan, and second, in the northern Bay of Bengal and over the Indochinese peninsula. The genesis of the air masses participating in the cloud formation also differs. In the first region this is air brought in by the southwest monsoon from the western and southern water areas of the Indian Ocean, while in the second region air masses participate in the convergence from the extreme eastern Indian and western Pacific Oceans.

The third region of maximum D_r values is located in the Southern Hemisphere and is a consequence of the activity of processes in the southern ITCZ branch. Attention is drawn to the meridional extension of the region of maximum dispersion values. This also can be explained by the seasonal migration of the southern ITCZ branch, and precisely: in April the ITCZ axis still occupies a position the farthest to the south from the equator, and in July it is the closest to the equator. Therefore the region of maximum D_r values confined to the ITCZ is extended. Its localization only in the central section of the Indian Ocean apparently is a peculiarity precisely of 1971.

As is apparent from fig 1,a the amount and region of spread of the greatest D_r values in the Southern Hemisphere are noticeably inferior to the analogous D_r characteristics in the Northern. This indicates that the atmospheric processes in the summer hemisphere occur more intensively than in the winter.

The confinement of the regions of maximum D_r amounts to the regions of ITCZ cloud accumulations permits the assumption that the intensity of the processes resulting in convergence of macro-scale currents in the lower atmospheric layers changes with periodicity of 2-3 weeks, eliciting, in turn, significant changes in the thermal balance of both the atmosphere and the underlying surface since the variability in cloud cover results in variations in the latent heat and fluctuations in the radiation streams.

In addition to the regions of high D_r values figure 1,a clearly traces the regions with low variability in the cloud cover as a consequence of the activity of atmospheric processes. This is primarily the Arabian peninsula, the eastern coast of Africa and the western water areas of the Arabian Sea. Over these regions on almost all of the daily satellite photographs without exception the cloud accumulations of the northern ITCZ branch of the Indian Ocean section for the space of more than 2,000 km are interrupted and are not connected to the ITCZ cloud systems over Africa [6]. Apparently, this is related to the existence over these regions during the entire examined period of a fairly strong (to 15-20 m/s) meridional southerly migration in the lower portion of the troposphere [9].

In the Southern Hemisphere in this period the winter monsoon dominates, especially pronounced near the Mozambique coast of Africa and Madagascar. These regions are distinguished by the least activity of the atmospheric processes and generally have few clouds [6]. On fig 1,a the region of least D_r values corresponds to them.

Now we will examine the processes lasting 3-6 days that we have agreed to call synoptic-scale fluctuations not directly linked to global shifts in the pressure and wind zones. In the tropical zone the cloud systems of such scale are associated with synoptic disturbances at different stages of development (from depression to tropical hurricane); their characteristic horizontal scale is several hundreds of kilometers.

In the period of the summer Indian monsoon the increased D_c values are confined to the near-equatorial water areas of the central and eastern sections of the Indian Ocean and the southeastern Bay of Bengal (fig 1,b). These are the main regions for the generation of tropical depressions. Especial attention should be given to the position of the isoline D_c=0.4 whose configuration almost precisely repeats the shoreline of the Bay of Bengal. A reduction in D_c over the continental regions, undoubtedly linked to the attenuation in tropical depressions during their emergence on land, once again indicates the link between the synoptic cloud cover fluctuations (3-6 days) and the tropical cyclogenesis. The southeastern regions of China are another region in the Northern Hemisphere where high D_c values were noted. Here the D_c maximum is also apparently linked to the tropical depressions and typhoons of the East China Sea.

In the Southern Hemisphere the activity of the tropical cyclogenesis is significantly reduced and the maximum spectral density observed in the southeast of the studied region is apparently linked to the fluctuations in the cloud cover on the tradewind front.

Thus, we have ascertained that in the period of the summer monsoon the regions of maximum low-frequency fluctuations in cloud cover do not coincide with the regions of synoptic fluctuations, that is over the Indian Ocean basin in the period of the summer monsoon processes of a varying scale simultaneously participated in the mechanism of cloud cover formation; here a distinct localization is observed in the fluctuations of a certain frequency range.

In winter in the Northern Hemisphere one can isolate four main regions of maximum values (fig 1,c) in the distribution of dispersion corresponding to global scale fluctuations (D_Γ).

The most significant of them is observed in the extreme southwest Indian Ocean with the maximum over the Strait of Mozambique and Madagascar. The second and third regions are located also in the Southern Hemisphere and occupy the central and eastern near-equatorial water areas of the Indian Ocean. If one compares the examined localization of the centers of maximum D_Γ values with the position in this same period of the ITCZ cloud accumulations [6], then it is easy to note their almost complete coincidence with each other. Thus, also in the Southern Hemisphere in the period of the summer monsoon the ITCZ cloud cover undergoes fluctuations with a period of 2-3 weeks. The fourth region of maximum D_Γ values is located in the Northern Hemisphere (winter) in southeast China. Large-scale fluctuations in the cloud cover here are linked to the activity of processes on the polar front which in the winter months in this region penetrates especially far to the south. The amounts of D_Γ confined to the polar front region are close to the D_Γ values in the ITCZ region.

Thus, the intensity of the polar frontogenesis is altered with the same frequency (and even with the same amplitude) as the intensity of the processes of macro-scale convergence of air streams in the Southern Hemisphere tropics. This can occur if in both hemispheres alternate intensification and attenuation of the meridional wind components is observed that results in aggravation both of the zone of convergence in the tropics and the fronts of temperate latitudes. It is noted in publication [4] that there are two circulation patterns in the atmosphere: one--with strong meridional and weak zonal air streams, the other--with intensive zonal movements and weak meridional exchange. Quasiperiodically transition occurs from one pattern to another, whereby the period is close to that examined by us. The impression is created that we have succeeded in tracing this phenomenon in the evolution of the cloud cover.

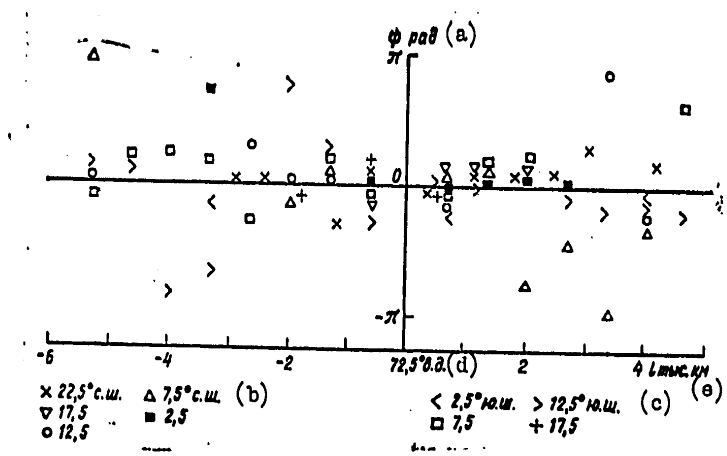

Figure 2. Dependence of Difference in Phases (ψ) of Cloud Cover Fluctuations with Period 14-21 Days on the Distance along the Latitudinal Circles

Key:
- a. rad
- b. northern latitude
- c. southern latitude
- d. eastern longitude
- e. thousand kilometers

In the distribution of the amount D_c (fig 1,d) the maximum values, as in the period of the summer Indican monsoon are observed in the near-equatorial regions of the summer hemisphere, that is where the tropical depressions are encountered most often in the northern winter [3]. The region of increased

D_c values over Indochina can be linked to the development of disturbances of a synoptic scale on the polar front. In the extreme southwest of the examined region large D_c values can be linked to the penetration of individual depressions from the ITCZ regions far to the south, and their regeneration on the polar front.

Now we will examine the spatial-temporal structure of the global atmospheric disturbances (T=14-21 days) that are reflected in the cloud cover variability. The task was set such that with the help of a cross spectral analysis a study was made separately of waves in the field of the cloud cover in the meridional and zonal directions. In the first case the section bounded by the equator and 5° n.l. was taken as the start of the reading from which the phase difference was computed. In the second case the computations were made from the meridional range 70-75° e.l. The function of the phase difference was computed for each five-degree square; the analysis used only the values with coherence exceeding 0.58 (here the evaluation of the phase spectrum possesses 80% reliability).

Figure 2 shows the results of the calculation for the function of phase difference (ψ) depending on the distance (for summer in the Northern Hemisphere). The values ψ are plotted with regard for the cartographic projection. Fluctuations in the cloud cover with period of 2-3 weeks have high coherence at the points located at different distances from the start of the reading. This is correct almost for the entire Indian Ocean basin--roughly from 20° s.l. to 25° n.l. As is apparent on fig 2, the difference in the phases does not depend on the distance, remaining close to zero. This indicates that at all points the fluctuations in cloud cover are synchronous, that is simultaneous increase or decrease occurs in the amount of cloud cover over the entire territory. The calculations of the phase difference showed that to the south of 20° s.l. movements are observed in the cloud systems from the west to the east. They are possibly linked to the formation of cold, high-altitude large-scale troughs from the equatorial side of the western migration of temperate Southern Hemisphere latitudes.

With the help of phase analysis a study was made of the waves of cloud cover (with T=14-21 days) in the meridional direction. It was found that on the background of practically simultaneous pulsations examined above, the fluctuations in the cloud cover at the equator and above Hindustan and Indochina are in the antiphase (this phenomenon is more clearly manifest to the east of 75° e.l.). This indicates the alternate activity of the processes on the northern and southern ITCZ branches.

The given conclusion is of great importance for predicting the intermittent situations in the Indian monsoon and confirms the hypothesis of one of the authors [5,6] that the maximum development of the monsoon cloud accumulations in northern India is observed at that period when near the equator on the southern ITCZ branch the cloud cover is almost completely eroded, and conversely, interruptions in the monsoon are linked to the maximum activity of cloud formation processes in the southern ITCZ branch.

The calculations made for the winter conditions of the Northern Hemisphere show that to the west of 70° in the Southern Hemisphere a high coherence is observed between the fluctuations in cloud cover in the junctions of the grid, while the phase difference is close to zero. This indicates that over the entire southwest section of the Indian Ocean and the adjacent regions of Africa a simultaneous increase or decrease in the cloud cover is observed. Thus, the results of a cross-spectral analysis indicate that large-scale pulsations in the cloud cover occur simultaneously over the entire territory encompassed by the monsoon circulation.

In conclusion we note that, despite the fact that the results are presented only for 2 years there are grounds to consider that the noted periodicity in the atmospheric processes manifest in the cloud cover is not a feature exclusively of 1971-1972, but is characteristic also for other years. This is primarily indicated by the observed confinement of these atmospheric processes to the macrocirculation objects such as the ITCZ, polar front, and others. The geographical localization and intensity of certain oscillations can be altered from year to year in accordance with the inter-annual variability in the general atmospheric circulation.

BIBLIOGRAPHY

1. Kislov, A. V. "Variability in the Tropical Cloud Cover as an Indicator of the Dynamic Processes in the Atmosphere," VESTNIK MOSKOVSKOGO UNIVERSITETA, SERIYA GEOGRAFIYA, No 3, 1978, pp 100-105.

2. Kryzhanovskaya, A. P. "Movement of Cyclonic Disturbances in the Tropical Zone," TRUDY GIDROMETTSENTRA SSSR, No 107, 1972, pp 85-98.

3. Kur'yanov, B. F.; and Medvedeva, L. Ye. "Harmonic Analysis of Stationary Random Processes," "Statistika i stokhasticheskiye sistemy" [Statistics and Stochastic Systems], No 8, Moscow, Izd-vo MGU, 1970, 56 p.

4. Monin, A. S. "Prognoz pogody kak zadacha fiziki" [Weather Forecasting as a Problem of Physics], Moscow, Nauka, 1969, 184 p.

5. Semenov, Ye. K. "Certain Peculiarities of the Intratropical Zone of Convergence from Observations from Meteorological Satellites," METEOROLOGIYA I GIDROLOGIYA, No 2, 1975, pp 22-29.

6. Semenov, Ye. K. "Peculiarities of the Cloud Accumulations of the Intratropical Zone of Convergence of the Indian Ocean Basin," METEOROLOGIYA I GIDROLOGIYA, No 6, 1977, pp 99-109.

7. "Catalog of Meteorological Satellite Data--ESSA-9 Television Cloud Photography," No 5, 323, 5, 324, 1971, Washington, D. C.

8. "Catalog of Meteorological Satellite Data--ESSA-9 Television Cloud Photography," No 5, 326, 1972, Washington, D.C.

9. Findlater, J. "Mean Monthly Airflow Levels over the Western Indian Ocean," GEOPHYS MEM, No 115, 1971, London, 53 p.

10. Krishmamurti, T. N.; and Bhalme, H. N. "Oscillations of a Monsoon System," J ATMOS SCI, Vol 33, No 10, 1976, pp 1937-1954.

11. Murakami, T.; and Ho, F. P. "Spectrum Analysis of Cloudiness over the Pacific," J METEOROL SOC JAPAN, Vol 50, No 4, 1972, pp 301-311.

12. Sikdar, D. N.; Young, J. A.; and Suomi, V. E. "Time-Spectral Characteristics of Large-Scale Cloud Systems in the Tropical Pacific," J ATMOS SCI, Vol 29, No 2, 1972, pp 229-239.

UDC 551.591:629.735.073

PROBLEM OF DETERMINING ATMOSPHERIC VISIBILITY AS APPLIED TO AIRCRAFT TAKE-OFF AND LANDING

Moscow METEOROLOGIYA I GIDROLOGIYA in Russian No 5, May 79 pp 57-61

[Article by Candidate of Technical Sciences S. L. Belogorodskiy, State Scientific Research Institute of Civil Aviation, submitted for publication 13 Jul 78]

Abstract. The extant visibility terminology as applied to aircraft take-off and landing operations is analyzed. A classification of terms is suggested according to four signs, as well as the terminology based on it; the classification is convenient for individualizing the requirements for visibility range information during aircraft take-off and landing. Suggestions are made for the most important trends in work to measure the actual visibility range of specific reference points used by the crew during take-off and landing.

[Text] One of the main conditions for guaranteeing the safe take-off and landing operations of aircraft is the correct determination of their position in space in relation to the take-off and landing strip (TLS). The fulfillment of this condition is attained by the crew's visual observation of the TLS, and in a number of cases, also by approaches to it. Here the maximum distance (range) at which the crew is guaranteed observation of the TLS and the approaches to it, or the reference points marking them is the most important characteristic of the meteorological conditions of take-off and landing.

In the documents regulating the meteorological analysis of civil aviation aircraft flights and the extant literature on these questions diverse terms are used to characterize these conditions: visibility, visibility range on the TLS, meteorological visibility range, flight visibility range, etc.

In a number of cases different terms are used to designate the same concepts, and converesely, the same terms are used for difference concepts. This concerns, in particular, the main term "visibility." Thus, in [3] and a number of documents regulating the meteorological analysis of civil aviation aircraft flights by visibility is meant the maximum distance at which the day and night reference points are visible (objects, light points). In the IKAO terminology [5] visibility is the possibility, determined by atmospheric conditions and expressed in units of distance, of seeing and identifying noticeable unilluminated objects during the day and noticeable illuminated reference points at night. In [1] it is indicated in relation to the term "visibility" that visibility range is meant by it, and so forth. In a number of documents visibility and visibility range on the TLS are viewed as similar concepts. Here visibility range is essentially the meaning for visibility [3].

There is no clearness in the structure of terms, definitions and use of the terms, and the derivatives from the main term "visibility." Thus, for example, the terms "vertical visibility" and "inclined visibility range vary in structure, although in the given case the distinctive feature is the direction of observation.

Without dwelling further on a discussion and criticism of the extant terminology we will move to an examination of the terminology we have suggested that is based on a classification of terms concerning atmospheric visibility as applied to the guarantee of take-off and landing operations.

The main term is visibility (visibility in the atmosphere)--the possibility, determined by atmospheric conditions, of seeing and identifying distant reference points (objects). The characteristic of visibility is the range of visibility--the maximum distance at which reference points (objects) are found and identified.

In accordance with the civil aviation documents currently in force under conditions of limited visibility the crew has the right to land if by the moment the decision making altitude has been reached reliable visual contact has been established with the ground reference points to determine the position of the aircraft in space in relation to the TLS.

Therefore, in speaking of visibility range as applied to the take-off and landing operations one should have in mind the visibility range at which detection and reliable identification of the ground reference points (objects) occur.

Visibility can be classified according to different signs. As applied to our tasks of greatest importance is the classification according to the following signs (fig 1):

--nature of observed reference points (objects);
--site of observation;
--direction of observation;
--time of day during which observation is made.

In the classification according to nature of observed reference points the latter can be subdivided into nonself-luminous and self-luminous (lights). The nonself-luminous reference points (objects) include artificial and natural elevations, clouds, TLS (pavement, axial line), special markers (screens, posts, flags, etc.) and so forth. The self-luminous reference points include single and group lights of constant and discrete (flashing) emission serving to illuminate and mark the TLS, taxiing roads, approaches and others, as well as lights (lamps) on the meteorological screens serving to determine the visibility range.

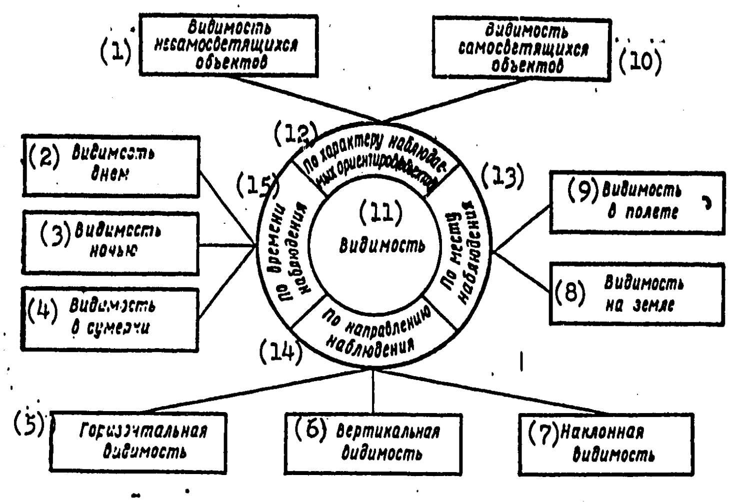

Figure 1. Classification of Visibility Terms

Key:
1. Visibility of nonself-luminous objects
2. Visibility during day
3. Visibility at night
4. Visibility at dusk
5. Horizontal visibility
6. Vertical visibility
7. Inclined visibility
8. Visibility on ground
9. Visibility in flight
10. Visibility of self-luminous objects
11. Visibility
12. According to nature of observed reference points (objects)
13. According to observation site
14. According to observation direction
15. According to observation time

We recall that the division of objects into nonself-luminous and self-luminous reflects the basic differences in the physical and biological processes of their perception by the human visual analyzer.

Depending on the observation site we note visibility on the ground and visibility in flight. As applied to the specific observation site on the ground one can distinguish visibility at the beginning of the TLS, visibility at the end of the TLS, visibility at the nearest homing radio station, etc.

With respect to observational direction visibility can be subdivided into horizontal vertical and inclined. In switching to visibility range we will speak of the range of horizontal visibility, range of vertical visibility, and range of inclined visibility (and not about the inclined range of visibility).

Finally, with respect to the time of day during which the observation is made one can distinguish visibility during the day, at night and at dusk. It should be noted that the classification of visibility according to the time of day is conditional to a certain degree since the change in visibility range according to time of day is linked to the change in brightness of the background. At the same time, depending on the characteristics of the surface on which the observed objects are located, the meteorological conditions at the moment of observation (cloud cover, fog), time of day and season (position of the sun on the celestial sphere), and other factors the brightness of the background can be significantly altered.

The classification given above is convenient for individualizing the requirements for visibility range information for take-off and landing.

In order to implement take-off and landing the crew needs to have information about the range of horizontal visibility on the TLS that determines the possibility of controlling the position and motion parameters of the aircraft during its take-off run, touchdown, and post-landing run. Since the take-off run and post-landing run can be carried out on the entire length of the TLS, then the information about visibility should also cover the entire length of the TLS. However, taking into consideration the difficulties in obtaining information along the entire length of the TLS and assuming that the spatial variability in visibility on this section is not great one can usually be limited to measurement of the visibility range at two-three TLS points.

During the landing approach in order to determine the position of the aircraft in space and the parameters of its motion in relation to the assigned landing trajectory the most important is the inclined visibility from the aircraft cockpit, i.e., the visibility in flight.

In order to make a decision on the possibility of landing the crew needs to observe a number of reference points sufficient for this purpose.

It should be indicated at once that the concept "sufficient" number of reference points is not unambiguous. In each specific situation the number of reference points that the crew needs to observe depends on the landing approach conditions. Thus, from the research results it is known that in order to determine the position of the aircraft and its deviations in relation to the prescribed rectilinear trajectory it is sufficient to see three-four lights on this trajectory. The extent of this section is less than 100 m. However such a number of reference points can be acknowledged as sufficient only with comparatively small deviations of the aircraft and low flight altitudes (30 m and less). In other cases a considerably greater number of reference points may be needed to evaluate the position of the aircraft and the parameters of its motion.

The section of the earth's surface observed (or the reference points on it) in the approach zone to the TLS depends not only on the visibility range, but also on the characteristics of the field of view of the aircraft pilots from the cockpit. We also note that in order to make a decision about landing the aircraft commander is not required to see the beginning of the TLS. In the existing minimums for landing the visibility range is computed such that the pilot during the approach to the decision making altitude can see a certain number of lights or other reference points on the course of the TLS axis in the approach zone.

Thus, for the conditions of landing minimums of the first IKAO category it is assumed that the pilot must see by the moment of reaching the decision making altitude (60 m) the section of lights on the course of the TLS axis extending 300 m.

In all take-off and landing cases under conditions of limited visibility the crew needs information about the visibility range of specific reference points that can be used to evaluate the position and motion parameters of the aircraft. Thus, for example, during the take-off of an aircraft during the day it is important to have information about the visibility range of the TLS and marking of its axial line (with regard for the condition of the TLS surface and marking) in the given specific illumination conditions. Under night conditions it is necessary to have information about the visibility range of the TLS lights and the axial line with the characteristics of the lights that are specific for the given take-off conditions (degree of brightness at which the lights are turned on). To make a decision about landing it is necessary, first to have information about the visibility range in flight of specific reference points in the zone of landing approach (for example, at night--approach lights), and second, the visibility range on the TLS.

As is known, currently the domestic AMSG [Air Weather Station of the Civil Air Fleet] is measuring the visibility only on the ground in a horizontal direction (range of horizontal visibility). Here the meteorological visibility range* during the day and the visibility range of a single light (about 45 cd) at night are taken as the visibility range. This visibility range is used as the visibility range on the TLS if the TLS is not equipped with lights of high intensity (LHI). If the TLS is equipped with lights of high intensity (TLS landing lights with light strength no less than 10,000 cd) then the visibility range of the TLS landing is taken as the visibility range on the TLS.

The terms "meteorological visibility" and "range of meteorological visibility are more correct.

Thus, only in the latter case the crews of aircrafts are given information about the visibility range of specific reference points. In all the other cases, as practical experience has shown, the crews receive information about the visibility range that does not correspond to a certain degree to the actual visibility range of specific reference points, which has a negative effect on the regularity and safety of flights. As a consequence of this the search for the methods and means of determining the actual visibility range of reference points used by the crew during take-off and landing of aircraft is an important task for improving the safety and regularity of flights of civil aviation aircraft.

In order to solve the aforementioned problems it is necessary to expand the front of scientific research and experimental design work. Currently of greatest importance are the works to determine the range of inclined visibility of group lights and markers, as well as certain others. Taking into consideration that the information about the range of meterological visibility apparently in the near future will remain the initial to determine the visibility range of specific reference points, it should be acknowledged that it is important to perfect the techniques for observing it with regard for the specific problems of the meteorological analysis of aviation, as well as to develop algorithms for computing the visibility of real objects along the TLS according to observational results.

BIBLIOGRAPHY

1. Gavrilov, V. A. "Vidimost' v atmosfere" [Visibility in the Atmosphere], Leningrad, Gidrometeoizdat, 1966, pp 6-7, 38-40, 119-125.

2. "Nastavleniye gidrometeorologicheskim stantsiyam i postam" [Manual for Hydrometeorological Stations and Posts], No 3, Pt 1, Moscow, Gidrometeoizdat, 1969, 201 p.

3. "Nastavleniye po meteorologicheskomy obespecheniyu grazhdanskoy aviatsii (NMD-GA-73)"[Manual for Meteorological Analysis of Civil Aviation (NMD-GA-73)], Moscow, Gidrometeoizdat, 1973, pp 6-8.

4. "Praktika nablyudeniya za dal'nost'yu vidimosti na VPP i peredachi soobshcheniy o ney" [Practical Observations of Visibility Range on the TLS and Transmission of Information about It], IKAO circular 113-AN/85, Montreal, 1973, pp 1-34.

5. "Sbornik terminov IKAO" [Collection of IKAO Terms], Doc 9110, Vol 11, Montreal, 1974, pp 92, 110.

UDC 551.593

CONSIDERATION OF ATMOSPHERIC SPHERICITY IN CALCULATIONS OF THE BRIGHTNESS OF THE DAYTIME SKY

Moscow METEOROLOGIYA I GIDROLOGIYA in Russian No 5, May 79 pp 62-65

[Article by V. Ye. Pavlov, Astrophysical Institute of the Kazakh SSR Academy of Sciences, submitted for publication 2 Aug 78]

Abstract. Results are analyzed from measurments of the brightness of the daytime sky in the 340-360 nm near-ultraviolet spectral range with large solar zenith angles. Observations were made under steppe conditions with good atmospheric transparency. It is shown that the replacement of secants of solar zenith angles and the observed point of the sky by appropriate atmospheric mass values makes the theoretical brightness values computed for the plane-parallel model closer to the real. Such agreement exists all the way to the onset of ultraviolet dusk, when the solar disk disappears on the veil background created by multiple-diffused light.

[Text] In solving a number of practical problems it often proves necessary to know the brightness distribution over the daytime sky in the ultraviolet spectral range when the solar zenith angle exceeds 80°. Making such observations is a fairly labor-intensive process and is linked to the designing of special apparatus [1]. Therefore the natural question arises as to the possible use of some approximate formulas or tables to evaluate the background of the descending diffuse radiation. The majority of them have been derived and computed as applied to the case of the plane-parallel atmospheric model. If its optic thickness τ is not great and the brightness of the sky is mainly governed by primary light diffusion then the simplest method for considering atmospheric sphericity is replacement in the formulas of single diffusion of the secants of solar zenith angles Z_0 and the observed point of the sky Z by the appropriate values of atmospheric masses m_0 and m [7,10]. In a number of cases such an approach is completely justified [5,9]. However the plane-parallel model of the atmosphere is often used also in computations of the intensity of multiple-diffused radiation [8,12]. This work covers an examination of the question of how permissible such approximations are with large Z_0.

Analyses were made of observational data of the brightness of the sky I in the 340-360 nm spectral range obtained on a quartz spectrometer [1] in the steppe near the settlement of Kirbaltabay in the Alma-Atinskaya oblast in the summer of 1973 and 1976. The uniform underlying surface with low albedo value [6] and open horizon made it possible to measure the amounts I in units of S (πS--spectral solar constant) all the way to Z_0, $Z \leq 89°$ [3]. At the same time the spectral atmospheric transparency was determined and the stability of its optic properties was controlled [2,7].

Initially for the zenith angles Z_0, $Z \leq 75°$ when the manifestations of atmospheric sphericity are insignificant, a comparison was made of the experimental values I and the theoretical I_t computed on the assumption of a plane-parallel homogeneous model with spherical indicatrix scattering [11]. In order to avoid the effect of the indicatrix factor the scattering angle φ was taken as equal to 60° [6]. It was found that I and I_t on the average agree fairly well among themselves if the albedo of single diffusion of the medium ω is taken as fluctuating from 1.00 to 0.98. The latter value mainly characterizes the atmospheric conditions in Kirbaltabay in 1976 where as compared to 1973 the dust content rose noticeably as a consequence of soil erosion. Therefore in the further calculations of I_t with large Z_0 and Z we used that specific value of ω that satisfied a whole series of observations of I with small Z_0 and Z. The differences in I_t for ω=1.00 and ω= 0.98, generally speaking, are small. For example, in the solar almucantar Z_0=Z=88.3° with τ=1.00 the I_t respectively equal 0.0039 and 0.0036.

The role of the multiple effects in the formation of the field of descending diffuse radiation thatincreases with a rise in Z_0 and Z alters to a considerable degree the pattern of brightness distribution over the sky [3]. It is possible that the shape of the distribution curves is affected also by the atmospheric sphericity. Therefore it is necessary to preliminarily analyze the observed angular relationship of I in different almucantars so that the comparison of I with the calculated values I_t is justified. Examination of 25 distributions of I (ψ) with respect to the azimuth angles ψ read off from the sun demonstrated that with Z_0>85° for each specific day the type of function I(ψ)/I(90°) changes little with variations in Z from 10 to 89°. As an example figure 1 gives such curves for Z=80, 20 and 10° in two spectral sections. It is not very likely that their asymmetry is a consequence only of the indicatrix effect. If Z_0=87.4° and Z=10° then the scattering angles φ corresponding to the azimuths 0 and 180° are 77.4° and 87.4°. Then with values of the molecular τ_R and aerosol τ_D of the optic thicknesses 0.527 and 0.185 that occur in the 380 nm spectral region (fig 1) the summary indicatrix of scattering $f(\varphi)=f_R(\varphi)+F_D(\varphi)$ even in the case of single diffusion of light in the range $77.4° \leq \varphi \leq 87.4°$, cannot be altered 1.5-fold for any type of distribution of particles with respect to sizes. Most likely the type of relationship I=I(ψ) is governed to a considerable degree by the atmospheric sphericity.

Based on the aforementioned, with Z_0>85° it is best of all to determine the weighted mean of I for each almucantar Z>10° not from the scattering angles φ but from the azimuths as

$$\overline{I(\psi_0)} = \frac{2\pi \int_0^{\pi} I(\psi) \sin\psi \, d\psi}{4\pi}.$$

It follows from the observations that $\psi_0=60°$. A comparison of the observed brightness I with the theoretical I_t computed from tables [11] on the assumption of the spherical indicatrix of diffusion was made precisely for the azimuth angles 60°.

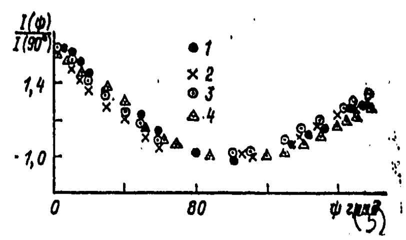

Figure 1. Amplitude Relationship of Relative Brightness of Sky in Spectral Region 360 nm(1,2) and 340 nm (3,4)

Key:
1. $z_0=88.3°$; $z=80°$
2. $z_0=85.9°$; $z=10°$
3. $z_0=85.6°$; $z=20°$
4. $z_0=87.4°$; $z=10°$
5. deg

Previously we had already compiled experimental values of I with theoretical I_t computed in the plane-parallel approximation [3]. It was shown that in the solar almucantar with $Z_0 \approx 89°$ the discrepancies between them on the average reach a two-fold amount, whereby $I > I_t$. Now, following [7,8,10, 12], by using the theoretical values I_t we will understand by sec Z_0 and sec Z the atmospheric masses m_0 and m. Such an approach significantly improves the convergence of I and I_t which is indicated by the data of fig 2. The points lie fairly well on the straight line whose angle of slope to the x-axis is 45°. Finally, the amounts I_t coincide well with the results of solving the equation of transfer of radiant energy in a heterogeneous spheric atmosphere with real indicatrix with consideration for its polarization properties. Such calculations using the Monte Carlo method were made by M. A. Nazaraliyev [3]. The values of intensity I_t in the solar almucantar with $\varphi \approx \psi = 60°$, $\tau=0.9$ and $\omega=1.00$ are given in table 1.

There is hardly any physical sense in such a replacement of secants of zenith angles by the atmospheric masses since the brightness of the sky with large Z_0, Z is mainly governed by multiple-diffusion of light. It should be viewed simply as a convenient empirical approach that improves the convergence of I and I_t.

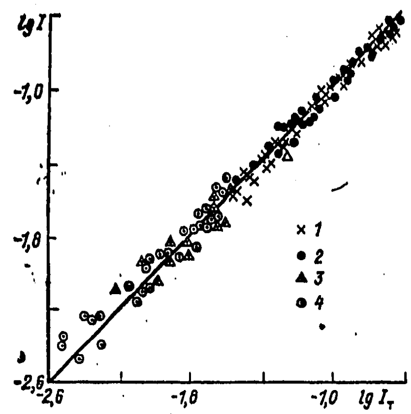

Figure 2. Comparison of Observed Values of Brightness of the Sky I (60°) in Solar (1,3) and Other (2,4) Almucantars with Theoretical I_t with Small (1,2) and Large (3,4) of Zenith Solar Angles

Key: 1,2. $z_0 < 85°$ 3,4. $z_0 \geq 85°$

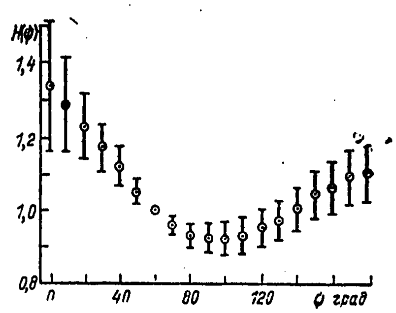

Figure 3. Function H(ψ) from Observations in Steppe

In order to compute the intensity of the scattered light in any point of the sky with Z_0>80° the amount I_t should be multiplied by the function H (ψ)= I(ψ)/I(60°) that takes into consideration the azimuth relationship of brightness. Its appearance with the mean values $\overline{\tau}_R$=0.60, $\overline{\tau}_D$=0.25 and Z> 10° with

Table 1.

Z_0 град (1)	m_0	I_τ	
		$m_0 = \sec Z_0$	Монте-Карло (2)
85	10,4	0,019	0,021
88	19,8	0,0076	0,0073
89	27,0	0,0054	0,0053

Key:
1. degrees
2. Monte Carlo

the corresponding root-mean-square deviations is depicted in fig 3. With the subsequent reduction in the zenith angle of the observed point Z the asymmetry of curve $H(\psi)$ drops, and for calculation of the brightness of the sky at the zenith one can assume that $H(\psi)=1$.

Such simplest semi-empirical methods of computation, in addition with those previously proposed [4,6] can prove convenient in practice if the required accuracy of evaluating the intensity is not greater than 25%.

BIBLIOGRAPHY

1. Boyko, P. N.; Pavlov, V. Ye.; and Teyfel', Ya. A. "Spectropolarimeter of Daytime Sky for Ultraviolet Spectral Region," "Rasseyaniye i pogloshcheniye sveta v atmosfere" [Scattering and Absorption of Light in the Atmosphere] Alma-Ata, Nauka, 1971, pp 67-69.

2. Golovachev, V. P.; Zarubaylo, V. T.; Pavlov, V. Ye.; and Teyfel', Ya. A. "Determination of Aerosol Optic Atmospheric Mass According to Brightness of Sky in Ultraviolet Spectral Region," "Rasseyaniye sveta v zemnoy atmosfere" [Scattering of Light in the Earth's Atmosphere], Alma-Ata, Nauka, 1972, pp 234-240.

3. Yegorova, L. A.; Nazaraliyev, M. A.; Pavlov, V. Ye.; and Rabinina, N. G. "Intensity of Direct and Scattered Ultraviolet Radiation in Large Atmospheric Masses," IZVESTIYA AN SSSR. FIZIKA ATMOSFERY I OKEANA, Vol 13, No 4, 1977, pp 420-424.

4. Yegorova, L. A.; Pavlov, V. Ye.; Ryabinina, N. G. "Approximate Method for Calculating Distribution of Intensity of Short-Wave Diffuse Radiation over Daytime Sky," METEOROLOGIYA I GIDROLOGIYA, No 2, 1976, pp 106-108.

5. Livshits, G. Sh. "Rasseyaniye sveta v atmosfere" [Scattering of Light in the Atmosphere], Pt 1, Alma-Ata, Nauka, 1965, 177 p.

6. Pavlov, V. Ye.; Ryabinina, N. G.; Teyfel', Ya. A.; Smirnov, V. V. "Transparency of the Atmosphere, Brightness of the Diurnal Sky and Reflecting

Ability of the Underlying Surface in the Near Ultraviolet Spectral Region," "Pole rasseyannogo isluchenlya v zemnoy atmosfere" [Field of Scattered Radiation in Earth's Atmosphere] Alma-Ata, Nauka, 1974, pp 3-31.

7. Pyaskovskaya-Fesenkova, Ye. V. "Issledovaniye rasseyaniya sveta v zemnoy atmosfere" [Study of Light Scattering in the Earth's Atmosphere], Moscow, Izd-vo AN SSSR, 1957, 217 p.

8. Rozenberg, G. V. "Sumerki" [Dusk], Moscow, Fizmatgiz, 1963, 380 p.

9. Sushkevich, T. A.; Rayevskaya, I. S. "Pervyy poryadok rasseyniya sveta v bezoblachnoy sfericheskoy atmosfere" [First Order of Light Scattering in Cloudless Spherical Atmosphere], Preprint of Institute of the Problem of Mechanics of the USSR Academy of Sciences, No 118, 1976.

10. Fesenkov, V. G. "Theory of Brightness of Daytime Sky with Spherical Earth," ASTRONOMICHESKIY ZHURNAL, No 32, Issue 3, 1955, pp 265-281.

11. Carlstedt, J. L.; and Mullikin, T. W. "Chandrasekhtar's X- and Y-Functions," THE ASTROPHYSICAL J. SUPPLEMENT SERIES, Vol 12, No 113, 1966, pp 449-586.

12. Dave, J. V. "Multiple Scattering in a Nonhomogeneous Rayleigh Atmosphere," J. ATMOS. SCI., Vol 22, No 3, 1965, pp 273-279.

APPROVED FOR RELEASE: 2007/02/08: CIA-RDP82-00850R000100080016-5

UDC 551.465.11

INFLUENCE OF THE BOTTOM RELIEF ON THE GEOSTROPHIC MOTION OF A STRATIFIED ZONAL FLOW

Moscow METEOROLOGIYA I GIDROLOGIYA in Russian No 5, May 79 pp 66-71

[Article by Candidate of Physical and Mathematical Sciences V. F. Kozlov, N. A. Kropinova, and M. A. Sokolovskiy, Far East State University, Pacific Ocean Oceanological Institute DVNTs of the USSR Academy of Sciences, submitted for publication 9 Oct 78]

Abstract. The problem of the interaction of the geostrophic zonal flow with disturbances of the bottom relief in the form of an axisymmetric underwater hill and an infinite meridional range is solved numerically. The role of stratification and velocity shear in the approach stream on the structure of the topographical eddies formed in it is clarified.

[Text] Analysis of the current measurement results in the ocean lead to the conclusion that the irregularities in the bottom relief affect the spatial-temporal variability of circulation (see, for example, publication [5] and its bibliography). In this respect it is important, in particular, to examine the problem of the interaction of a large-scale current with isolated bottom disturbances.

This article is a natural continuation of publications [1, 4] that were carried out in this direction in the framework of a model set-up based on the theory stated in [3]. Thus, in (4) the example is examined of a zonal kinematically uniform linearly stratified flow running against an obstacle in the form of an axisymmetric underwater hill. [1] studies the dependence of the vertical structure of topographical current disturbances on stratification and shear (constant) of the approach stream velocity. Below an examination is made of the most general case of velocity distribution according to the parabolic law, and the results are discussed from numerical calculations of the flow characteristics over an underwater hill and over a meriodional range in cases of shearless flow and a linear velocity shear with hyperbolic density distribution [2].

Following publications [1,3,4] we write the main equation

$$Q_\eta S_{\zeta\zeta} - Q_{\eta\zeta} S_\zeta - Q_{\zeta\zeta} S = 0, \qquad (1)$$

which must be integrated with the additional conditions

$$S|_{\zeta=0} = 0, \quad S|_{\zeta=1} = -Q_\eta, \qquad (2)$$

$$Q(0, \eta, \zeta) = \Phi(\eta, \zeta), \qquad (3)$$

where the functions $Q(\xi, \eta, \zeta)$ and $S(\xi, \eta, \zeta)$ are linked to the hydrodynamic pressure by the correlations

$$p = \rho_0 gz + \delta^* gH^* Q, \quad S = \int_0^\zeta (Q_\xi - \zeta Q_\zeta)\, d\zeta, \qquad (4)$$

while $\xi = \ln \frac{H(x, y)}{H^*}$, $\eta = \ln \frac{\Omega(y)}{\Omega^*}$, $\zeta = \frac{z}{H(x, y)}$ --dimensionless variables.

Here $H(x,y)$ and $\Omega(y)$ designate the assigned depth of the ocean and the Coriolis parameter, while the asterisks mark the corresponding characteristic amounts. The components of velocity and density are expressed by the functions Q and S according to the formulas

$$u = -(TH_y S_\zeta + PQ_\eta), \quad v = TH_x S_\zeta, \quad w = PH_x S, \quad \rho = \rho_0 + RQ_\zeta, \qquad (5)$$

where $T = \delta^* gH^* (\rho_0 \Omega H)^{-1}$, $P = \delta^* gH^* \Omega_y (\rho_0 \Omega^2)^{-1}$, $R = \delta^* H^* H^{-1}$, while ρ_0 and δ^* designate the mean density and characteristic disturbance of density. From the first two correlations (5) it is apparent that T and P are the coefficients with topographical and planetary horizontal velocity components.

We adopt condition (3) in the form

$$\Phi(\eta, \zeta) = -\frac{e^{2\eta}}{\varkappa} \{1 + \gamma_1 [\zeta - \gamma_2 (\zeta - \gamma_3)^2]\} - $$
$$- \frac{1 + \gamma}{\gamma^2} \ln(1 + \gamma\zeta) + \frac{\zeta}{\gamma} + \frac{1}{2}, \qquad (6)$$

where $\varkappa = \delta^* gH^* \Omega_y (\rho_0 U \Omega^{*2})^{-1}$. This corresponds to the following distribution of characteristics of an undisturbed stream (with $H=H^*$):

$$u = -PQ_\eta = U\{1 + \gamma_1 [\zeta - \gamma_2 (\zeta - \gamma_3)^2]\}, \quad v = w = 0, \qquad (7)$$

$$\rho = \rho_0 + \delta^* \left\{ \frac{\zeta - 1}{1 + \gamma\zeta} + \gamma_1 \frac{e^{2\eta}}{\varkappa} \left[\gamma_2 (\zeta - \gamma_3) - \frac{1}{2} \right] \right\}. \qquad (8)$$

The problem (1)-(3) was solved numerically according to the difference scheme briefly stated in [3].

Correlations (7) and (8) make it possible to trace the interrelationship of the fields of velocity and density (following from the initial equation system of the theory of the "ideal" thermocline [3]) in the region with level bottom. By assigning the density distribution we will predetermine at the same time the zonal flow structure. However, for greater clarity we will here, by assigning with the help of coefficients γ_i different vertical profiles u, determine from (8) the corresponding changes ρ. At the same time we will discuss the results of several variants of numerical computations of the topographical component of velocity S_ξ and vertical velocity S presented in figure 1 for $\xi = -0.1$, $\eta = 0$ (which corresponds to $H = 0.9045\ H^*$, $\Omega = \Omega^*$) and $U > 0$.

If the velocity has a constant shear, i.e., $\gamma_2 = \gamma_3 = 0$ (this case is examined in [4], then the vertical structure ρ does not depend on the kinematics of the flow, and the density field can be zonal, while precisely $\rho = \tilde{\rho} = \rho|_{\gamma_1=0} + \rho^*$, where $\rho^* = \gamma_1 U \Omega^2 \cdot \text{const}$. Density $\rho|_{\gamma_1=0}$ can be an arbitrary function of the vertical coordinate; here we have adopted the hyperbolic distribution [2]. The parameter $\gamma > 0$ characterizes the degree of deviation of the density profile from the linear; with $\gamma \to 0$ we will have a linear distribution, while with $\gamma \to \infty$ we obtain a barotropic liquid with $\rho = \rho_0$.* In the numerical experiments we assigned to γ the values $10^3, 10^{-3}$ and 10; by analogy with [1] we will conditionally call these three cases "barotropic," "linear," and "hyperbolic" respectively.

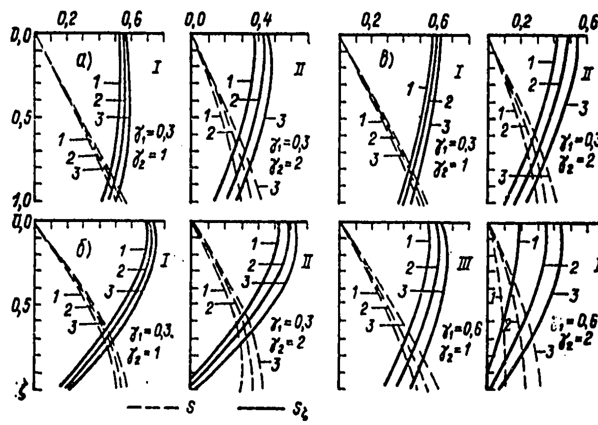

Figure 1. Profiles of Vertical Velocity S and Topographic Component of Horizontal Velocity S_ξ in "Barotropic" (a), "Linear" (b) and "Hyperbolic" Cases.
Velocity of the undisturbed flow has parabolic distribution (7). Numbers 1,2 and 3 refer to values $\gamma_3 = -0.1;\ 0;\ 0.1$ respectively.

---

*This is true only with $\gamma_2 = 0$.

If $\gamma_1 \neq 0$ and $\gamma_2 \neq 0$ then the velocity profile H=H* becomes parabolic, whereby the size of its deviation from the linear is characterized by the product $\gamma_1\gamma_2$. A linear term appears here in the density distribution, and now $\rho = \tilde{\tilde{\rho}} = \tilde{\rho} + \gamma_2 \rho^* \zeta$. Consideration for the parameter γ_3 results in a change in the depth of occurrence of the velocity maximum of the approach stream (this depth also depends on γ_2: $\zeta_{max} = \gamma_3 + \frac{1}{2\gamma_2}$), and in the density field of (8) here we make yet another addition of the zonal structure and obtain $\rho = \tilde{\tilde{\rho}} + \gamma_3 \rho^*$.

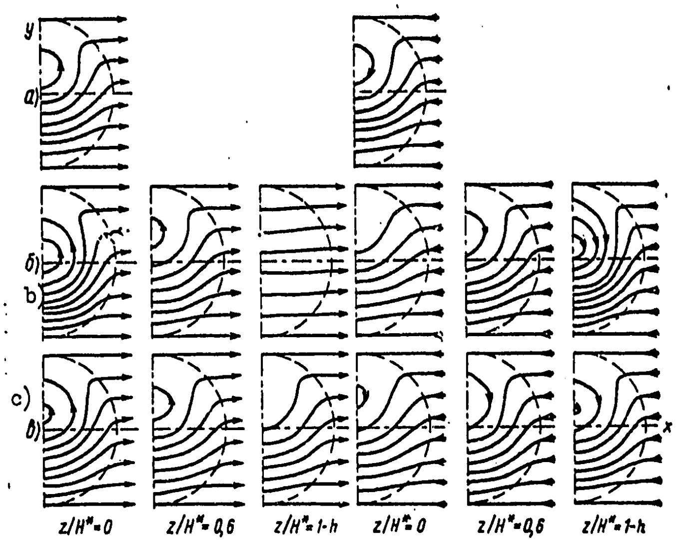

Figure 2. Isobars--Current Lines of Horizontal Motion over Underwater Hill of Type (9) in "Barotropic" (a), "Linear" (b) and "Hyperbolic" (c) Cases for Kinematically Uniform Flow. On the left side of the figure U>0, on the right U<0.

It is apparent on figure 1 how the topographical velocity reacts to all these changes: with an increase (decrease) in the deviation of the planetary velocity profile from the linear, as well as with the elevation (deepening) of ζ_{max} the intensity of the topographical movement is attenuated (intensified) at all levels. Such situations are also possible where the topographical velocity alters its sign (b, II; c, IV); this corresponds to the different directions of vorticity in the upper and deep layers. Attenuation in the topographical motion is always linked to a reduction in vertical velocity.

In contrast to the case examined in [1] of a constant velocity shear for the current model in the majority of the examined cases it is characteristic for the topographical velocity model to be present on a certain intermediate level.

We will examine the example of a kinematically uniform flow ($\gamma_1=0$) running against an underwater axisymmetric hill for which the bottom relief looks like

$$H(x,\ y)=H^*\begin{cases}1-h\left(1-\dfrac{x^2+y^2}{L^{*2}}\right)^2, & x^2+y^2\leqslant L^{*2}\\ 1, & x^2+y^2>L^{*2}.\end{cases} \qquad (9)$$

We assume $H^*=4$ km, $L^*=100$ km, $h=0.025$, $|\varkappa|=\left(\frac{\pi}{2}\right)^2$. Figure 2 illustrates the effect of the stratification parameter γ on the dynamics of this flow. Here and on figure 3 due to the symmetry only the right half of the pressure field is presented; the dotted line marks the external boundary of bottom relief disturbance.

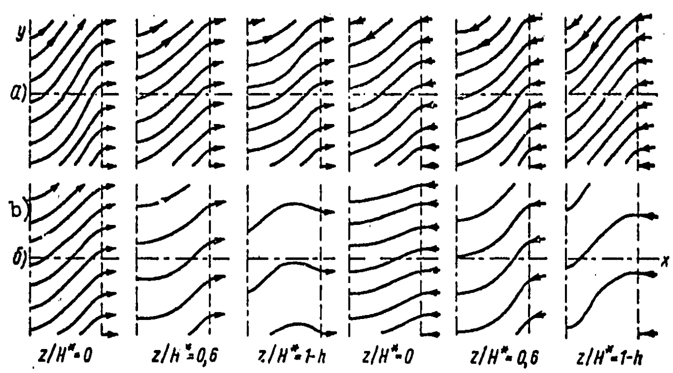

Figure 3. Isobars of Horizontal Motion over Underwater Meridional Ridge of Type (10) in "Hyperbolic" Case for Shearless Flow (a) and Flow with Constant Velocity Shear (b). From the left U> 0, from the right U< 0.

The calculations show that in the "barotropic" case ($\gamma=10^3$) the motion is practically two-dimensional, therefore isobars are presented on the figure only of one level z=0 for the easterly and westerly flow directions. They differ very insignificantly both from each other, and from the curves $\Omega H^{-1}=$ const (not given here) coinciding with the isobars for a uniform liquid, since $\rho=\rho_0$ from (4) and (2) $\overline{Q}=Q(\eta-\xi)=Q\{\ln[\Omega H^*(\Omega^*H)^{-1}]\}$ evidently follows.

Figure 2b presents the isobars for the surface, intermediate and benthic levels in the "linear" case $\gamma=10^{-3}$. They actually are identical to the corresponding lines on figures 2 and 3 of publication [4] where $\gamma=0$ is assumed. Over the northern slope of the hill a cyclonic (anticyclonic) eddy is formed whose intensity attenuates (intensifies) with depth for the easterly (westerly) flow. By comparing this figure with figure 2c we note that in the more realistic "hyperbolic" case the vertical structure of the eddy formation forming over the hill has the same, but not as pronounced nature. A comparison of all three series of this figure results in the conclusion that stratification has a considerable effect on the dynamics of the eddy topographical motion. This influence is manifest as follows: with an increase in the deviation of the density profile from the linear the intensity of the eddy motion attenuates in the upper and intensifies in the lower (intensifies in the upper and attenuates in the lower) layers for the easterly (westerly) flow, so that in the limit barotropic case it becomes constant with respect to the vertical.

In the following example a study is made of the effect of the velocity shear of the approach stream on its eddy disturbances with motion over a meridional ridge in the form

$$H(x,\ y) = H^* \begin{cases} 1 - h\left(1 - \frac{x^2}{L^{*2}}\right)^2, & |x| \leq L^*, \\ 1, & |x| > L^*. \end{cases} \tag{10}$$

Here the amounts H*, h and L* are the same as above. Figure 3 presents the isobars for the levels $zH^{*-1}=0$; 0.6 and 1-h in the "hyperbolic"case. Figure 3a illustrates the behavior of the isobars (lines of current) of a shearless flow, and figure 3b--the flow for which the coefficient of linear shear equals -0.6. In both cases the current meeting the underwater range is deviated in the southeasterly (southwesterly) direction with U>0 (U<0), while passing over the ridge it alters direction to the northeast (northwest), and again becomes zonal immediately after the ridge. A somewhat different behavior of the isobars is observed in the benthic layer in the presence of a velocity shear when in the peripheral section of the region over the ridge a shift occurs in the sign of meridional velocity; this is explained by the fact that with a rise in the velocity shear in the approach stream and with a reduction in the relative depth HH^{*-1} the topographical velocity S_ζ is attenuated with depth, and even can alter its sign in the benthic layer (fig 2 in [1]), and consequently, alter the sign of ν as well (see expression (5)). For the kinematically uniform easterly flow, as in the previous example, the vorticity is attenuated with depth; in the case of a westerly flow the vertical change in the eddy movement occurs nonmonotonically: its intensity rises with depth from the surface to a certain level, and then insignificantly attenuates. In the presence of shear velocity both for easterly and for westerly flows the amount of vorticity rises with depth, while the intensity of motion attenuates. The rise in vorticity with depth is explained by the fact that the topographical eddy component of the horizontal motion S_ζ diminishes slower than the planetary component Q_η.

The given examples convince one of the importance of considering the vertical distributions of density and velocity of a geostrophic zonal flow in studying the eddy motion occurring in it over the disturbed bottom relief, and also make it possible to note the laws illustrated above governing the corresponding transformations of a disturbed flow. Further studies in the case of bottom topography of the examined scale must, in our opinion, be based on a more general quasigeostrophic model.

BIBLIOGRAPHY

1. Kashirikhina, N. A.; Sokolovskiy, M. A. "Effect of Stratification and Velocity Shear on Topographical Motion in the Ocean," "Volnovyye protsessy v krayevykh oblastyakh okeana" [Wave Processes in the Marginal Ocean Regions], Yuzhno-Sakhalinsk, 1978.

2. Kozlov, V. F. "Application of One-Parametrical Models of Density to a Study of Thermocline Circulation in an Ocean of Finite Depth," IZVESTIYA AN SSSR. FIZIKA ATMOSFERY I OKEANA, Vol 4, No 6, 1968, pp 622-633.

3. Kozlov, V. F."Geostrophic Motion of Stratified Liquid over Uneven Bottom," IZVESTIYA AN SSSR. FIZIKA ATMOSFERY I OKEANA, Vol 13, No 9, 1977, pp 961-970.

4. Kozlov, V. F.; and Sokolovskiy, M. A. "Stationary Motion of Stratified Liquid over Uneven Bottom (Geostrophic Approximation on β-Plane)," OKEANOLOGIYA, Vol 18, No 4, 1978, pp 581-586.

5. Huppert, H. E.; and Bryan, K. "Topographically Generated Eddies," DEEP-SEA RES., Vol 23, No 8, 1976, pp 655-679.

UDC 532.5+556.535.6

COEFFICIENT OF TURBULENT DIFFUSION OF SEDIMENTS AND CALCULATION OF THEIR CONCENTRATION DISTRIBUTION IN A FLOW

Moscow METEOROLOGIYA I GIDROLOGIYA in Russian No 5, May 79 pp 72-86

[Article by Candidates of Physical and Mathematical Sciences S. M. Antsyferov and R. D. Kos'yan, Institute of Oceanology, USSR Academy of Sciences, submitted for publication 4 Sep 78]

Abstract. The goal of the work is to perfect the method of analytically describing the distribution of suspended sediment concentration proposed by the traditional diffusion model for a stationary forward flow. Reasons are examined for the discrepancy sizes of coefficients of turbulent particle diffusion and turbulent liquid mixing. Based on the introduced ideas and a generalization of the experimental material an expression is compiled for the sediment diffusion coefficient that takes into account peculiarities of particle behavior in the benthic flow region. The obtained expression that comprises the foundation for the desired solution is also experimentally confirmed.

[Text] Movement of suspended sediment is an important component of the dynamics of the river bed evolution. A considerable portion of the solid run-off of rivers in the suspended state is carried out to the shore zone of the sea in whose dynamics this form of movement also plays a very important role. The suspended sediments made a considerable contribution to the formation of reservoir patterns and to the transfer of detrital material on the entire continental ocean shelf.

One of the main problems of suspended sediment dynamics is the problem of the vertical distribution of particle concentration in a uniform steady-state forward flow. The solution to this problem is not only the first step on the path to determining the flow of sediments transported by the current, but also the foundation for compiling analogous solutions for the conditions of wave and mixed (waves on current) flows.

The lack of a detailed description of the turbulent structure of "clean" water flows (without foreign inclusions) and the shortage of information about the interaction of solid particles with a liquid and among themselves do not yet make it possible to involve comparatively accurate mathematical models for the corresponding constructions [3, 7]. Usually less strict solutions of the diffusion theory are used for this purpose. Here a number of stipulations are introduced that significantly limit the application of the obtained solutions. However, the information that has been accumulated by now, as it seems to us, already permits certain limitations to be removed by putting in their place an evaluation of the effect of the corresponding factors. This work has set the task of revealing, based on experimentally obtained information the main factors that affect the diffusion of particles, and of introducing certain physical ideas about this process. On this basis, by generalizing the experimental material it is proposed to improve the solution of the diffusion model for a stationary flow having thus expanded the boundaries of its applicability.

For the case of a uniform planar flow without cross currents and with a steady-state distribution of turbidity the equation of turbulent diffusion looks like

$$\varepsilon_S \frac{\partial S(z)}{\partial z} + \omega S(z) = 0, \qquad (1)$$

where z--vertical coordinate directed upwards from the bottom;
S(z)--value of concentration of suspended sediments on level z averaged with respect to time;
ε_S--coefficient of turbulent diffusion of sediments;
ω--sinking velocity of particles.

The solution to equation (1) is the expression

$$S(z) = S_c \exp\left(-\omega \int_0^z \frac{dz}{\varepsilon_S}\right). \qquad (2)$$

where S_c--value of concentration S(z) on fixed level z=c.

In order to determine the absolute values of the concentration, evidently, one should have the value of this amount on some known level (for example, the value of benthic turbidity). For this purpose usually the path of its direct measurement is suggested since the available empirical relationships are reliable only in a very narrow range of conditions.

The distribution of relative concentration of suspended particles with respect to the vertical flow is determined by the coefficient of type ε_S.

Further, the amount ε_S is usually identified with the coefficient of turbulent mixing of a liquid (ε_W) that is determined by the law of distribution with respect to the vertical of the averaged horizontal flow velocity. The traditional assumption $\varepsilon_S = \varepsilon_W$, evidently, denotes the introduction of a number of limitations on the corresponding solutions.

The solutions formulated in the framework of this assumption have been analyzed by us in publication [4], where it has also been shown that the most precise is the variant based on the law of distribution of velocities suggested by I. K. Nikitin [6]. For this case the amount ε_W is defined as follows:

$$\varepsilon_W = \frac{v_*^2 z^2 (1 - z/H)}{2,8\, v_* z + 15,7\, \nu}, \tag{3}$$

where v_*--dynamic velocity;
H--depth of flow;
ν--kinematic coefficient of liquid viscosity.

In the case of low liquid viscosity, when the contribution of the amount 15.7ν can be ignored, (3) switches to an expression that differs from the widespread formula of H. Rouse [12] for ε_W only by the value of the Karman constant equal to 0.36 in this case. Expression (3) differs most significantly from Rouses formula on the flow surface where it yields finite values of concentration while Rouses formula yields a hypothetical zero value.

Such a traditional approach does not consider a number of factors and it is not always justified to ignore them. We will examine the main, from our viewpoint, reasons for the discrepancy in the amount ε_S and ε_W.

1. It is known (see, for example, [5]), that the coefficient of diffusion of a "trace" passive admixture ($\varepsilon_{S\,0}$) can already differ from ε_W as a consequence of the fact that the first is determined directly by the mixing of the liquid mass, while the second, characterizing the continuous medium, can be determined also by pressure pulsations. Thus, $\varepsilon_{S\,0} \neq \varepsilon_W$. However, the discrepancy of these amounts is not great and further formulations here will be made without considering it.

2. A part of the pulsation energy of the flow is spent on suspending and maintaining the particles in suspension. On the other hand, the particles that are suspended but break away from the liquid are a certain lattice placed in the liquid that apparently is also capable of making distortions in the fine structure of the flow. Due to these reasons the frequency spectrum of turbulence can be deformed. Thus, the coefficient of mixing a liquid with suspension $\varepsilon_{W(S)}$ can differ from that for clean water, i.e., $\varepsilon_{W(S)} \neq \varepsilon_W$. And since the effect of these factors rises with an increase in concentration, the greatest distortions will evidently occur in the benthic region.

3. The energy of the turbulent pulsation vertical components responsible for movement of particles rises from the bottom to a certain level z_k (according to [6] z_k=(0.18-0.20)H) above which it is altered little. Generally in the benthic region only part of the turbulent pulsations possess the energy necessary toinvolve the particles in such motion when the latter practically completely repeat the movements of the surrounding volumes of liquid. Correspondingly, precisely here the greatest time lag of the particles will be manifest and the discrepancy between the amounts ε_S and $\varepsilon_{W(S)}$ will be the most noticeable.

The energy of pulsation movement rises the farther from the bottom, as a consequence of which there is a reduction in the discrepancy between the values ε_S and $\varepsilon_{W(S)}$. Generally above a certain level $z_r \leq z_k$ the particles will strive to follow practically all the components of turbulent movement of the liquid. Judging from the results of the experiments of V. Vanoni and G. Nomicos [14] the value z_r depends not only on the hydrodynamic pattern of the flow and the particle characteristics, but also on their concentration. For the zone $z > z_r$ the traditional solutions to the diffusion model can already be used (with limitations following from points 1 and 2). With respect to this boundary the suspension-carrying flow was conditionally divided into zones called the benthic region and the main mass of the flow [1,2,4].

4. Finally, the irregular bottom is also a factor of turbulization. The energy of turbulent pulsations developing as a consequence of the bottom irregularity has the maximum values on the upper boundary of the turbulent boundary layer, and rapidly is reduced to zero in its limits (see, for example [11]). It is also reduced fairly rapidly above this boundary. Instrument measurements of the concentration in the limits of the boundary layer have not yet been successfully made. In the subsequent presentation we will make a reading along the z axis, strictly speaking, from the upper boundary of this layer, since we exclude from examination the processes occurring in direct proximity to the bottom. As compared to the depth of the flow the thickness of the boundary layer is negligible, therefore it will not figure in the further formulations.

Analysis of the works on the covered questions shows (see, for example, [4]) that due to the difficulties in setting up physical studies of such type the available results are incomplete, not always reliable, and in certain cases are debatable. Thus, the question of the correlation of amounts ε_S and ε_W that is basically important in order to expand the applicability of the diffusion model is solved by introducing one [8,9] or two [10] coefficients of proportionality. Here the possibility of changing this correlation with a reduction in absolute values ε_W (for example, as one approaches the bottom) or with a change in concentration is in no way considered. Therefore for a further analysis we will involve the results of an empirical generalization of the experimental material with respect to the distribution of suspended particle distribution.

Publication [2], based on ideas about the two-layer model of the suspension-carrying flow has suggested an expression to describe the vertical concentration distribution over the entire flow mass in which the isolated variant of the diffusion theory--$S^{II}(z)$ is supplemented by the empirical relationship for the benthic region--$S^{I}(z)$

$$S(z) = S^{I}(z) + S^{II}(z) = S_{c_1} \exp\left\{-0{,}083\left(\frac{\rho_T-\rho}{\rho}\right)\left[\frac{g}{\nu^2}\left(\frac{\omega}{u_Д-\omega}\right)^2\right]^{1/3} \times \right.$$

$$\left. \times\ (z-c_1)\right\} + S_{c_2} \exp\left\{-\left(\frac{2{,}8\,\omega}{v_*}+\frac{15{,}7\,\nu\omega}{Hv_*^2}\right)\ln\left(\frac{z}{H-z}\,\frac{H-c_2}{c_2}\right)+\right.$$

$$\left. + \frac{15{,}7\,\nu\omega}{v_*^2}\left(\frac{1}{z}-\frac{1}{c_2}\right)\right\}, \qquad (4)$$

where S_{c_1} and S_{c_2}--values of function $S(z)$ on fixed levels $z=c_1$ and $z=c_2$; here c_1 is selected without fail in the benthic region of the flow, while c_2--in the main mass (above 0.3H from the bottom);

ρ and ρ_T --density of liquid and solid particles respectively;

g--acceleration of free fall;

$u_Д$--benthic velocity (velocity on level of upper boundary of turbulent boundary layer).

The obtained expression made it possible to compute the distribution of particles over the entire mass of a uniform steady-state forward flow and withstood verification well with respect to all the admissible materials of laboratory studies.

At the same time the two-layer model is not free of a number of significant shortcomings. First of all this is the presence of two norming multipliers and a certain indefiniteness in the instructions in relation to selecting the points for measuring the values of the norming concentrations.

We will attempt to construct a solution to the diffusion theory with the same range of applicability as the two-layer model, but without its shortcomings.

Taking into consideration the considerations stated above, we will look for a solution, assuming that in the zone of operation of the traditional diffusion model in the main mass of the flow the discrepancy in the amounts ε_S and ε_W can be ignored. We will attempt to consider the benthic region with the help of a certain multiplier α that equals a unit above z_T and approaches zero as it approaches the bottom. In addition, the values α must depend on the sinking velocity of particles and the hydrodynamic pattern of the flow, since the level above which the classic diffusion scheme is applicable is located farther from the bottom the greater the sinking velocity and the lower the dynamic velocity. Generally one can write that

AND
NO. 5, MAY 1979
13 AUGUST 1979 (FOUO) 2 OF 2

$$\alpha = \alpha(\omega,\ v_*,\ z,\ H). \tag{5}$$

In the benthic region as a consequence of the bottom irregularity additional turbulization develops that also makes a definite contribution to the suspension and movement of particles in the suspension. Generally the coefficient of additional mixing ε_δ depends on the properties of the particles and the liquid, distance from the bottom, parameter of bottom irregularity, and benthic velocity of flow. Therefore we will write it thus:

$$\varepsilon_\delta = \varepsilon_\delta(\rho,\ \rho_T,\ \nu,\ \omega,\ u_\Delta,\ z,\ \delta), \tag{6}$$

where δ--mean linear size of projections of bottom irregularity.

With z=0 the amount ε_S is completely determined by the bottom irregularity and becomes equal to ε_δ. At the same time in expression (4) at the bottom the contribution to the value S(z) of the second component as compared to the first can be ignored. Then it is easy to obtain the value $\varepsilon_{\delta,0}$ with z=0. Assuming

$$S(0) = S_{c_1} \exp\left(-\omega \int_{c_1}^{0} \frac{dz}{\varepsilon_{\delta,0}}\right) = S_{c_1} \exp\left\{-0{,}083\left(\frac{\rho_T - \rho}{\rho}\right) \times \right.$$

$$\left. \times \left[\frac{g}{\nu^2}\left(\frac{\omega}{u_\Delta - \omega}\right)^2\right]^{1/3} (-c_1)\right\}, \tag{7}$$

we obtain $$\varepsilon_{\delta,0} = \frac{\rho}{0{,}083\,(\rho_T - \rho)}\left[\frac{\nu^2 \omega\,(u_\Delta - \omega)^2}{g}\right]^{1/3}. \tag{8}$$

The energy of turbulent formations generated by friction of the water flow on the irregular bottom rapidly disappears with spread into its mass. The corresponding reduction in ε_δ the farther from the bottom is considered by introducing the function f(z, δ). Then

$$\varepsilon_\delta = \varepsilon_{\delta,0}\, f(z,\ \delta). \tag{9}$$

Now we will express ε_S with regard for the introduced concepts α and ε_δ:

$$\varepsilon_S = \alpha(\omega,\ v_*,\ z,\ H)\, \varepsilon_W + \varepsilon_\delta. \tag{10}$$

By assuming expressions for ε_W according to (3) and having used the considerations of dimensionality, we rewrite (10) as follows:

$$\varepsilon_s = \frac{v_*^2 z^2 \left(1 - \frac{z}{H}\right)}{2{,}8\, v_* z + 15{,}7\, \nu}\, \alpha\left(\frac{\omega}{v_*}, \frac{z}{H}\right) + \frac{\rho}{0{,}083\, (\rho_T - \rho)} \times$$

$$\times \left\{ \frac{\omega}{g} \left[\nu (u_1 - \omega)\right]^2 \right\}^{1/3} f\left(\frac{z}{\delta}\right). \qquad (11)$$

The selection of classes of functions approximating the relationships $\alpha\left(\frac{\omega}{v_*}, \frac{z}{H}\right)$ and $f(z/\delta)$ was made by us according to the data on the vertical distribution of sediment concentration obtained in experiments [1,13]. For this in each case with fixed ω, v_* and δ the experimental values of $\varepsilon_S(z)$ are determined as follows.

After differentiating expression (2) with respect to z we obtain:

$$\frac{S_c}{S(z)} \cdot \frac{d\left[\frac{S(z)}{S_c}\right]}{dz} = -\frac{\omega}{\varepsilon_s(z)}. \qquad (12)$$

From here

$$\varepsilon_s(z) = -\frac{\omega S(z)}{\frac{dS(z)}{dz}}. \qquad (13)$$

The approximate values are found from the smoothed experimental curves S(z)

$$\frac{dS_i(z)}{dz} = \frac{1}{2}\left[\frac{S_i(z_{j+1}) - S_i(z_j)}{z_{j+1} - z_j} + \frac{S_i(z_j) - S_i(z_{j-1})}{z_j - z_{j-1}}\right]. \qquad (14)$$

Here the index i designates the number of the fraction, while j--the successive number of level, the farther from the bottom, at which the values S_i are taken.

The found series of values ε_S made it possible to search for the following completely satisfactory approximations:

$$\alpha\left(\frac{v_*}{\omega}, \frac{z}{H}\right) = \mathrm{th}\left(\frac{v_*}{\omega}\frac{z}{H}\right), \qquad (15)$$

$$f\left(\frac{z}{\delta}\right) = \exp\left(-\frac{z}{\delta}\right). \qquad (16)$$

With regard for (8), (9), (15) and (16) one can write:

$$\varepsilon_s = \frac{v_*^2 z^2 \left(1 - \frac{z}{H}\right)}{2{,}8\, v_* z + 15{,}7\, \nu}\, \mathrm{th}\left(\frac{v_*}{\omega}\frac{z}{H}\right) + \frac{\rho}{0{,}083\, (\rho_T - \rho)} \left[\frac{\nu^2 \omega (u_1 - \omega)^2}{g}\right]^{1/3} \times$$

$$\times \exp\left(-\frac{z}{\delta}\right). \qquad (17)$$

Table 1. Comparison of Calculated and Experimental Values of Coefficient of Turbulent Diffusion of Particles

$\frac{z}{H}$	(1) ε_s по ф-ле (17) / ε_s опытное (3)	(1) ε_s по ф-ле (3) / ε_s опытное (3)	(2) ε_s по Раузу / ε_s опытное (3)
0,06	0,74±0,05	1,40±0,10	1,67±0,12
0,08	0,93±0,06	1,74±0,12	2,11±0,15
0,1	0,89±0,06	1,49±0,10	1,87±0,11
0,15	1,09±0,08	1,69±0,08	2,21±0,11
0,2	1,16±0,08	1,55±0,08	1,98±0,10
0,3	1,41±0,08	1,62±0,08	2,16±0,09
0,4	1,42±0,08	1,51±0,08	1,95±0,09
0,5	1,36±0,08	1,40±0,08	1,89±0,08
0,6	1,30±0,08	1,32±0,08	1,96±0,09
0,7	1,24±0,08	1,25±0,08	1,79±0,09
0,8	1,14±0,08	1,14±0,08	1,47±0,10
(4) Среднее по всем горизонтам	1,15±0,07	1,46±0,06	1,92±0,07
(5) Среднее по пяти первым горизонтам	0,96±0,07	1,57±0,06	1,97±0,09

Key:
1. according to formula
2. according to Rouse
3. experimental
4. Mean for all levels
5. Mean for five first levels

In order to illustrate the comparability of the amounts obtained directly from data of experiments and according to formula (17) table 1 gives the ratios of these amounts, averaged with respect to the data of all involved measurements for the selected levels. For comparison this same table gives the same correlations for the case where the amount ε_S is taken as equal to ε_W, which in turn was computed according to Rouses formula. The table also indicates the errors in averaging the ratio $\varepsilon_{S,calcul}/\varepsilon_{S,measur}$ according to the data of all experiments. The lower line of the table shows the values averaged with respect to all levels.

It follows from the data of the table that the found expression is in better correspondence with the experimental data than others. An especially good coincidence of the measured and calculated amounts is observed in the benthic region of the flow.

By substituting (17) into (2) we obtain the sought for expression that describes the relative distribution of concentration of suspended deposits with respect to the vertical:

$$S(z) = S_c \exp\left\{ -\omega \int_c^z \frac{dz}{\dfrac{v_*^2 z^2 (1 - z/H)}{2,8\, v_* z + 15,7\, \nu} \operatorname{th}\left(\dfrac{v_*}{\omega} \dfrac{z}{H}\right) + \dfrac{\delta}{0,083\, (\rho_T - \rho)} \left\{ \dfrac{\omega}{g} [\nu (u_\text{д} - \omega)]^2 \right\}^{1/3} \exp\left(-\dfrac{z}{\delta}\right)} \right\}. \tag{18}$$

Equation (18) is easily integrated by the numerical method. The values computed with respect to (18) agree well with the values obtained according to formula (4) that was previously verified according to all the available experimental data [2]. However, here the found expression is free of the shortcomings of the two-layer model and provides a physically more substantiated description of the behavior of particles in the benthic region of the flow.

BIBLIOGRAPHY

1. Antsyferov, S. M.; and Debol'skiy, V. K."Certain Features of the Transport of Detrital Material on a Shelf," "Litodinamika, litologiya i geomorfologiya shel'fa" [Lithodynamics, Lithology and Geomorphology of a Shelf], Moscow, Nauka, 1976, pp 74-84.

2. Antsyferov, S. M.; and Kos'yan, R. D. "Vertical Distribution of Suspended Sediments in Forward Flow," METEOROLOGIYA I GIDROLOGIYA, No 8, 1976, pp93-98.

3. Kos'yan, R. D. "Calculation of Concentration of Suspended Detrital Material in Water Flows of Upper Shelf Section," "Gidrofizicheskiye protsessy i protsessy vzaimodeystviya v more" [Hydrophysical Processes and Processes of Interaction in the Sea], Moscow, Nauka, 1979 (at press).

4. Kos'yan, R. D.; Antsyferov, S. M.; and Yefremov, S. A. "Applicability of Diffusion Theory to Calculations of Sediment Distribution in Open Flow," METEOROLOGIYA I GIDROLOGIYA, No 1, 1976, pp 79-87.

5. Monin, A. S.; and Yaglom, A. M. "Statisticheskaya gidromekhanika" [Statistical Hydromechanics], Pt 1, Moscow, Nauka, 1965, 639 p.

6. Nikitin, I. K. "Turbulentnyy ruslovoy potok i protsessy v pridonnoy oblasti" [Turbulent River Bed Flow and Processes in Benthic Region], Kiev, Izd-vo AN UkrSSR, 1963, 124 p.

7. Fridman, B. A. "Theories of Motion of Suspended Sediments," "Dinamika i termika rechnykh potokov" [Dynamics and Thermal Conditions of River Flows], Moscow, Nauka, 1973, pp 37-49.

8. Carstens, M. R. "Accelerated Motion of Spherical Particles," TRANS. AMER. GEOPHYS. UNION, Vol 33, No 5, 1952, Washington.

9. Ismail, N. M. "Turbulent Transfer Mechanism and Suspended Sediment in Closed Channels," TRANS. AMER. SOC. CIV. ENGRS., Vol 117, 1952.

10. Jobson, H. K.; and Saira, W. W. "An Experimental Investigation of the Vertical Mass Transfer of Suspended Sediment," PROC. XIII CONGR. INT. ASS. HYDR. RES., Vol 2, 1969, pp 111-121, Kyoto.

11. Lungren, H. "Turbulent Currents in the Presence of Waves," "Proc. of the 13th Coastal Eng. Conf. Vancouver, 1972, pp 623-634.

12. Rouse, H. "Modern Conception of the Mechanics of Fluid Turbulence," TRANS. AMER. SOC. CIV. ENGRS., Vol 102, 1937.

13. Taggart, W. C.; Yermoli, C. A.; Montes, S.; and Ippen, A. T. "Effect of Sediment Size and Gradation on Concentration Profiles for Turbulent Flow," "M.I.T. Lab. Water Resour. and Hydrodyn. Rept. No 152, 1972, 154 p.

14. Vanoni, V.; and Nomicos, G. N. "Resistance Properties of Sediment-Laden Streams," TRANS. AMER. SOC. CIV. ENGRS., Vol 125-1, 1960.

UDC 532.543

ANALYSIS OF TURBULENCE SPECTRAL CHARACTERISTICS WITH RIDGED ROUGHNESS OF THE BOTTOM

Moscow METEOROLOGIYA I GIDROLOGIYA in Russian No 5, May 79 pp 80-86

[Article by N. A. Melekhova, All-Union Scientific Research Institute of Physicotechnical and Radiotechnical Measurements, submitted for publication 18 Dec 78]

Abstract. A study is made with ridged roughness of the bottom of the characteristic groupings of extremum values of spectral density functions marked by increased drops both in frequency and in the value of spectral density. The hypothesis is advanced that the observed drops determine the boundaries of the eddy structural formations existing in the flow. A similar distribution pattern is noted with respect to the flow depth of Euler scale turbulence, and scales determined from the frequency of the first maximum spectral drop. The frequencies at which the indicated drops are observed have a tendency towards multiplicity.

[Text] The spectrum of flow velocity turbulent pulsations is continuous-discrete. It was previously indicated that in the spectral density functions of velocity pulsation components characteristic groupings are observed of the extremum values marked by increased drops both in frequency and in the spectral density value [2]. It has been noted that the characteristic extremum values linearly depend on the number of the corresponding extremum. Here the slope of the line of maximums of the spectral density functions coincides with the slope of the line of minimums.

This work analyzes the distribution of characteristic frequencies and their spectral density for pulsations of the longitudinal velocity component with respect to the verticals along ridged roughness. Recordings of velocity pulsations by a two-component mechanotron converter were used as the initial realizations. Measurements were made in a trough 25.5 m long, 0.5 m high, and 0.6 m wide, where the correct periodic forms were simulated in the form of fixed ridges 1.75 m long and 0.09 m high made of medium-sized gravel to 0.01 m. The surface of the ridges was fixed by a cement solution. Eight ridges were arranged over the bottom of the trough. Thus, the given relief had unchanged characteristics with respect to the width of the flow. The depth of the flow over the crest of the ridge was 21 cm, the mean velocity--47 cm/s. The geometric correlations for the ridges roughly corresponded to ridges observed under low water conditions in the Polomet' River. Thus, from the 1960 observational data a movement was noted over the gravel-sand bottom of the river of ridges up to 1.5 m long and 0.1 m high with mean velocity of the current 47 cm/s [3]. A study was made of the stationary pattern of the water flow with Reynolds and Froude numbers computed with respect to mean velocity and equal respectively to $1 \cdot 10^5$ and 0.33. Six measuring verticals were arranged over the fourth and fifth ridges (fig 1). The mechanotron converter was fastened with the help of a water gage on a moving cart.

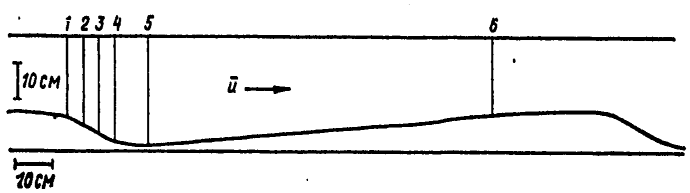

Figure 1. Placement of Measuring Verticals along Fourth and Fifth Ridges

The two-component mechanotron converter is an electric-vacuum lamp containing two plane-parallel two-cathode mechanotron systems of longitudinal control [1], whereby the planes of the electrodes of both mechanotron systems are oriented perpendicular to each other. Each of the two mechanotron systems of the converter possesses sensitivity only in one direction, and precisely: with the movement of the anode perpendicular to the planes of its electrodes. The mobile component of the converter is a light tubular rod connected to the control pin and mechanotron anode; it is 10 cm long. A sphere made of foam plastic 0.5 cm in diameter is fastened on its end. A reduction in the influence of side effects of the flow on the converter rod was attained by screening the latter with a shield. During measurement of the velocity pulsations the rod with the sensitive component-sphere was immersed in the flow. The action of the converter is based on the use of the dependence of the output electric signal of the mechanotron on resistance during the spatial flowing of the flow over its sensitive component. Here a shift occurs in the mechanotron rod that is proportional to the strength of action of the flow on the sensitive component. The link between the velocity and strength of action of the flow on the sensitive component of the converter is determined by the formula of complete resistance of a body during its spatial flowing that is known in technical hydromechanics

$$P = C \gamma S, \frac{u^2}{2},$$

where C--dimensionless coefficient of resistance whose amount depends on the shape of the sensitive component and equals 0.5 for a sphere;

γ--liquid density;
S--area of the largest section of the sensitive component perpendicular to the direction of flow;
u--velocity of flow.

The movement of the rod and the mechanotron anode connected to it under the influence of a flow results in a change in the currents in the mechanotron cathode circuits, and as a result, in a change in the output signals of two bridge measuring schemes to which the mechanotron is connected. Here the amounts of the output signals are proportional to two mutually perpendicular components of the vector of flow strength applied to the end of the pin. The output signals of the mechanotron converter were recorded by a N-327 type self-recorder that then were translated onto punched cards (or punched tape) with the help of a semiautomatic digital converter of logging diagrams type F-001. The length of realization with respect to time was 41 s, the quantization spacing--0.04 s. The spectral density functions were computed by the method of rapid Fourier transformation on a BESM-1 type computer.

The kinematic structure of a flow with the ridge roughness indicated above was studied in publication [5], where the multiple-modality of the obtained spectral density functions of the velocity pulsation components was indicated. Here we will analyze for the sample one of the functions, for example, S_u for pulsations of the longitudinal velocity component--second vertical Y=0.8 cm. The analysis fixed the frequencies of successive maximums and minimums, and their ordinal number of arrangement on the spectral curve. Here the numbering of the maximums coincided with the numbering of the minimums located to the right of them. Consequently the minimum frequency was higher than the maximum frequency of the same number or pair. Further, a determination was made of the difference in spectral densities ΔS of the maximum and minimum of each pair (we will conditionally call it the spectral drop) and difference in the frequencies Δf of the minimum and maximum (correspondingly the frequency drop). The analysis results are presented in table 1.

On figure 2, with respect to the dependences of the observed spectral ΔS and frequency Δf drops on the corresponding frequency of the pair minimum one can note the presence of six pairs in the frequency range to 10 Hz with increased values of the indicated drops. Thus, the maximum spectral drop is noted for the pairs with ordinal numbers 1, 5, 8, 11, 13 and 18 with frequencies of the minimum of these pairs respectively 0.84, 3.06, 5.08, 7.02, 8.17, 9.84 Hz. The maximum frequency drop is observed for pairs with ordinal numbers 1, 4, 7, 11, 13 and 18 with frequencies respectively of 0.84 2.41, 4.80, 7.02, 8.17, and 9.84 Hz. As is apparent from the analysis, the frequencies of the pair minimum for which the maximum spectral and frequency drops are observed can coincide or somewhat differ from each other. We will successively enumerate six of the indicated maximum drops. The dependence of their frequencies on the number of drop n is a straight line (fig 2). This circumstance indicates the close link between the frequency and spectral drops and their multiplicity.

Table 1. Frequencies and Spectral Density of Successive Pairs of Maximums and Minimums for Spectral Density Function S_u of Longitudinal Velocity Component and Differences of Spectral Densities S and Frequencies f of Maximum and Minimum of Each Pair (second vertical, Y=0.8 cm)

	(a) Номер пары								
	1	2	3	4	5	6	7	8	9
f_{max} гц (b)	0,12	1,04	1,68	1,91	2,84	3,56	4,07	4,94	5,22
f_{min} гц (b)	0,84	1,33	1,84	2,41	3,06	3,92	4,80	5,08	5,30
Δf гц (b)	0,72	0,29	0,16	0,50	0,22	0,36	0,73	0,14	0,08
S_{max} дБ (c)	7,2	—0,4	—2,4	—2,4	—3,6	—8,0	—9,8	—12,4	—15,7
S_{min} дБ (c)	—3,8	—6,5	—5,8	—8,3	—14,8	—13,0	—14,0	—17,6	—18,0
ΔS дБ (c)	11,0	6,1	3,4	5,9	11,2	5,0	4,2	5,2	2,3

	(a) Номер пары								
	10	11	12	13	14	15	16	17	18
f_{max} гц (b)	5,42	6,24	7,24	7,74	8,32	8,60	8,89	9,25	9,54
f_{min} гц (b)	5,72	7,02	7,38	8,17	8,46	8,76	9,12	9,40	9,84
Δf гц (b)	0,30	0,78	0,14	0,43	0,14	0,16	0,23	0,15	0,30
S_{max} дБ (c)	—12,2	—4,4	—9,2	—1,6	—12,3	—12,4	—14,0	—13,8	—13,8
S_{min} дБ (c)	—17,0	—14,4	—12,0	—14,0	—14,6	—15.0	—15,0	—15.2	—17,4
ΔS дБ (c)	4,8	10,0	2,8	12.4	2,3	2,6	1,0	1,4	3,6

Key:
- a. Number of pair
- b. Hz
- c. db

As indicated above, on the spectral characteristic one can note several frequencies at which the maximum spectral drops are observed. We will examine the distribution with respect to depth of flow of the first three indicated frequencies for the spectral characteristics of the longitudinal velocity component on the fourth vertical--respectively f_1, f_2 and f_3 (table 2). As is apparent from the table the nature of the distribution with respect to flow depth of the amounts f_1, f_2 and f_3 is similar. All the points of discontinuity of the indicated curves are repeated. Such an analysis of the distribution of maximum spectral drops with respect to the flow depth on all the measuring verticals confirms the pattern of similarity described above. This can be explained by the single source of emergence of the drops. Probably the observed drops can be viewed as boundaries of local structural formations existing in the flow. In this case, the observed multiplicity of the drops

Table 2. Distribution with Respect to Depth of Flow of Frequencies of First Three Maximum Spectral Drops f_1, f_2 and f_3 for Functions of Spectral Density of the Longitudinal Velocity Component on the Fourth Vertical

Y см	f_1 Hz	f_2 Hz	f_3 Hz
0,30	0,90	2,92	3,64
1,45	2,76	4,86	6,60
3,45	2,12	3,00	5,08
6,70	0,90	2,77	4,14
8,70	1,56	2,70	4,22
11,70	0,62	1,26	2,56
15,70	0,32	2,20	3,92
27,80	0,54	3,48	4,50

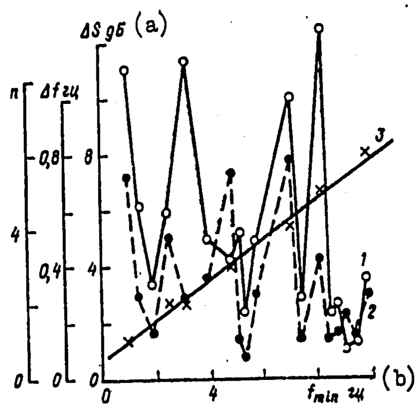

Figure 2. Change in Range to 10 Hz of Spectral ΔS(1), Frequency Δf(2) Drops and Ordinal Number n of Maximum Spectral and Frequency Drops (3) Depending on Frequency of Minimum f_{min} of Successive Pairs of Minimums and Maximums with Respect to the Spectrum of the Longitudinal Velocity Component (Second Vertical Y=0.8 cm).

Key:
a. db
b. Hz

can be explained as follows: during the interaction of eddies at the site of their meeting as a consequence of the inverse rotation the breakdown of the boundary is possible, and the emergence of a doubled eddy that, in turn, can form a quadrupled eddy, and so forth. The multiplicity of the drops as boundaries of the eddy formations can also be determined by the multiplicity of the turbulence scales in the flow.

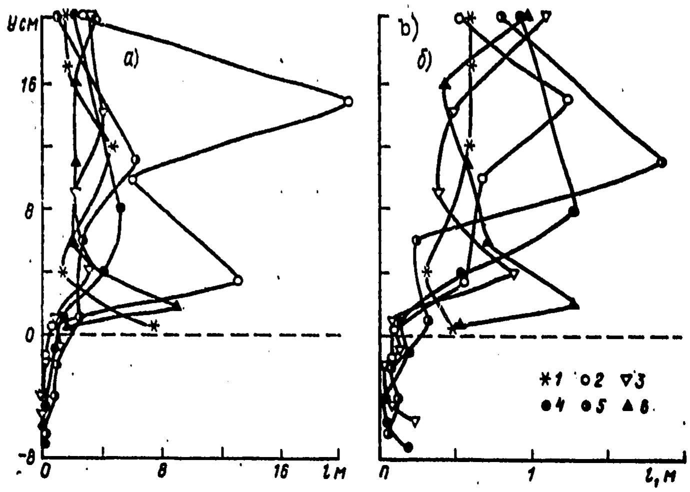

Figure 3. Distribution with Respect to Verticals of Ridge (1-6) of Euler Time Scales l Determined with Respect to Time of Zero Correlation (a) and Scales l_1 Computed with Respect to Frequency f_1 of First Maximum Spectral Drop (b) for Longitudinal Velocity Component.

It is important to explain the pattern of transformation of the eddy formations with respect to depth of the flow. For this purpose a computation was made of their dimensions by two methods: with respect to time of the zero correlation τ_0 and with respect to the frequency of the first maximum spectral drop f_1 for all the studied verticals along the ridge respectively by the formulas

$$l = 4\,\bar{u}\,\tau_0, \quad l_1 = \frac{\bar{u}}{f_1},$$

where $\bar{u}$--local velocity.

The Euler turbulence scale l, in contrast to the l_1 scale is not a direct geometric dimension of the eddy formation, but is the summary effect of the interaction of the eddies of different sizes that have different energy levels (a certain summary averaged eddy). However, the qualitative course of changes in scales l and l_1 with respect to flow depth on all the verticals along the ridge remains the same (fig 3). All the points of discontinuity in the comparable curves are repeated, and the inequality $l > l_1$ is maintained with respect to the absolute value. Such a pattern of distribution with respect to depth of the summary eddy and the eddy determining the boundary of transition from one structural formation to another can occur in the case if the assumption on the multiplicity of the turbulence scales existing in the flow is true. It should be noted that the dimensions of the eddy

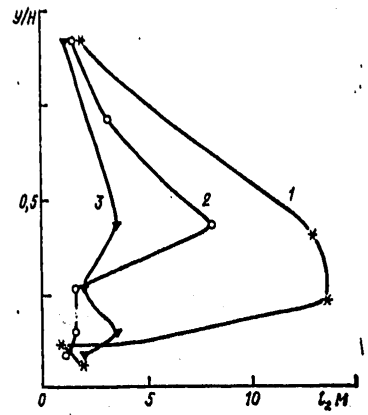

Figure 4. Distribution with Respect to Depth of Flow of Euler Turbulence Scales l_2 of Longitudinal Velocity Component with Small-Scale Bottom Roughness.

formations in the lower part of the ridge are significantly smaller than in the transit portion of the flow.

The stratified structure of the region of the ridge lower part and the transit section of the flow has previously been discussed in publications [6,7]. Thus, for example, in the joint study of the nature of the change with respect to flow depth of the root-mean-square deviations in longitudinal and vertical velocity components, the moment of correlation between them, and the coefficient of turbulent exchange an assumption was made on the existence directly in the benthic region of the lower part, besides the roll occupying the main part of the lower portion, a roll of smaller dimension. The boundaries of the layers were determined according to the points of discontinuity in the course of the comparable curves of distribution. The layers in the transit portion of the flow had greater extent with respect to depth than in the region of the lower portion. The separation into layers is noted also on the curves of distribution l and l_1 with respect to all verticals, only they can be more or less pronounced (fig 3).

For a ridgeless bottom the distribution with respect to depth of flow of the Euler turbulence scales l_2 (fig 4) provides the basis for the separation of the upper and lower layer between which the boundary depends on the dimension of bottom roughness. Studies of pulsations in the steady-state flow velocity (mean velocity on the order of 60 cm/s) were made by a two-component mechanotron converter in a trough 7 m long, 0.2 m wide and 0.4 m high with the following types of small-scale bottom roughness: 1--smooth glass bottom of trough, 2-- glass balls 0.24 cm in diamter, and 3--glass balls 2 cm in diameter. The balls were glued with nitroenamel right up to the glass sheets which were then placed on the bottom of the trough. The interface between the layers for a smooth bottom are located lower, on the relative level Y/H=0.1 than for the two other comparable types of bottom roughness for which the indicated level equals 0.25. Consequently, the extent of the upper layer for a smooth bottom is higher than in the other two cases. A trend is observed towards reduction in the maximum value of the Euler turbulence scale with a rise in the bottom roughness. If the observed maximum values of l_2 are compared with different types of roughness with the length of the trough, then with a smooth glass bottom this scale equals two lengths of the trough (14 m), with balls 0.24 cm in diameter--roughly the length of the trough (8 m), and with balls 2 cm in diameter--half the length of the trough (3.5 m). Thus, all the analyzed maximum values of the Euler turbulence scale have a multiple bond to the length of the trough. The coefficient of multiplicity, i.e., the ratio of the maximum value of the Euler turbulence scale to the length of the trough is determined by the dimension of roughness. With a rise in roughness the coefficient of multiplicity is reduced. It is evident that the most low-frequency oscillations in the troughs are determined by the frequency computed from the length of the trough, or its harmonics depending on the bottom roughness. The division into layers with small-scale roughness is similar to the division into layers of the transit portion of the flow with ridge roughness. Here the eddy region of the lower portion which is characterized by significantly smaller dimensions of the eddy structural formations than for the transit portion of the flow is excluded.

Conclusions

1. In the functions of the spectral density of velocity components characteristic groupings are observed of the extremum values marked by increased drops both with respect to frequency, and with respect to the value of spectral density (respectively the frequency and spectral drops). The frequencies at which the indicated maximum drops are noted are multiples of each other.

2. With ridge roughness of the bottom the zone of the lower part, like the transit part of the flow has a stratified structure. The dimensions of the eddy structural formations in the transit portion of the flow significantly exceed the dimensions of these formations in the region of the ridge lower portion. With ridgeless small-scale roughness the division into layers is similar to the transit portion of the flow.

3. The qualitative course of changes with respect to depth of the Euler scales and the scales that determine the boundary of transition from one structural formation to another is the same, which is a confirmation of the hypothesis on the multiplicity of the turbulence scales existing in the flow. The multiplicity of the turbulence scales also governs the multiplicity of the boundaries of eddy formations marked by increased drops both with respect to frequency and with respect to the value of spectral density.

4. In the troughs with ridgeless bottom the maximum Euler turbulence scale computed with respect to the time of the zero correlation for the longitudinal velocity component has a multiple link to the length of the trough. The multiplicity coefficient is determined by the type of bottom roughness.

BIBLIOGRAPHY

1. Berlin, G.S.; and Rozentul, S. A. "Mekhanotronnyye preobrazovateli i ikh primeneniye" [Mechanotron Converters and Their Application], Moscow, Energiya, 1974, 240 p.

2. Denisov, Yu. A.; Maslov, V. K.; Melekhova, N. A.; and Mikhaylova, N. A. "Distribution of Characteristic Frequencies in Spectrum of Turbulent Velocity Pulsations," TRUDY VNIIFTRI, No 34(64), 1977, pp 43-51.

3. Korchokha, Yu. M. "Study of Ridge Motion of Sediments in Polomet' River," TRUDY GGI, No 161, 1977, pp 98-119.

4. Loytsyanskiy, L. G."Mekhanika zhidkosti i gaza" [Mechanics of Liquid and Gas], Moscow, Nauka, 1973, 847 p.

5. Melekhova, N. A. "Study of Kinematic Structure of Flow with Ridge-Shaped Bottom," GIDROTEKHNICHESKOYE STROITEL'STVO, No 2, 1977, pp 30-34.

6. Melekhova, N. A.; Mikhaylova, N. A. "Turbulent Exchange in Flow with Ridge Bottom," METEOROLOGIYA I GIDROLOGIYA, No 4, 1978, pp 82-87.

7. Melekhova, N. A. "Correlation Analysis of Velocity Pulsations with Rough Bottom," TRUDY VNIIFTRI, No 34(64), 1977, pp 30-36.

UDC 633.11:577.95

INFLUENCE OF WEATHER ON SIZES AND DEPTH OF THE TILLERING NODE OF WINTER WHEAT

Moscow METEOROLOGIYA I GIDROLOGIYA in Russian No 5, May 79 pp 87-92

[Article by Candidate of Biological Sciences A. I. Mitropolenko, Krasnograd Experimental Station, submitted for publication 30 Oct 78]

Abstract. Studies have established that depending on the agrometeorological conditions after the epicotyl stops growing further differentiation into nodes and internodes occurs in the tillering node of winter wheat, previously formed internodes gradually expand and growth cones are carried to the soil surface. The tillering node enlarges, while the protective function of the near-surface soil layer is reduced, especially in plants of early sowings.

[Text] In our country winter wheat is the most important food crop. However, in individual years the grain harvest is sharply reduced as a consequence of the death or damage to the plants from unfavorable wintering conditions. Many researchers have indicated that the hibernation of plants is determined by the state of the tillering node which is the most resistant to all possible fall-winter adversities. When it is preserved the plants are capable of regenerating roots, leaves, shoots, and of forming a good harvest [1-3, 7, 9-13, 15, 16].

We studied the process of tillering node formation (from the appearances of shoots to the end of the fall vegetation) and its carrying to the soil surface in plants of winter wheat in the fall period of vegetation under different conditions of growing.

The experiment work was carried out at the Krasnograd experimental station of the All-Union Scientific Research Institute of Corn in 1970-1978. Plants of eight studied types (zoned and long-term) were selected from a plot of sowing of 16 August, 7 and 25 September (early, optimal and late periods for the given zone). Morphophysiological studies of the growth cones were made according to the technique developed in the laboratory of plant development biology of Moscow State University [10]. Measurements were made of adjacent nodes and internodes of the forming tillering node or the developing underground stem of the main shoot, the number of formed metamers was counted, and their length and width were determined. The depth of occurrence of the tillering node was established according to the generally accepted technique [5]. The soil and air temperatures were determined with the help of soil, minimum and standard thermometers. The seeds were sown to a depth of 5-6 cm.

The most active factors affecting the depth of occurrence of the tillering node under natural conditions of growth according to A. I. Nosatovskiy are the intensity and duration of illumination, as well as the air temperature [15]. The lower the temperature at this time, the deeper the tiller node is laid. This is also indicated by the results of our experiments (table 1). Analysis of the data we obtained indicates that the conditions of the medium have a direct effect first of all on the epicotyl growth. Thus, the location of the tillering node from the soil surface directly depends on the length of this organ. Studies have established that the least intensive elongation of epicotyl cells occurs in plants of middle, and especially later sowings, as a consequence of which their tillering node is laid at a greater depth. The growth of the epicotyl in plans of early (August) sowings under conditions of intensive solar illumination and high temperatures is significantly intensified which promotes the carrying of the tillering node much closer to the soil surface.

Based on previously conducted extensive research [2, 7, 10, 12, 13, 17], as well as on our multiple-year data (tables 1-3) it follows that the depth of occurrence of the tillering node in winter wheat plants strongly varies due to the growing conditions. The depth of its placement in the soil is affected primarily by the planting periods, the precursors and strain peculiarities. As we see from the data of tables 1-3, the distance of the tillering node from the soil surface increases by the later sowing periods with respect to all the precursors, and to the greatest degree with respect to the fallow land. We did not find clear differences by strains in this respect, however, with respect to triticale Amphidiploid-206 we see its maximum approach to the soil surface in plants of the early sowing periods. In this respect density and type of the soil, depth of raking, and size of the seeds are of great importance. The depth of occurrence is affected the greatest by chlorocholine chloride (CCC, TUR) when the seeds are treated semidry before sowing. Deepening of the tillering node as compared to the control increases in plants from the treated seeds 1.5-2-fold, and reaches 4-6 cm [4]. Thus, by the time the winter vegetation ends in winter wheat there is a different depth of occurrence of the tillering node, often lower than 3 cm and not coinciding with that accepted for measuring soil temperature during hibernation [8, 12, 18]. Moreover, on individual fields there is a considerable spatial variation in the location of the tillering node in the near-surface soil layer [12] which is important for the hibernation of the node and the further formation of output by these plants.

It is also well known that the environmental conditions in the fall vegetation period do not promote the intensive development of vegetation cones in winter wheat plants. At this time the cone is mainly enlarged in volume

Table 1. Length of Epicotyl and Depth of Occurrence of Tillering Node in Relation to Weather Conditions

Indices		Sowing periods		
		16 Aug	7 Sep	25 Sep
Daily average air temperature during period "sowing-sprouts," °C		23.2	13.6	6.4
Daily average soil temperature at depth 5 cm during period "sowing-shoots," °C		27.1	15.2	7.0
Length of day in hours during this period		14.19	12.55	11.44
Cloud cover in points during the periods:				
"sowing-shoots"	general	4.3	5.2	5.8
	lower	3.0	3.4	3.6
"shoots-tillering"	general	3.3	5.6	7.2
	lower	1.7	3.7	5.2
"sowing-end of vegetation in fall period	general	5.8	6.4	6.8
	lower	4.2	4.7	4.9
Length of epicotyl, cm		3.95	3.30	1.80
Depth of occurrence of tillering node, cm		2.00	2.68	4.20
Number of days from shoots to tillering		19	25	47

by thickening and elongation, while at its base, as indicated by our studies, separation into nodes and internodes of the underground stalk occurs such that each of the newly formed metamers gradually carries to the soil surface growth cones of the main and lateral, more developed shoots, thus stretching and elongating the zone of the tillering node.

It is quite natural that the differentiation and dynamics of tillering node change in different plants of winter wheat in the fall period of vegetation do not at all occur in the same way. This process is affected the most by the duration and conditions of growth in the period "shoots-end of fall vegetation." In this case strain peculiarities, CCC treatment of the seeds and much more play the decisive role. And if, regardless of the time of sowing, the length of the rudimentary stem when the epicotyl stops growing usually equals 1.5-2.0 mm (measurement of the depth of laying and of occurrence of the tillering node is made at the site of attachment of the first rudimentary leaf), then in the next certain changes occur with the tillering node: in plants a very slow increase begins in the tillering node from the bottom to the top, as a result of which the growth cones of the main and lateral more developed shoots are carried considerably closer to the soil surface than occurred in the cessation of epicotyl growth.

Under comparatively favorable conditions of fall vegetation which are usually combined for plants of the early sowing periods intensified differentiation of the underground stem of the main shoot occurs, as well as intensive expansion of the tillering node from the bottom upwards (table 2). Moreover these plants by the end of the fall vegetation end the vernalization processes and already are at the third stage of organogenesis, which entails extension and elongation of the growth cone [3, 10].

Table 2. Depth of Laying of Tillering Node (mm), Dynamics of Its Development, and Distance (mm) between Soil Surface and Growth Cones of Main Shoot Depending on the Growing Conditions by the Time the Fall Vegetation Ends

(1) Показатели	1971			1972		
	(2) Сроки посева					
	16 VIII	7 IX	25 IX	16 VIII	7 IX	25 IX
(4) Глубина заложения узла кущения	20,0	27,5	28,7	20,0	26,8	42,0
(5) Длина подземного стебля от сближенных узлов и междоузлий, мм	13,1	7,2	3,5	11,7	6,8	2,6
(6) Число подземных междоузлий стебля	9,3	7,6	4,1	9,0	7,2	3,8
(7) Длина конуса нарастания	0,85	0,60	0,33	0,70	0,52	0,29
(8) Расстояние между конусом нарастания и поверхностью почвы	6,05	19,70	24,87	7,60	19,49	39,11

(1) Показатели	1973			1974			(3) Среднее		
	(2) Сроки посева								
	16 VIII	7 IX	25 IX	16 VIII	7 IX	25 IX	16 VIII	7 IX	25 IX
(4)	19,5	26,0	37,0	18,7	27,9	35,9	19,6	25,8	35,9
(5)	10,7	4,5	2,3	14,2	10,5	4,2	12,4	7,2	3,2
(6)	8,4	5,5	3,0	9,7	7,6	4,9	9,1	7,0	3,9
(7)	0,59	0,36	0,19	0,77	0,50	0,31	0,73	0,49	0,28
(8)	8,11	23,51	34,51	3,70	16,9	30,5	6,36	19,75	32,25

Key:
1. Indices
2. Sowing periods
3. Average
4. Depth of laying of tillering node
5. Length of underground stem from adjacent nodes and internodes, mm
6. Number of underground internodes of stem
7. Length of growth cone
8. Distance between growth cone and soil surface

reduction in the air temperature, decrease in the day and shortening of the fall vegetation period in plants of the middle planting periods somewhat delay differentiation and expansion of the underground stem, and as a result, promote the deeper laying of the tillering node.

Table 3. Depth (mm) of Laying of Tillering Node (A) and Distance (mm) between Growth Cone of Main Shoot and Soil Surface (B) Depending on Sowing Periods, Precursors, Crop and Strain Peculiarities, 1977

(1) Культура, сорт	(2) Сроки посева					
	16 VIII		7 IX		25 IX	
	A	B Б	A	B Б	A	B Б
			(3) *Черный пар*			
(4) Озимая пшеница Мироновская-808	19,4	12,6	26,0	21,5	30,0	27,0
(5) Мироновская-808 улучшенная	21,8	14,4	26,2	21,6	30,0	27,1
(6) Харьковская-63	19,4	12,6	26,1	21,8	31,0	28,4
(7) Днепровская-782	19,4	12,4	32,0	27,6	35,0	31,6
Ахтырчанка (8)	21,7	14,1	31,0	27,0	33,0	31,1
(9) Безостая-1	19,0	11,5	26,0	21,8	27,0	24,1
(10) Тритикале Амфидиплоид-206	11,4	4,0	27,0	22,7	28,0	25,0
			(11) *Горох на зерно*			
(4) Озимая пшеница Мироновская-808	18,5	13,1	21,9	17,7	27,0	24,3
(5) Мироновская-808 улучшенная	21,0	15,2	22,2	18,0	29,0	25,9
(6) Харьковская-63	18,5	12,2	21,0	17,2	30,0	27,0
Днепровская-782 (7)	21,0	14,3	24,0	19,8	32,0	29,8
(8) Ахтырчанка	20,0	14,2	21,3	16,9	31,0	28,2
			(12) *Кукуруза на силос*			
(4) Озимая пшеница Мироновская-808	16,0	10,1	22,2	19,6	25,1	21,9
(5) Мироновская-808 улучшенная	17,0	11,5	18,0	14,1	29,0	25,4
(6) Харьковская-63	20,0	14,9	20,0	16,3	31,1	28,0
(7) Днепровская-782	22,0	16,3	21,0	17,2	28,0	24,9
Ахтырчанка (8)	20,0	14,3	23,0	19,8	30,9	26,9

Key:
1. Crop, strain
2. Sowing periods
3. Fallow land
4. Mironovskaya-808 winter wheat
5. Mironovskaya-808, improved
6. Khar'kovskaya-63
7. Dneprovskaya-782
8. Akhtyrchanka
9. Bezostaya-1
10. Triticale Amphidiploid-206
11. Pea for grain
12. Corn for silage

In plants of the late sowing periods the rudimentary stems before going into winter are usually in the beginning of differentiation into nodes and internodes having small dimensions. The deepest laying of the tillering node in plants of these sowing periods, the insignificant development of the rudimentary stem and the growth cone practically do not alter the positions of the latter in the near-surface layer of soil.

As the studies showed, the more developed lateral shoots have the length of the underground stem, close to the length of the main shoot. Therefore the carrying of the growth cones to the soil surface is also observed in them. The same law occurs in all the uncovered plants regardless of the sowing periods.

The studies also show that the process of expansion of the tillering node of plants in the fall in different years does not occur in the same way, which is demonstrated by the data of tables 2 and 3. Thus, in plants of the early sowing periods it is increased, moving the growth cones in separate years to 1.5 centimeters, and on the average--somewhat over 1 centimeter. In plants of the optimal planting periods the tillering node expands less, and its size fluctuates within 0.5-1 cm. In plants of the late sowings it is changed little.

Table 3 presents data on the carrying of the growth cones in plants of winter wheat depending on the precursors and the sowing periods. Although the conditions in the fall of this (1977) year were anomalous for the plant development, growth of the underground stem and cone (daily average air temperature in September and October was 4-6°C lower than the mean for many years), nevertheless certain conclusions can be drawn. It was established that the distance between the growth cone and the soil surface in plants of the majority of the studied strains with respect to the non-fallow precursors is smaller than for the fallow, and that the underground stem develops better in winter wheat sown with respect to good precursors.

Thus, in the tillering node the position of the adjacent nodes and internodes does not remain unchanged after the growth of the epicotyl stops. Due to the absence in the fall period of conditions for the development of a rudimentary ear further differentiation into nodes of the internode occurs, the gradual elongation of the tillering node, and carrying closer to the soil surface of the growth cones of the main and more developed two-three shoots.

The maximum convergence of the growth cones to the soil surface in plants of the early sowing periods is promoted by: elongation of the epicotyl during the appearance of shoots, appearance of new and growth of previously formed nodes and internodes from bottom to the top, and increase in the dimensions of the growth cones passing to the third stage of organogenesis.

The given analysis that shows the movement of the cones to the surface of the soil is of definite importance from the viewpoint of the resistance of winter wheat plants to the unfavorable hibernation conditions, and primarily, to low temperatures. Based on the obtained experimental material it is possible to reveal one of the aspects of the death of the most developed shoots and the tillering node itself. Agrometeorologists [12, 18] indicate that at a depth of 2.5-3.0 cm the temperature on the average is higher by 3.5-8.5°C than on the soil surface. At the same time at a depth of 1-1.5 cm this difference reaches only 2-3°C, i.e., more severe conditions are created for the hibernation of the wheat. It is quite natural that at the depth we indicated for the placement of the growth cones in plants of August sowings (0.5-1 cm) the temperature difference here as compared to the depth of laying of the tillering node is even more reduced, despite the certain thermal-insulating role of the thickest herbage of these sowings [11]. This, in turn, has a fatal effect on the resistance of the most developed and closest growth cones to the soil surface. Moreover, these shoots always die earlier, even with equal temperature conditions for the entire tillering node [6,10].

The death of the most developed shoots with the preservation of the tillering nodes capable of generating new shoots and roots results in the fact that the winter wheat harvest is formed either on the late-fall shoots in which the growth cone is not differentiated, or of very poorly developed spring shoots [10]. Those great advantages in the harvest and early maturation that the winter wheat has over the spring wheat can be easily lost due to the death or even damage to the growth cones of the fall shoots [12].

It follows from the statements that the resistance of the plants of the early sowing periods to low temperatures is affected not only by the high degree of their development, with the consequences that follow from this, but also the very close location of the cones of the main and lateral shoots to the soil surface as a consequence of the change in the sizes of the tillering node. In such cases there is a sharp reduction in the protective function of the near-surface layer of soil. Moreover, they, according to [12] will be located in the soil layer in which the plants are exposed to the greatest measure to the effect of sharp temperature fluctuations. A somewhat reduced threat in this respect occurs for plants of the optimal periods, while for plants of the late plantings relatively more favorable conditions are formed.

Based on the given analysis we consider it expedient to make an additional measurement of the soil temperature at the depth of the tillering node of the main shoots by the time fall vegetation has ended, i.e., in the upper section of the tillering node.

BIBLIOGRAPHY

1. Bondarenko, V. I.; Pistunov, N. I.; and Khmara, V. V. "Zimovka ozimykh khlebov" [Hibernation of Winter Grains], 1972, 80 p.

2. Bondarenko, V. I. "Biologicheskiye osnovy vozdelyvaniya ozimoy pshenitsy v stepnoy zone Ukrainy" [Biological Foundations for the Cultivation of Winter Wheat in the Steppe Zone of the Ukraine], Author's abstract of doctoral dissertation, Khar'kov, 1973, 50 p.

3. Bondarenko, V. I.; and Mitropolenko, A. I. "Effect of Vegetation Conditions on the Growth, Development, Hardiness and Harvest of Strains of Winter Wheat in the Northern Ukrainian Steppe," BYULLETEN' VNII KUKURUZY, No 1(45), 1977, pp 59-63.

4. Grichenko, A. L. "Primeneniye CCC dlya povysheniya vyzhivayemosti pshenitsy v neblagopriyatnykh usloviyakh proizrastaniya" [Use of CCC to Increase Survival Rate of Wheat in Unfavorable Vegetation Conditions], Candidate dissertation (All-Union Scientific Research Institute of Corn), Dnepropetrovsk-Kiev, 1971, 210 p.

5. Dobrynin, G. M."Rost i formirovaniye khlebnykh i kormovykh zlakov" [Growth and Formation of Grain and Fodder Cereals], Leningrad, Kolos, 1969, 276 p.

6. Zadontsev, A. I.; and Bondarenko, V. I. "Hardiness and Productivity of Different-Aged Shoots of Winter Wheat and Rye Depending on Vegetation Conditions and Strain," AGROBIOLOGIYA, No 1, 1963, pp 44-50.

7. Zadontsev, A. I.; Pikush, G. R.; and Grinchenko, A. L. "Deepening of Tillering Node and Increase in Productivity of Winter Wheat under the Influence of Chlorocholine Chloride," VESTNIK SEL'SKOKHOZYAYSTVENNOY NAUKI, No 1, 1970, pp 26-32.

8. "Kratkiy agroklimaticheskiy spravochnik Ukrainy" [Concise Agroclimate Reference of the Ukraine], edited by K. T. Logvinov, Leningrad, Gidrometeoizdat, 1976, 255 p.

9. Kuperman, F. M. "Diagnosis of the State of Winter Sowings in the Fall-Winter Period by the Method of Charting the Decisive Hibernation Complexes," METEOROLOGIYA I GIDROLOGIYA, No 3, 1939, pp 83-91.

10. Kuperman, F. M. "Biologicheskiye osnovy kul'tury pshenitsy" [Biological Foundations for Wheat Cultivation], Pt 1, 1950, Pt 2, 1953, Moscow, Izd-vo MGU.

11. Mitropolenko, A. I. "Osobennosti formirovaniya vegetativnykh i reproduktivnykh organov ozimoy pshenitsy, eye zimostoykost' i produtivnost' v severnoy step USSR" [Peculiarities of the Formation of the Vegetative and Reproductive Organs of Winter Wheat, Its Hardiness and Output in the Northern Steppe of the Ukrainian SSR], Candidate dissertation (All-Union Scientific Research Institute of Corn], Dnepropetrovsk, 1974, p 228.

12. Moiseychik, V. A. "Agroklimaticheskiye usloviya i perezimovka ozimykh kul'tur" [Agroclimate Conditions and Hibernation of Winter Crops], Gidrometeoizdat, 1975, 296 p.

13. Mosolov, V. P. "Zimnyaya agrotekhnika" [Winter Agricultural Technology], Vol 2, Moscow, 1953, 488 p.

14. "Nastavleniya gidrometeorologicheskim stantsiyam i postam" [Instructions to Hydrometeorological Stations and Posts], No 11, Pt 3, Leningrad, Gidrometeoizdat, 1973, 288 p.

15. Nosatovskiy, A. I. "Pshenitsa (biologiya)" [Wheat (Biology)], Moscow, Sel'khozgiz, 1950, 407 p.

16. Tumanov, I. I. "Fiziologicheskiye osnovy zimostoykosti rasteniy" [Physiological Foundations for Plant Hardiness], Moscow-Leningrad, Sel'khozgiz, 1940, 366 p.

17. Tsybul'ko, V. S. "Effect of Strain Peculiarities and External Factors on Depth of Occurrence of Tillering Node of Winter Wheat," TRUDY KHAR'KOVSKOGO S-KH. IN-TA IM. V.V. DOKUCHAYEVA, Vol 18, 1959, pp 47-66.

18. Shul'gin, A. M. "Peculiarities of Climate Conditions of Winter Period in Southern USSR and Consideration of Them in Selecting Winter Wheats," "Metody selektsii zimostoykikh pshenits" [Methods of Selecting Hardy Wheats], Moscow, Sel'khozgiz, 1962, pp 142-151.

UDC 551.50:633.11(470.6)

AGROCLIMATE RESOURCES AND POTENTIAL YIELDS OF WINTER WHEAT GRAIN IN FOOTHILLS OF NORTHERN CAUCASUS

Moscow METEOROLOGIYA I GIDROLOGIYA in Russian No 5, My 79 pp 93-98

[Article by Candidate of Agricultural Sciences E. D. Adin'yayev, Gorskoye Agricultural Institute, submitted for publication 27 Oct 78]

Abstract. An examination is made of the agroclimate resources of the Northern Caucasus foothills and their effect on the formation of the biological output of winter wheat.

It is theoretically and experimentally established that with an efficient use of agroclimate resources of this region, without additional outlays for irrigation and fertilization the following yields of winter wheat grain can be obtained: for the Kabardino-Balkarskaya ASSR--18-25 centner/ha; Severo-Osetinskaya ASSR--19-32 centner/ha; and Checheno-Ingushskaya ASSR--15-24 centner/ha.

The findings serve as the basis for determining the need of the region for water and fertilizers for the planned yield level.

[Text] Among the problems of national economic importance whose solution is necessary for the growth and development of agriculture the first place belongs to the problem of the most complete and highly productive use of the land, its protection, and increase in soil fertility.

Planning of agricultural production and the measures for land use is implemented according to administrative oblasts, krays and republics. However, many oblasts, krays and republics differ in natural conditions, others are similar to each other in conditions and potentialities for agricultural development, and they can be viewed as single natural-agricultural complexes separated by administrative boundaries.

Under the extant natural-agricultural zoning one rayon includes the territories of the Kabardino-Balkarskaya, Severo-Osetinskaya and Checheno-Ingushskaya autonomous republics, otherwise called the Northern Caucasus foothills.

The natural-agricultural zoning of the Northern Caucasus foothills is based on an analysis of the natural conditions from the viewpoint of their value in agricultural production. Therefore the goal of our research is to find the most optimal methods for using the agroclimate resources of the Northern Caucasus based on an investigation of the natural conditions, and the knowledge of the laws governing the harvest in the system "plant-soil-climate-cultivation technology."

This work presents studies on the systemization of agrometeorological factors as applied to a determination of the size of potential winter wheat yields in the examined region.

Only the most important climate indices can be practically used for agroclimate zoning of the territory. These indices, in our opinion, must be fairly simple, clear and accessible. Many researchers mainly base zoning on consideration of temperature, air humidity, and amount of precipitation, since there are still few actinometric data for these purposes, while the amount of photosynthetically active radiation on the examined territory does not limit the development of agricultural crops.

Taking into consideration the most significant features of the soil-climate and economic conditions, as well as the extant production trend, habits and accumulated experience in the operation of the kolkhozes and sovkhozes of the Northern Caucasus foothills, in our opinion, one can separate three main natural-economic (agricultural) zones: plain (steppe), foothill, and mountain. The zones of plains and foothills of the republics are of great importance for agricultural production. They are arranged in the following order: grassy-wormwood steppe with insufficient moistening on chestnut brown soils; mixed grass-grassy steppe with unstable moistening on carbonate-chernozem soils; forest steppe (Agropyron-mixed grass meadow steppes) with unstable and sufficient moistening on leached, less often podsolized chernozems.

For the climate characteristics of the Northern Caucasus foothills data were used of the meteorological stations Mozdok, Prokhladnaya, Kotlyarevskaya, Terek, Mikhaylovskaya, Zamankul, Ordzhonikidzevskaya, Groznyy and Gudermes.

In the evaluation of climate as one of the factors of the general potential output of the land we used as a criterion the bioclimatic potential (BCP)--a complex amount that takes into consideration the effect of elements of the biochemical effectiveness of climate.

The bioclimatic potential in each specific case can be determined according to the equation

$$\text{BCP} = K_p \cdot \frac{\Sigma t > 10\,^{\circ}\text{C}}{1000\,^{\circ}\text{C}} - \text{ point}$$

where K--coefficient of biological output;

$\Sigma t > 10\,^{\circ}$C--sum of temperatures above 10°C;

1000°C--sum of temperatures on northern boundary of field cultivation.

Table 1. Scale of Biological Productivity (from D. I. Shashko, 1967)

Biological productivity	$\Sigma t > 10°C$	BCP
Very low	800	0.8
Low	800-1200	0.8-1.2
Reduced	1200-1600	1.2-1.6
Average	1600-2200	1.6-2.2
Increased	2200-2800	2.2-2.8
High	2800-3400	2.8-3.4
Very high	3400	3.4

The bioclimatic productivity of the land synthesizes in itself the effect on plant productivity of the main factors of their vital activity; heat and moisture supply. In order to evaluate the biological productivity of the land D. I. Shashko (1967) developed a scale constructed on the basis of the amounts of bioclimatic potential (table 1).

The relative amounts of potential productivity are translated into the crop yield according to the equation

$$m = \frac{K'_p}{K_p} \cdot 10 \quad \text{BCP}$$

where m--grain yield, centner/ha;

K'_p--coefficient of crop productivity (yield corresponding to 100°C sums of temperatures) according to empirical data (determined according to index of moistening M_d);

K_p--coefficient of biological productivity that depends on the moisture supply of plants and that is the ratio of maximum productivity under conditions of sufficient moistening to productivity with insufficient moisture.

The coefficient of biological productivity was defined by us from the formula

$$K_p = \frac{WT_v}{36R},$$

where W--productive moisture in meter layer of soil during spring maturation of wheat, mm;

T_v--period of spring-summer vegetation, ten-day periods;

36--number of ten-day periods in the year;

R--radiation balance during this period, kcal/cm^2.

The indices of biological productivity of a plowed field that we computed by zones of the Northern Caucasus republics proved to be considerably lower than the data of D. I. Shashko (table 2).

Table 2. Biological Productivity of Land for Main Zones of Northern Caucasus Foothills

(1) Республика	(2) Зона	$\Sigma t > 10°C$	(3) БКП	Biological productivity by $\Sigma t > 10°C$	Biological productivity by BCP
(4) Кабардино-Балкарская АССР	I	3377	2,30	high	elevated
	IIа	3377	2,27	"	"
	IIб	3253	2,44	"	"
(5) Северо-Осетинская АССР	I	3590	1,90	very high	average
	II	3110	2,61	high	elevated
	III	2800	2,64	elevated	"
(6) Чечено-Ингушская АССР	Iа	3658	1,54	very high	reduced
	Iб	3615	1,52		
	II	3335	2,27	high	elevated

Key:
1. Republic
2. Zone
3. BCP
4. Kabardino-Balkarskaya ASSR
5. Severo-Osetinskaya ASSR
6. Checheno-Ingushskaya ASSR

Table 3. Biological Potential of Productivity and Grain Yield (m) of Winter Wheat in Main Zones of Northern Caucasus Foothills

(1) Республика	(2) Зона	M_d	K'_p	K_p	(3) БКП	(4) m ц/га
(5) Кабардино-Балкарская АССР	I	0,25	0,86	0,68	2,30	28,9
	IIа	0,25	0,86	0,68	2,27	28,6
	IIб	0,28	0,92	0,75	2,44	30,0
(6) Северо-Осетинская АССР	I	0,19	0,67	0,53	1,90	23,9
	II	0,34	1,04	0,84	2,61	32,1
	III	0,43	1,16	0,94	2,64	32,5
(7) Чечено-Ингушская АССР	Iа	0,16	0,52	0,42	1,54	18,9
	Iб	0,16	0,52	0,42	1,52	18,7
	II	0,25	0,86	0,68	2,27	28,6

Key:
1. Republic
2. Zone
3. BCP
4. m centner/ha
5. Kabardino-Balkarskaya ASSR
6. Severo-Osetinskaya ASSR
7. Checheno-Ingushskaya ASSR

Analysis of the data of tables 1 and 2 shows that the biological productivity of the plowed fields on the territory of the Kabardino-Balkarskaya ASSR according to the sum of temperatures is classified as high, while according to Shashko's formula--only as elevated. A more contrasted relationship is revealed for the territory of the Severo-Osetinskaya ASSR whose biological productivity according to the sum of temperatures is very high, and according to BSP--reduced. In our opinion, such a difference is governed by the fact that in Shashko's calculations K_p is taken for all the climate zones as equal to a unit (K_p=1.0). At the same time, K_p in the Kabardino-Balkarskaya ASSR fluctuates from 0.68 to 0.75; in the Severo-Osetinskaya ASSR--from 0.53-0.94, and in the Checheno-Ingushskaya ASSR--from 0.42 to 0.68.

Having determined from the index of moistening ($M_d = \frac{p\text{(precipitation)}}{f\text{(evaporation)}}$) the zone of location of the farm it is easy to compute the possible grain yield of winter wheat (table 3).

The BCP is an integral index since it makes it possible to evaluate the yield obtained in different soil-climate conditions and different natural-botanical zones, in the same comparable units.

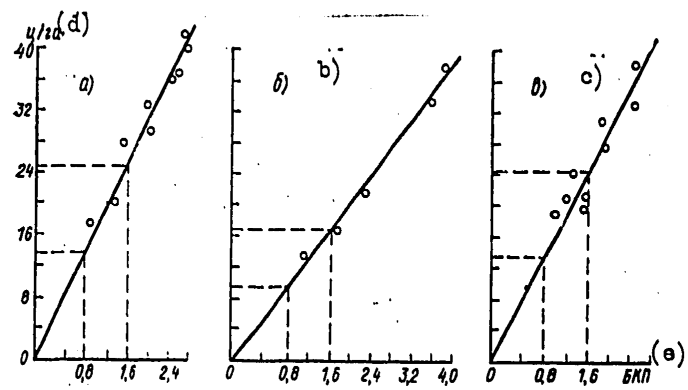

Figure 1. Relationship of Winter Wheat Yield (a, c) and Grains as a Whole (b) to Climate Potential

Key:

a. according to data of SSS of Northern Caucasus foothills
b. according to data of D. I. Shashko
c. according to data of experimental studies of author in Northern Caucasus foothills
d. centner/ha
e. BCP

In order to substantiate this conclusion we revealed the relationship of the bioclimatic potential of land productivity as compared to the yields obtained at the state strain-testing stations (SSS) located on the territory of the examined region. In Kabardino-Balkarskaya ASSR the winter wheat grain yield Bezostaya-1 for 1967-1975 according to strain-testing stations was from 26.4 to 44.2 centner/ha, in Severo-Osetinskaya ASSR--from 24.5 to 41.2 centner/ha, and in Checheno-Ingushskaya ASSR--from 26.1 to 31.4 centner/ha.

Figure 1 depicts the dependence of the averaged grain yield of this strain on the BCP in the examined region.

For comparability of the data taken from Shashko's graph that he compiled for all the grains as a whole (fig 1b) and that we compiled for the winter wheat (fig 1c) the sizes of winter wheat grain yields were determined for one unit of BCP. According to Shashko's data for one unit of BCP there is 1.09 centners of grain, and according to our calculations for Bezostaya-1 winter wheat in the examined region--1.54 centners; thus the difference is 0.45 centners or 41%. Shashko's method, in our opinion, is correct, but its use in different regions currently requires the introduction of appropriate corrections for the increased level of agricultural technology of the cultivated crops and genetic potential of the strains of winter wheat of the intensive type introduced into production.

Table 4. Biological Productivity of Winter Wheat with Natural Moisture Supply

(1) Республика	(2) Зона	(3) $\Sigma t > 10°C$ за весенне-летний период вегетации	(4) Сумма осадков за период с $\Sigma t > 10°C$, мм	(5) W мм в весенний период	(6) Всего продук. влаги с учетом коэф. их использов., мм	(7) Кв, м³/ц	(8) Возможный урожай, ц/га	(9) БКП
(10) Кабардино-Балкарская АССР	I	1620	204	81	224	1200	18,7	1,10
	IIа	1580	195	94	231	1100	23,4	1,07
	IIб	1555	217	120	272	1000	24,7	1,16
(11) Северо-Осетинская АССР	I	1572	185	85	215	1250	17,2	0,83
	II	1555	264	112	307	1100	27,9	1,31
	III	1526	330	87	318	900	35,3	1,43
(12) Чечено-Ингушская АССР	Iа	1746	170	90	209	1250	16,7	0,73
	Iб	1738	192	98	242	1100	22,0	0,73
	II	1580	235	95	260	1085	23,9	1,07

Key:

1. Republic
2. Zone
3. $\Sigma t > 10°C$ for spring-summer vegetation period
4. Sum of precipitation for period with $\Sigma t > 10°C$, mm
5. W mm in spring period
6. Total productive moisture with regard for coefficient of utilization, mm
7. Ke, m³/centner
8. Possible yield, centner/ha
9. BCP
10. Kabardino-Balkarskaya ASSR
11. Severo-Osetinskaya ASSR
12. Checheno-Ingushskaya ASSR

In relation to the fact that under production conditions the yields are usually lower than on the state strain-testing stations, we attempted to reveal the dependence on the BCP of the yield of the strain Bezostaya-1 obtained in our experiments on the soils with a varying degree of cultivation. In the Kabardino-Balkarskaya ASSR in experiments without the use of fertilizers under natural conditions of moistening for the years of study (1965-1976) in different climate zones 25.1-18.1 centner/ha were obtained, in the Severo-Osetinskaya ASSR--32.1-18.8 centner/ha, and in the Checheno-Ingushskaya ASSR--23.4-14.3 centner/ha (table 5). According to these data a graph was plotted (fig 1c) from which it follows that for one unit BCP 1.38 centners of grain are obtained or 0.16 centners less than according to the SSS data. One should draw the conclusion that the potential productivity of the same strain cultivated under production conditions, as a consequence of the noncorrespondence of the level of crop cultivation with the SSS is 14% lower. These data can be successfully used to substantiate the size of the yield in a specific farm located near the SSS.

Our calculations (table 3) and the experimental data (fig 1c) show that with the efficient use of climate resources of the studied region without additional outlays for irrigation and fertilization the following grain yields of winter wheat can be obtained: for the Kabardino-Balkarskaya ASSR--18-25 centner/ha, for the Severo-Osetinskaya ASSR--19-32 centner/ha, and for the Checheno-Ingushskaya ASSR--15-24 centner/ha.

In addition to the sum of temperatures the moisture supply of the sowings is the most precise expression of the plowed field productivity, and can be placed as the basis for a determination of the size of potential yields of dry biological mass ($Y_{биол}$):

$$Y_{биол} = \frac{\text{productive moisture}}{\text{coefficient of water consumption}}.$$

This relationship according to the definition of grain yield (Y centner/ha) can be determined as:

$$Y\ \text{centner/ha} = \frac{100\ П_в}{2.5\ К_в\ (100 - C)},$$

where $П_в$--moisture output, centner/ha;

$К_в$--coefficient of water consumption;

C--standard moisture content of crop, %;

2.5--ratio of main product to secondary (for winter wheat 1.5 or 2.5).

The productive moisture is formed from its amount in the meter layer of the soil before the renewal of vegetation of the winter crops, precipitation falling in the spring-summer period of vegetation with regard for the coefficient of its utilization.

The greatest quantity of productive moisture (300 mm) in the meter layer of soil is observed in the III zone of the Severo-Osetinskaya ASSR: average (264 mm) in the II zone, and the least (185 mm)--in the I zone. The coefficients of water consumption obtained on the basis of the experimental data showed their inverse relationship to the sum of effective temperatures: in the I zone it was 1200 m^3/centner; in the II zone--1100 m^3/centner and in the III zone--900 m^3/centner of grain. Therefore the fluctuations in the

Table 5. Calculation of Possible Grain Yields of Winter Wheat with Natural Moisture Supply in Northern Caucasus Foothills, 1965-1976

(1) Республика	(2) Зона	(3) Урожай (ц/га) по данным:		
		(4) экспериментальных исследований	(5) влагообеспеченности	(6) ГСУ
(7) Кабардино-Балкарская АССР	I	18,1	18,7	26,4
	IIа	23,6	23,4	41,8
	IIб	25,1	24,7	44,2
(8) Северо-Осетинская АССР	I	18,8	17,2	21,6
	II	25,3	27,9	38,0
	III	32,1	35,3	41,2
(9) Чечено-Ингушская АССР	Iа	14,3	16,7	26,1
	Iб	19,6	22,0	29,2
	II	23,4	23,9	31,4

Key:
1. Republic
2. Zone
3. Yield (centner/ha) according to data
4. of experimental studies
5. of moisture supply
6. SSS
7. Kabardino-Balkarskaya ASSR
8. Severo-Osetinskaya ASSR
9. Checheno-Ingushskaya ASSR

yields reach considerable amounts: the greatest possible yield of winter wheat grain with respect to moisture supply (35.5 centner/ha)--in the III zone of the Severo-Osetinskaya ASSR, the medium (27.9 centner/ha)--in the II zone, and the least (17.2 centner/ha)--in the I zone.

Similar calculations were made also for the zones of other republics of this region (table 4).

The results of calculations of the possible winter wheat grain yields made on the basis of the experimental data we obtained and from moisture supply differed insignificantly (table 5). For dry conditions these methods of calculation are completely applicable and serve as the foundation for a determination of the need for water for the planned level of productivity.

It should be considered that the yield sizes are governed by the moisture supplies formed from productive water in the soil and precipitation of the vegetation period, and they are close to the mean multiple-year data. The size of the yield obtained on the SSS is affected not only by the thermal, water and air patterns, but also by the higher level of agricultural technology, as well as the potentialities of the genotype placed in the first generation of the initial material. These data can also be used in selecting a highly productive strain for productive sowings with correction for the moisture supply of the plants in each specific case.

Consequently, with the natural moisture supply the potential winter wheat grain yields in different agroclimatic zones of the Northern Caucasus foothills fluctuate from 16 to 35 centner/ha. The further rise in the yield of this crop requires an improvement in the moisture supply of the sowings by means of irrigation.

The data that we obtained according to the BCP can be used to compute a more efficient pattern of irrigation in the Northern Caucasus foothills and the optimal use of the soil fertility.

UDC 551.576.11:535.317.1

USE OF IMAGE TECHNIQUE TO STUDY CLOUD AND FOG MICROSTRUCTURE

Moscow METEOROLOGIYA I GIDROLOGIYA in Russian No 5, May 79 pp 99-105

[Article by Candidate of Physical and Mathematical Sciences V. V. Smirnov, and G. F. Yaskevich, Institute of Experimental Meteorology, submitted for publication 4 Jul 78]

Abstract. Possibilities are discussed and ways are shown for improving holographic, shadow, and television methods of studying cloud and precipitation microstructure based on the use of partially coherent illumination, as well as spatial image filtering.

[Text] The diversity of shapes and broad range of concentration, sizes and velocities of cloud and precipitation particles pose serious requirements for the corresponding measuring apparatus. In these terms the optic-electronic methods [1] are the most accepted; they are based on comparatively well revealed links between the parameters of the microstructure of aerodisperse media and the degree of deformation of the optic emissions transmitted through the medium.

Below is a brief examination of the possibilities of improving the so-called "image" methods, i.e., methods based on the formation and automatic analysis of optic images of microobjects in a suspended state and in flows.

Features of Image Methods

Holographic methods. There are several published descriptions of cloud holographic camera modifications (see, for example, [2, 5, 6]) to obtain "frozen" three-dimensional images (holograms) of individual cloud sections. Here the assembly of moving microobjects is illuminated by an intensive impulse of laser radiation with a high degree of temporal and spatial coherence. The hologram is recorded on high-resolution photo-sensitive materials. With the subsequent restoration of the images from the hologram usually the standard microscope technique and sources of continuous coherent radiation are used. The automatic analysis of holograms is made with scanning with respect to the plane and depth of the restored image by a television microscope aperture connected to a computer device. The discreteness of the measurement process and the labor intensity of processing the holograms, complexities in selecting the defocussing images in the presence of coherent noises, as well as a certain awkwardness and high cost of the holographic cameras restrain the broad use of holography.

Shadow spectrometry. The so-called shadow spectrometry of Knollenberg [18] has become considerably widespread in practice; it is based on the formation of optic image elements of single moving microobjects in the plane of the discrete photoreceiver guide bar (matrix). In the initial state the photoreceivers are illuminated by an intensive continuous laser beam with a high degree of spatial coherence. During the flight of a particle through the working volume of the instrument its image, and more precisely, the diffraction shadow from the particle screens a certain number of photoreceivers from direct exposure.

Knollenberg shadow spectrometers are used for the continuous measurement of concentration and dimensions of cloud and rain drops in the interval of diameters 10-4500 μm. These instruments are comparatively simple and are subject to automation, but in contrast to the holographic cameras, they do not permit visualization of the state of the assembly of particles as a whole.

Television methods. It is not difficult to see that the shadow spectrometers are a particular solution of the television (TV) methods in which the role of the TV horizontal scan is played by the photoreceiver guide bar, while the role of the frame scan--by the movement of the monitor in the cloud or particles in relation to the monitor.

In certain designs of TV analyzers [1, 7, 17] the classic schemes of automated TV microprojection systems are realized with impulse source of illumination.

The operating principle of the television analyzer described in [7] is briefly reduced to the following. The impulse light source is started at the moment of the reverse course of the TV beam with respect to the vertical. Through the microscope optics the light impulses illuminate the photolayer of the TV transmitting tube. If at the moment of exposure an object is located in the plane of sighting of the microscope the corresponding segment of the TV screen is unilluminated. During the direct course of the TV scan there is successive reading of information "for storage" and the videosignal at the camera outlet records the corresponding jumps in the level of the "black," their number, and duration are proportional to the dimensions of the object. Certain algorithms of the automatic analysis of TV images designed for obtaining data on the disperse composition of aerosols and the corresponding schematic solutions are described in [4, 7, 10, 11].

On the whole one can include among the advantages of the television methods:

--the possibility of recording on a magnetic carrier and visualization of the studied process on the TV monitor screen;

--complete automation of measurements and making of measurements in a real time scale;
--fairly broad interval of countable concentration (to 10^5-10^6 cm^{-3}) and dimensions (from 2 μm to several mm) of microobjects of fairly arbitrary shape and composition moving with velocities from units of mm/s to tens of mm/s (using laser impulse sources of light the upper limit of velocity can be increased by an order [17];
--simplicity of the metrological base of TV monitors since they can be calibrated directly during the measurements according to standard immobile test objects.

The main and important limitation of such type of TV device, as by the way, also of all microphotographic systems designed to study particles in flows, is the deformation of images of microobjects removed from the plane of sighting.

The microprojection optic systems with sources of noncoherent radiation are characterized by the shallow depth of sharpness: $z \approx 10$-100 μm. With large z the edges of the image are gradually eroded, while the signal amplitude drops. The use for selection of defocussing images of amplitude threshold schemes [7] is ineffective in a broad interval of microobject dimensions, since the amplitude of the videosignal from small particles diminishes during their defocussing considerably faster than from large particles. The limitation in the depth of the visual field results, in turn, in an exacerbation of the informative characteristics of the instrument, i.e., to small volumes of sampling. Thus, with the use of the television counter described in [7] the effective size of the countable volume for particles of radius 2-20 μm equals 0.25 mm^3, which requires exposures lasting about 10 s for a representative series of measurments to be obtained.

As shown in [13, 14] the indicated limitations can be overcome if one considers that generally the nature of the microobject image that is displaced in relation to the sighting plane depends not only on its size, degree of defocussing and geometry of the optic system, but also on the coherent properties of the radiation source. We will examine these questions in more detail.

Role of Radiation Coherence

We will assume that the microobject of spherical shape is located in the visual field of the TV microscope at a distance z from the sighting plane. The distribution of light intensity in this plane is determined by the superposition of waves--incident, diffracted, reflected from the object, and passing through it--and depends on the properties of the light beam, position of the object in relation to the sighting plane, as well as its optic properties.

1. With noncoherent illumination the summation of the listed waves results in the erosion of the edges of the defocussed image and exception complexity of its analysis.

2. If coherent light beams are used for illumination then the interaction of the aforementioned waves yields an interference pattern that is essentially a Gabor hologram [6]. A quantitative analysis of such a pattern when several particles fall in the counting volume is fairly complicated due to the mutual imposition and presence of coherent noises.

Figure 1 presents densitograms obtained during a single scanning of the image of polymethyl methacrylate particles of radius r=150 μm. The particle is displaced in relation to the sighting plane a distance of z=2, 30, 70 mm with completely coherent illumination (a, b, c) and a distance 10 mm with partially coherent illumination (fig 1, d). With short distances to the sighting plane pulsations in the signal on the edges of the impulse are a consequence of Fresnel's diffraction (fig 1,a). In the far field ($z \gg r^2/\lambda \sim 50$ mm) Fraunhofer diffraction is manifest (fig 1,c). It is apparent from the figure that with the use of coherent illumination the diffraction pattern can occupy a considerable part of the visual field of the optic system, impairing the automatic analysis due to the mutual imposition and appearance of additional interference maximums and minimums.

3. Serious outlooks for the image methods are yielded by the use of partially coherent illumination that can be obtained by reducing the temporal or spatial coherence. First, with such illumination the diffraction pattern occupies a considerably smaller part of the visual field, second, one can obtain more accurate information about the particle with comparatively large shifts in it in relation to the sighting plane. As compared to the source of noncoherent radiation the sources of partially coherent radiation produce an increase in the effective depth of the counting volume by more than an order, while as compared to the coherent sources they make it possible to guarantee the conditions for the emergence and recording only of one (first) diffraction ring (see the densitogram in fig 1, d), whereby it is found [16] that its width has little dependence on the particle sizes, and is only linked to the position of the particle in relation to the sighting plane with displacements in the microobjects all the way to units cm.

Television images of spherical particles with radius 26 and 20 μm displaced in relation to the sighting plane by 3 mm are obtained in fig 2,b with the help of a bright-field TV microscope based on a vidicon and source of impulse illumination with length of coherence (6-7) $\bar{\lambda}$, where $\bar{\lambda} \simeq 0.45$ μm. The photography illustrates the possibility of confident recording only of the first diffraction ring. The intensity of the other rings is found on the level of TV tube noises. To the left on the photograph an image of spheres of the same size as those in the sighting plane is visible.

The videosignal from the intersection of the defocussed image has the appearance of a bipolar impulse, which makes it possible to automatically determine the location of the object in relation to the sighting plane (with respect to the width of the ring), precisely determine the size and concentration of the objects falling outside the sighting plane, as well as "electrically" regulate the size of the counting volume along the microscope axis [14]. It is necessary to note that the value of the peculiarities indicated above in

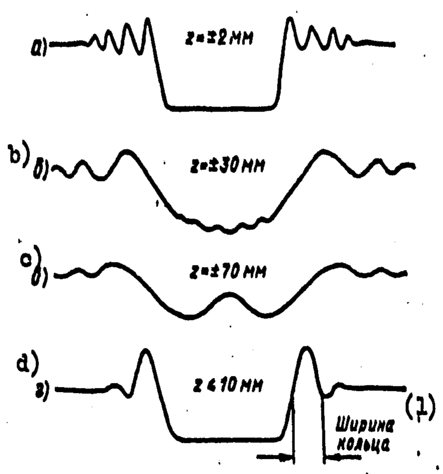

Figure 1. Densitograms of Image of Microsphere for Fresnel's Region (a), Intermediate (b) and Fraunhofer (c) with Coherent Illumination and for Fresnel's Region with Partially Coherent Illumination (d).

Key:
1. Width of ring

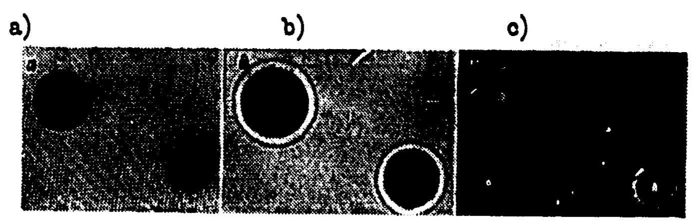

Figure 2. Television Images of Microspheres with Partially Coherent Bright-Field Illumination (a, b) and After Spatial Filtering (c).

the structure of the diffraction pattern of the microobject illuminated by partially coherent light has a more general nature since it provides the prerequisites for the creation of holographic systems operating in a real time scale [15], and for an improvement in the accuracy of the Khollenberg shadow spectrometers due to the electrical selection of signals from the defocussed particle images.

Thus, the examined method of obtaining and analyzing a TV diffraction picture-microhologram obtained with partially coherent illumination makes it possible to solve the problem of the automatic processing of defocussed images of the microobjects. A shortcoming of the method remains the relatively low information content (frequency of changing the subjects cannot exceed the frequency of frames, while the size of the frame is limited by the required resolution), as well as the small upper limit for measuring the motion velocity of microobjects (on the order of units of cm/s with magnification of the microscope of tens of times) that is governed by the peculiarities of the exposure of the photolayers in the bright field pattern.

The method of recording the tracks of rapidly moving particles that is usually realized with illumination by the method of a dark field through recording on a photolayer of a sequence of spots of radiation scattered by the microobject does not solve the problem since the task of measuring the object dimensions requires preservation of information if only about its contour. We will examine one of the ways to overcome the indicated limitations.

Spatial Filtering of Images

As noted, the pattern of bright field is inapplicable since each successive impulse (from the bundle of light impulses during the reverse course of the frame scan) will "erase" the previously recorded potential relief on the photolayer. With the help of track methods an undistorted image of the microobjects is not successfully obtained, and in addition, separation of the boundaries of the counting volume is very complicated.

Nevertheless, the use of the modern methods of optic processing of images makes it possible to obtain in a pattern of a dark field clear images of the contours of objects, and at the same time, additional information about their spatial position [13]. Those images possess such properties that are obtained after double differentiation of the initial image. As is apparent from fig 2,c with the realization of the second derivative the contour of the object is formed as a dark line surrounded from both sides by bright bands; the dark line stresses the smallest details of the surface structure of the microobject.

The experiments not discussed here show that although with defocussing of the similarily formed images there is a certain widening of the contour line and the bright bordering bands, the center of the line corresponds to the contour of the focussed image, while the width of the bright bands can serve as the criterion for a shift in the object in relation to the sighting plane. Thus, the transition to a dark field pattern by spatial filtering of images makes it possible to obtain more complete information about the moving microobjects (size, concentration, shape, velocity, direction and trajectory of movement).

TV Devices

The application of the new approaches examined above to the use of image methods made it possible to create a number of automatic TV analyzers of moving microobjects that are distinguished by fairly high accuracy of measurements, as well as comparative simplicity and universality.

a)

b)

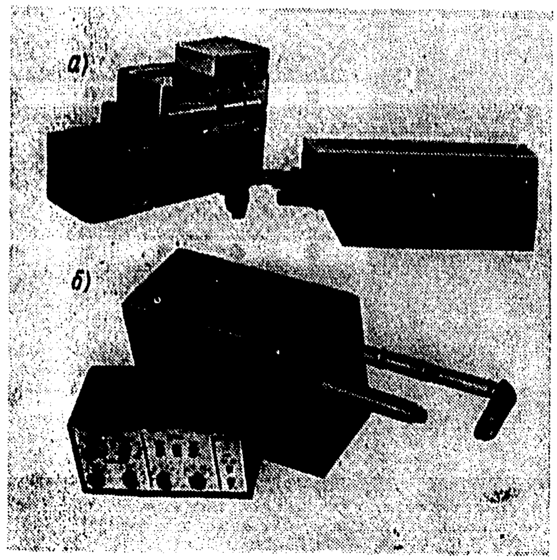

Figure 3. Overall View of TV Analyzers of Moving Microobjects Based on Superorthicon (a) and Vidicon (b)

Figure 3,a shows a photograph of the TV monitor "Mars" for measuring the disperse composition of aerosol particles assembled on the base of an LI-225 superorthicon, a PTU-101 industrial TV unit, and bright-field microscope optics. The monitor is equipped with a set of standard microlenses with magnification 1-10^{x} selected remotely from the control panel, and heaters of microscope optics to prevent their "sweating" during operation in cold chambers and media containing aqueous aerosol. The automated operating cycle of the instrument is preset by a timer that synchronizes the operation of the impulse condenser, the television-computer device, and a 10-channel storage block with output of data onto digital reading and a punch-card machine. The measurement range of the microobject dimensions is 4-1000 μm with concentration of them to 10^4 cm^{-3}.

The TV monitors on modern superorthicons provide "signal-noise" about the size of 10 and the remaining signal with frequency of exposure 50 Hz in the second half-frame less than 10% of the main, but do not always meet the requirements of high homogeneity of the background and compactness of the apparatus, and are also complicated to tune and operate. In this sense the impulse TV analyzers on vidicons guarantee the best indices [13]. However, their increased drift reduces the frequency of information output from 50 to 10-20 Hz, while the reduced sensitivity requires higher energy of flash of 5-10-fold.

The universal TV analyzer based on a half-inch vidicon shown in fig 3,b can operate in a pattern of bright and dark field (with filtering of the lowest spatial frequencies in the image spectrum); it has a built-in generator of bundles of powerful light impulses which makes it possible, in addition to visualize and measure the dimensions and concentration of particles, to control their velocity and direction of movement in the velocity interval of 4-500 cm/s.

Examples of Using TV Technology

We will examine a number of examples of the specific application of TV devices in the practical research of the Institute of Experimental Meteorology.

a) b) c) d) e)

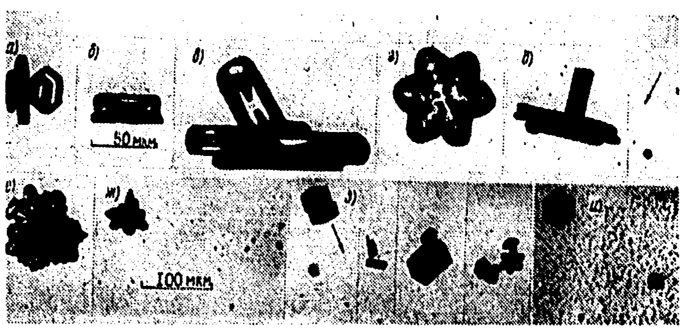

f) g) h) i)

Figure 4. TV Images of Crystalline Fog Particles

1. Microstructure of crystalline fog. One of the promising trends in the use of TV impulse devices is the study of the dimensions, shape, orientation and velocity of movement of crystalline cloud and fog particles. Figure 4 presents individual TV images of crystals formed in several seconds after the effect of artificial nuclei of crystallization (silver iodide) on supercooled aqueous fog in a 100 m^3 thermobarochamber.

The scale of the images shown in fig 4 b and g refers respectively to the upper and lower series of photographs. The use of partially coherent illumination of the working volume of TV monitors made it possible to obtain fairly sharp images of the particles even when they were comparatively far from the sighting plane. For example, the particle in fig 4, d is at a distance on the order of 1.5 mm. The field of gravity forces on all photographs is directly downwards along the plane of the photograph. In figure 4 b and h the arrows indicate the direction of flow movement.

Analysis of these and other TV subjects indicates a number of peculiarities of the microstructure of crystalline fog that were previously not discussed in the literature. Thus, under certain conditions of influence roughly 50-60% of the total quantity of the observed crystalline particles are aggregates made of two-four crystalline particles of simple shapes. It is important that the aggregates are formed primarily by the contact of incoming pieces of crystals, and apparently can be broken down during their settling on the backing.

a) b) c)

Figure 5. Individual Examples of Use of TV Monitors

It is important to also note that judging from the readings of the TV monitors a crystallized cloud always has a noticeable number of particles of spherical shape (see the subjects of fig 4, e, g, i).

2. Spatial distribution of drops in fog. In various types of theoretical models of microphysical processes in clouds it is usually assumed that the distribution of droplets in space is subordinate to Poisson's statistics. It is evident that the most suitable for the purposes of verifying this hypothesis is the use of TV analyzers that have a small optically formed working volume. Corresponding tests [8] in a cloud chamber 3200 m^3 in volume with a TV counter [7] that has counting volume of 0.05 mm^3 confirmed that during the formation and dissipation of "adiabatic" fog the spatial distribution of drops 3-22 μm in diameter can be described by Poisson's statistics.

3. Precipitation of crystalline particles on charged bodies. The TV subject in figure 5, a illustrates the result of precipitation of particles of a crystalline cloud on a single negatively charged sphere (intensity of the electrical field on the surface about 6 kv/cm). It is apparent that the precipitating particles form unique branches with branching shoots. It is important that the intensity of precipitation and the configuration of the branches depend not only on the amount, but also the sign of the charge of the sphere. In [19] the analogous technique was used to investigate the electrostatic precipitation on a sphere of liquid drops.

4. Formation of drops in a generator with vibrating needle. Figure 5, b depicts the possible operation of a TV monitor as a TV stroboscope, and simultaneously the possibility of obtaining information on the particle dimensions with dark field illumination. The first is attained by synchronization of frequencies and phases of the needle oscillations, periodically immersed into a capillary with water [12], the frequency of the flashes of the impulse condenser and frequency of the frame scan. The second effect is attained by illumination of the droplets at angles from 0 to 2π with the help of wide-aperture optics. The frequency of generation of the drops 30 µm in diameter equals 250 Hz.

5. Recondensation for evaporation of crystals. With the help of a TV monitor operating in a pattern of impulse dark field exposure for the first time observations were made of the phenomenon of formation of a tail of secondary drops behind a crystal moving in a beam of radiation of a carbon dioxide laser with density of power about 1 kw/cm^2 [3]. The working volume of the TV monitor ($1.2 \times 0.8 \times 0.25$ cm^3) was formed in a laser beam with exposure by three flashes of ISSh-100-3 impulse lamps lasting 2 µs and frequency 1 kHz. As is apparent from the TV subject on figure 5, c, during evaporation of the ice crystal 40 µm in size in less than 1 µs (with air temperature -20°C) a tail is formed of recondensed small particles, while the crystal during evaporation begins to move in the direction of the radiation spread.

In conclusion we will note that the TV methods are efficient also with automated measurement of the structure of various types of microheterogeneities on backings or slides, in particular, in an analysis of aerosol samples on a slide [9] and tracks of fragments of nuclear fission on solid track detectors [4].

BIBLIOGRAPHY

1. Belyayev, S. P.; Nikiforova, N. K.; Smirnov, V. V.; and Shchelchkov, G. I. "Optiko-elektronnyye metody izucheniya aerozoley" [Optic-Electronic Methods of Studying Aerosols], Moscow, Energiya, 1978 (at press).

2. Birger, Ye. M.; Zakharov, V. M.; Karlov, S. P.; and Razumov, L. N. "Use of Impulse Holography to Study Atmospheric Aerosol," METEROLOGIYA I GIDROLOGIYA, No 1, 1977, pp 44-52.

3. Volkovitskiy, O. A.; Denisova, V. V.; Ivanov, Ye. V.; and Kolomeyev, M. P. "Experimental Study of the Effect of Condensation during the Effect of CO_2-Laser Radiation on Cloud Media," TRUDY IEM, No 13(58), 1976, pp 95-107.

4. Zhuk, I. V.; Malakhov, V. A.; Malykhin, A. P.; and Smirnov, V. V. "Television Counter of Fission Fragment Tracks," PRIBORY I TEKHNIKA EKSPERIMENTA, No 3, 1975, pp 179-181.

5. Kolomeyev, M. P. "Possibility of Obtaining Holographic Images of Ice Crystals," METEOROLOGIYA I GIDROLOGIYA, No 7, 1977, pp 111-113.

6. "Lazery" [Lasers], collection of articles edited by V. P. Pavlov, Moscow, Nauka, 1977, pp 86-113.

7. Malakhov, V. A.; and Smirnov, V. V. "Television Counter of Cloud Particles," TRUDY IEM, No 4(38), 1973, pp 70-93.

8. Savchenko, A. V.; and Smirnov, V. V. "Certain Laws Governing the Spatial Distribution of Cloud Particles," TRUDY IEM, No 4(38), 1973, pp88-100.

9. Smirnov, V. V. "Use of Television Unit to Examine and Photograph Aerosol Particle Samples," "Materialy 8-y mezhvuz. konf. po aerozolyam" [Materials of Eighth Conference of Schools of Higher Education on Aerosols], Odessa, 1968, pp 34-35.

10. Smirnov, V. V. "Isolation and Analysis of Characteristic Dimensions of Objects by Methods of Television Automatics," TEKHNIKA KINO I TELEVIDENIYA, No 12, 1970, pp 17-24.

11. Smirnov, V. V. "Generatory na tunnel'nykh diodakh" [Tunnel-Diode Generators], Moscow, Energiya, 1971, 46 p.

12. Smirnov, V. V. "Generator monodispersnykh kapel'" [Generator of Mono-Dispersed Drops], Patent No 486806, BYULLETEN' IZOBRETENIY, No 37, 1975.

13. Smirnov, V. V.; Goncharov, N. V.; and Yaskevich, G. F. "Television Analyzer of Aerosol Microstructure 'Taran'," "Materialy 3-y Vsesoyuzn. konf. po aerozolyam" [Materials of Third All-Union Conference on Aerosols], Yerevan, Vol 1, 1977, Moscow, Nauka, 1977, pp 148-149.

14. Smirnov, V. V.; and Yaskevich, G. F. "Ustroystvo dlya formirovaniya i schityvaniya izobrazheniy dvizhushchikhsya mikroob"yektov" [Device for Formation and Metering of Images of Moving Microobjects], Patent No 578647, BYULLETEN' IZOBRETENIY, No 40, 1977.

15. Smirnov, V. V.; and Yaskevich, G. F. "Formation and Analysis of Holograms in Partially Coherent Light," "Optika i spektroskopiya" [Optics and Spectroscopy], 1978 (at press).

16. Yaskevich, G. F. "Structure of Defocussed Images with Partially Coherent Illumination," TRUDY IEM, No 14(59), 1976, pp 94-103.

17. Lilie, L. E.; Crove, T. C.; and Carvey, D. M. "In situ Ice Crystal Counting by Means of a Laser-Television Camera System,""Abstr. of Internat. Cloud Physics Conf." (Boulder, Colorado, 26 July-6 August, 1976), 1976, pp 29-30.

18. Knollenberg, R. G. "Three New Instruments for Cloud Physics Measurements: the Second Spectrometer, the Forward Scattering Spectrometer, and the Active Scattering Spectrometer," "Proceed. Intern. Cloud Physics Conf. (Boulder, Colorado, 26 July-6 August, 1976), 1976.

19. Smirnov, V. V. "Electrostatic Collection of Aerosol Particle on a Sphere at Intermediate Reynolds Number," J. Aerosol Sci., Vol 7, 1976, pp 473-477.

UDC 551.509.615:(182.2+183.022)

FOG DISSIPATION WITH THE HELP OF SURFACE-ACTIVE SUBSTANCES

Moscow METEOROLOGIYA I GIDROLOGIYA in Russian No 5, May 79 pp 106-112

[Article by Doctor of Physical and Mathematical Sciences M. V. Buykov, and Candidate of Physical and Mathematical Sciences V. I. Khvorost'yanov, Ukrainian Scientific Research Hydrometeorological Institute, submitted for publication 11 Jul 78]

Abstract. A survey is made of the theoretical and experimental works on fog dissipation with the help of surface-active substances, and the outlook for further research is discussed.

[Text] Dissipation or prevention of formation of fog is of great value for guaranteeing the operation of aviation and other types of high-speed transportation. Currently, methods have been developed and are being used in practice for dissipation of supercooled (temperature below -3°C) fog. Supercooled fog is in the metastable state, and introduction of ice crystals into the fog in the necessary concentration results in the disappearance of drops and improvement in visibility. Operational systems of supercooled fog dissipation are working in a number of airports in Europe and North America.

However the majority of fogs are warm (over the European territory of the Soviet Union--70%, on the territory of the United States--95% [13, 30]). Although fairly many methods have been proposed for improving visibility in warm fog [20,30], only the methods based on forced evaporation of drops (thermal, hygroscopic, use of helicopters) have reached the stage of field experiments, while the thermal method has been practically employed in certain countries.

The method based on introduction into the fog of vapors of surface-active substances (SAS) is the most attractive in many respects. Modification of the surface of cloud particles by SAS can influence the processes of fusion and fragmentation of drops, or the processes of condensation or evaporation by reducing the coefficient of water condensation. Only the latter effect is important for fog.

The introduction of SAS vapors into the volume of air before fog formation and their adsorption on the surface of cloud nuclei of condensation must lower the coefficient of condensation, strongly retard their condensation growth under conditions of changing humidity, and delay their transformation into cloud drops [12]. Since under natural conditions air cooling and increase in the relative humidity can be continued, then a reduction in the activity of the nuclei by SAS vapors can prevent the formation of fog only during a certain time interval. The introduction at this stage of a small number of unmodified condensation nuclei can result in fog formation with larger drops and greater visibility range.

It is suggested in [27] that the SAS vapors have the strongest effect on activation of the smallest nuclei, while activation of a small number of large nuclei results in the formation of fog made of larger drops.

Over 20 years have passed since the formulation of the idea of passivation of condensation nuclei for the purpose of fog dissipation, and in this time a large volume of theoretical, laboratory and field work has been carried out whose analysis will also be covered in this survey.

Theory of condensation growth of passivated drops. The fundamentals of the theory of passivation of the condensation growth of an individual drop in an atmosphere containing SAS vapors have been developed by B. V. Deryagin and Yu. S. Kurgin [9, 25]. With the help of the method of the boundary sphere to describe the transfer of molecules of water and SAS equations were obtained for the change in radius r and the degree of filling of the monolayer S. In the equation for the velocity of drop growth the experimentally established fact [23] is taken into account that with the attainment of S of a certain value S_{kp} a very rapid reduction in α occurs. Therefore one can approximately assume that with $S<S_{kp}$ (i.e., in the presence of the adsorption layer) $\alpha=\alpha_c$. For cetyl alcohol $S_{kp}=0.976$ [23], $\alpha_c=3.5\cdot10^{-5}$ [8, 18].

An important role in the problem of passivation is played by the critical oversaturation of water vapor Δ_{kp} [9, 25] that is defined as supersaturation during which breakdown of the SAS condensation monolayer occurs on the growing drop. In [9, 25] the critical supersaturation was determined with the help of a study on the asymptotics of the solution to the Deryagin-Kurgin equations with great times, and in [10]--by a qualitative analysis of the equations the lower and upper limits for Δ_{kp} were established. In publications [10, 17] it was assumed that during supersaturation equal to the critical, the degree of filling of the monolayer is not altered with time, and by this method an explicit expression was obtained for Δ_{kp} on the condition that absorption occurs in a diffusion pattern, while the growth of the drop in a kinetic pattern. Calculations according to this formula yield for the main fraction of nuclei of condensation (0.08-0.27 μm) values of Δ_{kp}=4-12%. These calculations did not take into consideration the presence of salt in the drops. However, the calculations made in [29, 31] with regard for salinity, with somewhat different hypotheses yielded approximately the same values.

In the majority of publications the Deryagin-Kurgin equations were solved with the starting condition $S_{kp}=1$, which corresponds to the complete filling of the monolayer. It is important to also examine that case where the non-passivated drop is carried into an atmosphere supersaturated with water vapor and containing SAS vapors ($S(0)=0$). The solution to these equations with such a condition was obtained in [5] by approximate analytical and numerical methods. It was shown that during supersaturations that considerably exceed the typical values for real fog, the passivation time is short: for the starting radius $r_0=20$ µm with $\Delta=0.7\%$ S reaches the value S_{kp} in 200 s, whereby the drop radius is increased less than 2-fold. With supersaturations typical for radiation fog, the passivation time does not exceed several tens of seconds, and the radius of the drop is increased by several percents. It is shown in [5] that the passivation time is proportional to the initial drop radius.

Laboratory studies of growth in passivated drops. The first experimental data that confirm the existence of the passivation effect were obtained in [12, 23]. Detailed experimental studies of adsorption of cetyl alcohol vapors during the growth and evaporation of individual drops of water and saline solutions 2, 150 and 300 µm in size are described in [8, 18]. Besides the condensation coefficient for a passivated drop α_c the amounts of the diffusion coefficients and pressure of the saturated vapors of cetyl alcohol, the equilibrium adsorption constant, and so forth were determined.

The experimental values of the critical supersaturation determined by the different methods (7% [18], 5-6% [16], 5-7% [19]) agree well among themselves and with the theoretical values given above.

The passivation effect of condensation growth of drops growing on condensation nuclei was confirmed with the help of the method of flow ultramicroscopy [21], different-temperature diffusion flow chamber [19], jet method [1,2]. In [1,2] it was shown that in the interval of moisture 80-100% passivation of nuclei made of aluminum chloride results in a reduction in the modal radius and dispersion of drops grown on modified nuclei.

If the initially passivated nuclei grow in the atmosphere that does not contain cetyl alcohol vapors, then, according to [2] breakdown of the monolayer occurs in 3-4 s.

Experimental studies of the passivation process in fog chambers. All the studies with individual drops were conducted either with fixed supersaturation or with fixed humidity and diminishing supersaturation (growth in drops on hygroscopic nuclei), while the formation of natural fog occurs under conditions of growing relative humidity, which is governed by air cooling. In addition, in the formation of drop distribution with respect to sizes a broad spectrum of cloud nuclei of condensation participate, whereby the adsorption of SAS vapors can have a varying effect on the nuclei of different sizes. This makes it necessary to conduct theoretical and experimental studies on the SAS action under conditions close to the real. Research in fog chambers that to a certain degree simulate the real conditions serve this purpose.

The first experiments to study the growth in passivated nuclei of condensation in fog chambers were made in [15]. It was demonstrated that the modification by SAS vapors of the insoluble condensation nuclei does not affect the properties of the forming fog in the adiabatic chamber. Fog formation on passivated soluble condensation nuclei in [15] was investigated under isothermic conditions with a rise in humidity not reaching 100%, while in [16]--in and adiabatic chamber. The delay time in fog formation under the influence of isothermic conditions was 45 s, and under adiabatic conditions--3-4 s. This difference in the delay times can be explained by the fact that under isothermic conditions the nuclei grow with humidity not greater than 100%, approach the equilibrium size, and the monolayer is not punctured. During adiabatic cooling the rate of growth of supersaturation is 1.4%/s and within 3-4 s reaches the critical supersaturation, after which the monolayer is broken down and growth occurs in the absence of passivation.

A reduction in optic density of fog during the action of isothermic conditions is explained by the fact that the time for reaching the equilibrium size of the drop growing on a particle of salt is inversely proportional to the water condensation coefficient that for passivated nuclei is by several orders smaller than for the controls [8, 18]. Therefore for short observation times in [16] the dimensions of the drops that grew on passivated nuclei will be smaller than on the controls.

A detailed study of the effect of cetyl alcohol vapors on fog formation in an adiabatic chamber was made in [28]. In one series of experiments SAS was added to a chamber containing a formed fog. Then compression was carried out in the chamber during which a monolayer of cetyl alcohol was formed on the fog drops. After compression expansion was started that lasted about 25 min, then the fog began to dissipate as a consequence of the warming of the chamber. The difference between the development of passivated and nonpassivated fog in visibility range and in drop distribution with respect to sizes was observed both during compression, and during expansion: visibility in the passivated fog was worse than in the control; the drop spectrum was narrower, while the number of drops was greater in the passivated fog. By the end of the stage of expansion the properties of the passivated and control fog were identical. A natural breakdown in the passivated fog occurred slower than the control.

In the other series of experiments the vapors of cetyl alcohol were introduced into the chamber before the beginning of expansion, i.e., passivation of the condensation nuclei occurred. After a 30 minute delay expansion occurred.

The visibility range in the passivated fog was greater than in the control, during the first 10 minutes of expansion (fig 1). In 2.5 min the visibility range in the passivated fog 2.5 km, in the control--0.6 km. After 10 minutes the properties of both fogs begin to coincide. The natural breakdown of the passivated fog occurs more slowly than that of the control.

Based on these experiments [28] draws a conclusion about the unsuitability of passivation to prevent fog formation.

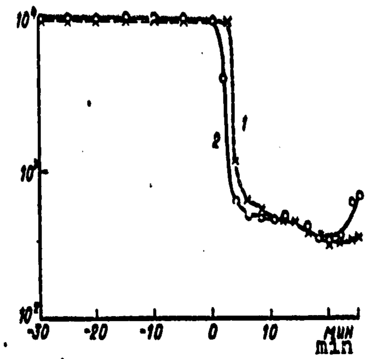

Figure 1. Visibility Range (feet) in Passivated (1) and Control (2) Fogs Measured in Fog Chamber. Expansion in Chamber Begins with t=0 (Figure taken from publication [28]).

Numerical Modeling of Evolution of Passivated Fog in Chambers. In publication [31] the results are given of a numerical solution to the Deryagin-Kurgin equations, equations for temperature and supersaturation. Corrections were made in the equations for velocity of condensation growth of drops for the curvature and salinity of drops.

At the starting moment in time all the nuclei were located in equilibrium with the medium with 98% relative humidity, and were covered with a monolayer of cetyl alcohol. It was assumed that the chamber was filled with cetyl alcohol vapors whose summary amount in the vaporous phase and adsorbed state was not further altered. In certain calculations the cetyl alcohol density vapor exceeded the saturation and the condensation of cetyl alcohol on the surface of drops was taken into consideration. The majority of calculations were made with velocity of cooling 2°C/h until fog formation and 0.75°C/h after its formation. The problem was solved for one sea (total concentration 433 cm^{-3}) and two continental spectra of nuclei (1000 and 4000 cm^{-3}).

The calculations demonstrate that with the start of cooling supersaturation begins to rise, reaching for the sea spectrum of nuclei the maximum value 0.11% in the control fog and 2-9% in the passivated fog depending on the initial concentration of SAS vapors. A sharp drop in supersaturation in the passivated fog further was governed by a puncture in the monolayer on small drops (according to [10], $\Delta_{kp} \sim r_0$ with small r_0), which results in an increase in the rate of condensation growth a hundred times. As a result of this the drops with destroyed monolayer begin to overtake the passivated drops in their growth.

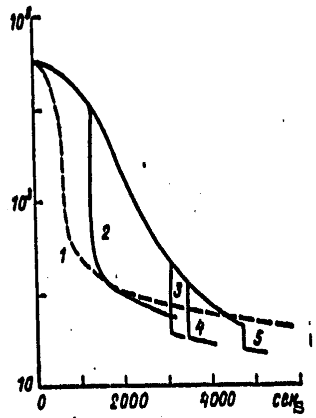

Figure 2. Visibility Range (m) in Control and Passivated Fog, Computed for Conditions of Fog Formation in Expansion Chamber with Starting Rate of Cooling 2°C/h; Sea Type of Spectrum of Condensation Nuclei. Different Starting Concentration of Cetyl Alcohol Vapors in Chamber Correspond to Different Curves. (Figure taken from publication [31]).

Key:
1. 0
2. $6 \cdot 10^{-11}$ g/cm^3
3. $8 \cdot 10^{-11}$ g/cm^3
4. 10^{-10} g/cm^3
5. $2 \cdot 10^{-10}$ g/cm^3

Figure 2 shows the dependence of visibility range on the time for different starting values of density of cetyl alcohol vapors. The visibility range in the passivated fog is higher than in the control until the monolayer begins to break down on small drops, then it is sharply reduced and becomes 2-3 times narrower than in the control fog. The duration of existence of the improved visibility in the passivated fog depends on the starting concentration of cetyl alcohol vapors and for nuclei of the sea type comprises from 20 to 70 min. For nuclei of the continental type the general nature of processes is preserved, however an exacerbation of visibility occurs somewhat earlier. On the whole the results of these calculations are in qualitative agreement with the experiments described in [28].

Analogous calculations for drops formed on sea nuclei of condensation and passivated by natural means are given in [29].

Calculation of the growth of a group of passivated and nonpassivated drops of pure water in a chamber (starting radius 1 µm, concentration--500 cm^{-3}, rate of cooling 1.7°C/h) made in [17] on the condition of the existence of a monolayer at all moments of time, showed that within 20 min the size of the passivated drop is two times smaller than the nonpassivated, and within 1 h their dimensions coincide.

Results of field experiments. Experiments under full-scale conditions to prevent fog with the help of SAS were made in Australia and the Soviet Union. In Australia [24] the experiments were made over reservoirs located in connecting mountain valleys up to 600 m deep, and up to 20 km long. The modification was carried out during the entire night from 21.00 to 6.00-7.00 with the help of an aerosol generator with output of 25 kg/h that discharged into the atmosphere submicron particles of higher alcohols. A total of four experiments were made. In two of them in the region of operation of the generator no fog was formed, in one an elevation was observed in the lower boundary of fog at altitude 100 m and rain in the zone of operation of the generator, and in the last test the entire arm of the mountain valley in which the generator was located was entirely clear of fog. During the carrying out of the work in eight cases fog was observed that was not modified. In viewing these observations as the control experiments the authors [24] came to the conclusion that the experiments were successful in having an effect since only in one of the control cases was a continuous fog formed in that place where no influence was made on the fog. However, the authors note that in two cases the movement of air was not in that direction where the dissipation occurred, and in three cases out of four the volume proved to be free of fog that could not be passivated with 25 kg/h output of the reagent.

Fog that was modified as described in [24] is not radiation fog, but is formed as a consequence of the establishment of breeze circulation in the mountain valleys filled with water: during the night the valley slopes are colder than the mirror of the reservoir and runoff of air from the slopes must result in the emergence of ascending currents. In fact, according to [24] the fog is always formed at a certain altitude and is lowered to the water surface, i.e., is a cloud with descending lower boundary, while the radiation fog is generated near the earth. In this case, passivation of the nuclei by SAS vapors must result in the elevation of the lower boundary. According to [17, 31] delay in fog formation can be about an hour, with ascending movements about 3 cm/s this results in an elevation of the lower boundary by 100 m.

Two series of experiments were conducted in the USSR.

In 1971 a group of Odessa University set up tests in the region of Baryshevka settlement in the Kievskaya oblast. The reagent (shebekinskiy alcohol C_{17}-C_{23}) was introduced with the help of an aerosol generator with capacity 250 g/h. The fog that was modified was generated in the valley of the Trubezh River and its thickness did not exceed 4 m. The modification was started before the fog formation ; to evaluate the effect the method of control and experimental area was used. Sixteen tests were made on the modified area and 6 observations were made of natural fog development. During modification the delay in fog formation on the test section as compared to the control was 20-70 min. Under natural conditions fog developed the same on both sections [22, 26].

In September 1972 experiments on fog dissipation with the the help of SAS were set up by the group of the Institute of Physical Chemistry of the USSR Academy of Sciences in the floodplain of the Seym River in the region of Ryl'sk [11, 26]. Photography carried out from a balloon demonstrates that around the aerosol generator in the fog there is a dark spot indicating, apparently, the fog dissipation. The area of the spot is 3500-5000 m^2 (according to special report of the executors) and the visibility range in this zone was improved 3-4-fold.

The field experiments made in the USSR strongly differ in the meteorological conditions from the Australian experiments therefore it is impossible to compare them.

Delays in fog formation (20-70 min) attained by the introduction of SAS in the tests made by the group of Odessa State University are comparable in amount to the results of calculations for the chambers [17, 31], although they also considerably exceed the experimental value (10 min) obtained in [28]. It is possible that this difference is governed by the too great cooling rate in [28].

From the description of the tests made by the groups from Odessa State University and the Institute of Physical Chemistry it follows that evidently in the zone of SAS generator action the fog is not formed at all, and the delay time was determined according to the flow of fog from the control area. Apparently, passivation of condensation nuclei resulting in the growth of supersaturation of the water vapor in the zone of generator action can intensify the precipitation of dew on the soil (condensation on the soil) and at the same time create a certain dehydration of the near-surface air layer. With the coefficient of turbulent exchange 5 cm^2/s in an hour a layer can be dehydrated of about 2 m, which is commensurate with the thickness of the fog described in [22].

Numerical modeling of evolution under natural conditions of passivated radiation fog. The model that takes into consideration the main meteorological factors that affect fog development, and that permit a description of the kinetics of the processes occurring during the effect on fog by SAS vapors has been developed in [3, 4, 6]. The system of equations of the model includes equations of dynamics of the planetary boundary layer and equations of transfer of heat, moisture, and long-wave radiation; it takes into account the heat and moisture exchange with the soil.

In order to describe the microphysical processes in fog the kinetic equation is used for the function of drop distribution according to dimensions. The model makes it possible to compute as the functions of altitude and time the temperature, humidity, wind velocity, coefficient of turbulent mixing, rate of radiation cooling, as well as the microphysical characteristics--supersaturation and drop spectra. The use of this approach to simulate the natural development of fog made it possible to describe many observed features of its development, as well as to predict a number of new effects [3,4,6]. Due to the insufficient power of the computer the model does not compute in

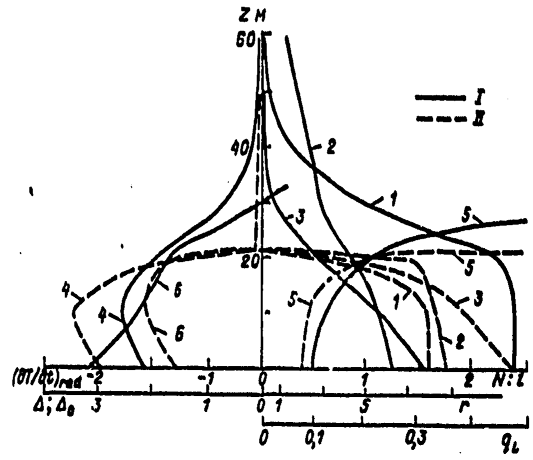

Figure 3. Concentration $N \cdot 10^5$ g^{-1} (1) and Mean Radius r μm (2) of Drops; Water Content q_L g/kg (3); Rate of Radiation Cooling $(\frac{T}{t})_{rad}$ x 10^{-3}°C/s (4); Visibility Range $l \cdot 10^2$ m (5); Supersaturation $\cdot 10^{-4}$g/kg; $_0 10^{-6}$ g/kg (6); t=1 h 40 min. I--with modification; II--without modification.

detail the process of activation of condensation nuclei and their transformations into drops, in particular, it does not consider the effect of curvature, salinity and reverse transition of the drops into nuclei. However, the delays computed in [17] for passivated drops of pure water are close to the delays found with precise computation of passivated condensation nuclei [31].

Calculations of the evolution of modified fog were made with the following values of parameters: velocity of geostrophic wind--3 m/s, initial humidity--90%, temperature on surface 10°C, the calculations were made for night conditions. The atmosphere contains SAS vapors whose concentration is sufficient for formation of a saturated monolayer on fog drops. As shown in [5] the formation of a monolayer occurs in the time that is much shorter than the characteristic time for fog formation, therefore from the moment of SAS introduction the drops were considered passivated.

In the calculations at first a reduction was observed in the temperature of the soil and adjacent air layer governed by the radiation cooling, and within 1 h 10 min--fog formation. Figure 3 presents the condition of the fog in 30 min of its development (1 h 40 min from the start of metering) when the greatest difference is observed in the development of the modified and control fogs. The greatest increase in visibility range (1.5-fold) is reached at altitude 10 m. In the lower 20-meter layer the mean drop radius and water content are lower, while the drop concentration is greater in the modified fog than in the control. This is explained by the deceleration in drop growth, however not by three orders as it should be in correspondence with the change in condensation coefficient. As follows from figure 3, supersaturation in the modified fog is 100 times greater therefore the rate of growth during modification is only 1.5-fold less. An analogous increase in supersaturation in the passivated fog has been established in [31]. Thus, the fog as a thermodynamic system is subordinate to the Le Chatelier principle, according to which in the system subject to external modification processes emerge that strive to compensate for its effect [14]. The somewhat lower increase in the visibility range in this model as compared to the calculations for the chamber [17, 31] is governed by the fact that passivated drops carried into the region of negative supersaturation are evaporated slower and the number of completely evaporated drops is reduced on the upper boundary of the fog, i.e., their concentration increases. This same effect explains the great thickness of the passivated fog, and the existence of its upper layers in negative supersaturation.

With the further development the visibility in the passivated fog is worse, while its thickness is greater. In those cases where the natural fog is separated from the earth and is converted into low cloudiness, during modification near the earth the fog is preserved with visibility range 300 m.

Numerical experiments were also conducted where the introduction of a reagent into an already formed fog was simulated. Here it was established that the increase in the visibility range was smaller than in the case examined above.

Thus, the results of the numerical experiment on fog simulation agree with the results of the calculations for chambers and chamber experiments [17, 28, 31], and predict a number of new effects governed by the intensification of colloidal stability of a passivated fog.

Conclusion. The research carried out in the last 20 years on the use of SAS for fog dissipation shows that this method can result only in the delaying of fog formation. Modification of the formed fog intensifies its colloidal stability.

Experimental studies in chambers and numerical modeling of fog formation for conditions close to the natural demonstrated that an improvement in visibility in the passivated fog lasts longer than an hour. Although in field experiments made in Australia the improvement in visibility lasted for several hours, however the authors express doubt as to the reliability of the findings. In this respect the thorough verification of the hypothesis advanced in the article about the more abundant dew precipitation resulting in dehydration of the lower air layer in the zone of passivation of condensation nuclei, in particular for thick fogs is of great importance. Unfortunately, as of yet the idea about the introduction of additional condensation nuclei into the zone of passivation to reduce the excess supersaturation of water vapor has not been realized. For this purpose one can use, for example, the insoluble condensation nuclei, which according to [15], are not subject to passivation.

In order to obtain the final conclusion about the effectiveness of using SAS for fog dissipation it is necessary to continue the full-scale studies providing tests with a full set of measurements of fog characteristics and meteorological parameters. In the area of theory the primary task is numerical modeling of the effect on fog with a detailed description of the process of activation of condensation nuclei and fulfillment of calculations for the conditions close to the conditions of carrying out the experiment.

BIBLIOGRAPHY

1. Bakhanova, R. A.; and Silayev, A. V. "Evaluation of Retardation of Drop Growth on Passivated Nuclei of Aluminum Chloride," TRUDY UKRNIGMI, No 95, pp 71-81.

2. Bakhanova, R. A.; and Silayev, A. V. "Study of Drop Growth on Passivated Condensation Nuclei with Relative Humidity Less than 100%," TRUDY UKR-NIGMI, No 103, 1971, pp 126-136.

3. Buykov, M. V.; and Khvorost'yanov, V. I. "Numerical Modeling of Fog Formation and Stratus in the Boundary Atmospheric Layer on Dry Under-lying Surface with Regard for Microphysical Properties," TRUDY UKRNIGMI, No 146, 1976, pp 24-46.

4. Buykov, M. V.; and Khvorost'yanov, V. I. "Numerical Modeling of Radiation Fog and Stratus with Regard for Microsctructure over Moist Underlying Surface," TRUDY UKRNIGMI, No 152, 1977, pp 36-56.

5. Buykov, M. V.; and Khvorost'yanov, V. I. "Theory of Passivation of Fog Drops by Vapors of Surface-Active Substances," TRUDY UKRNIGMI, No 152, 1977, pp 57-63.

6. Buykov, M. V.; and Khvorost'yanov, V. I. "Formation and Evolution of Radiation Fog and Stratus in Boundary Atmospheric Layer," IZVESTIYA AN SSSR. FIZIKA ATMOSFERY I OKEANA, Vol 13, No 4, 1977, pp 356-370.

7. Buykov, M. V.; and Khvorost'yanov, V. I. "Microphysical Model of Evolution of Fog with Introduction of Vapors of Surface-Active Substances," EKSPRESS-INFORMATSIYA. METEOROLOGIYA, No 1(48), 1977, pp 1-9.

8. Deryagin, B. V.; Fedoseyev, V. A.; and Rozentsvayg, L. A. "Study of Adsorption of Cetyl Alcohol Vapors and Its Effect on Evaporation of Water Drops," DOKLADY AN SSSR, Vol 167, No 3, 1966, pp 617-620.

9. Deryagin, B. V.; and Kurgin, Yu. S. "Theory of Passivation of Conden-sation Growth of Fog Drops by Vapors of Cetyl Alcohol," KOLLOIDNYY ZHURNAL, Vol 34, No 1, 1972, pp 36-42.

10. Deryagin, B. V.; and Kurgin, Yu. S. "Question of Passivation of Conden-sation Growth of Fog Drops by Cetyl Alcohol Vapors," DOKLADY AN SSSR, Vol 216, No 5, 1974, pp 1087-1090.

11. Deryagin, B. V.; Leonov, L. F.; Prokhorov, P. S.; Malikov, B. A.; and Zelotarev, I. A. "Laboratory Studies and Field Experiments to Prevent Radiation Fog Formation," INFORMATSIONNYY BYULLETEN', GUGMS, No 8, 1972.

12. Izmaylova, G. I.; Prokhorov, P. S.; and Deryagin, B. V. "Possibility of Surface Activation and Passivation of Condensation Nuclei of Water Vapors," KOLLOIDNYY ZHURNAL, Vol 19, No 5, 1957.

13. Koshelenko, I. V. "Fogs," TRUDY UKRNIGMI, No 155, 1977, 154 p.

14. Landau, L. D.; and Lifshits, V. M. "Statisticheskaya fizika" [Statistical Physics], Moscow, Nauka, 1964, 567 p.

15. Leonov, L. F.; Prokhorov, P. S.; Yefanova, T. A.; and Zolotarev, I.A. "Possibility of Passivation of Condensation Nuclei by Cetyl Alcohol Vapors," FIZIKA AERODISPERSNYKH SISTEM, No 2, 1970, pp 13-20.

16. Leonov, L. F.; Prokhorov, P. S.; and Zolotarev, I. A. "Passivation of Condensation Nuclei of Sodium Chloride by Cetyl Alcohol Vapors," FIZIKA AERODISPERSNYKH SISTEM, No 5, 1972, pp 7-11.

17. Leonov, L. F.; Prokhorov, P. S.; and Malikov, B. A. "Conditions for Preserving the Screening Effect of SAS Monolayers on Water Drops Growing in a Supersaturated Medium," KOLLOIDNYY ZHURNAL, Vol 39, No 3, 1977.

18. Rozentsvayg, L. A.; Deryagin, B. V.; and Fedoseyev, V. A. "Effect of Cetyl Alcohol Monolayer on Condensation Growth of Drops of Aqueous Solutions," DOKLADY AN SSSR, Vol 176, 1967, pp 635-638.

19. Silayev, A. V.; Royev, L. M. "Study of Fog Formation on Natural and Artificial Condensation Nuclei in Different-Temperature Flow Chamber," "Trudy IV i V vsesoyuznykh mezhvuzovskikh konferentsiy po ispareniyu goreniyu i gazovoy dinamike dispersnykh sistem" [Proceedings of Fourth and Fifth All-Union Conference of Schools of Higher Eduction on Evaporation, Combustion and Gas Dynamics of Disperse Systems], Kiev, Naukova Dumka, 1967, pp 200-205.

20. Solov'yev, A. D. "Physical Bases for Methods of Modifying Warm Fog," "Issledovaniya po fizike oblakov i aktivnym vozdeystviyam na pogodu" [Studies on Physics of Clouds and Active Weather Modification], Moscow, Gidrometeoizdat, 1967, pp 209-217.

21. Storozhilova, A. I. "Passivation of Hygroscopic Condensation Nuclei by SAS Adsorption from Gas Phase," FIZIKA AERODISPERSNYKH SISTEM, No 1, 1969, pp 40-44.

22. Fedoseyev, V. A., et al. "Study of Effect of SAS on Generation of Radiation Fog," FIZIKA AERODISPERSNYKH SISTEM, No 7, 1972, pp 3-6.

23. Barnes, G.; and La Mer, V. "Retardation of Evaporation by Monolayers. Transport Process," 1962.

24. Bigg, E. R.; Brownscombe, J. L.; and Thompson, W. J. "For Modification with Long-Chain Alcohols," J. APPL. METEOROL., Vol 8, No 1, 1969, pp 75-82.

25. Derjaguin, B. V.; and Kurgin, Yu. S. "Theory of Passivation of the Growth of Water Condensation Nuclei by Cetyl Alcohol Vapor," "Proc. Seventh Intern. Conf. on Cond. and Ice Nucl., 1969, Prague-Vienna, p 461.

26. Derjaguin, B. V., et al. "Problems of Radiation Fog Prevention,""Proc. WMO/IAMAP Sci. Conf. on Weather Modification, 1973, Tashkent, pp 29-33.

27. Juisto, J. E. "Project Fog Drops, Investigations of Warm Fog Properties and Fog Modification Concepts," Cornell Aeronautical Labs, Inc. Rept., CR-72, 1964.

28. Kocmond, W. C.; Garrett, W. D.; and Macr, E. J. "Modification of Laboratory Fog with Organic Surface Films," J. GEOPHYS. RES, Vol 77, 1972, pp 3221-3231.

29. Podzimek, J.; and Saad, A. N. "Retardation of Condensation Nuclei Growth by Surfactant," J. GEOPHYS. RES., Vol 80, No 24, 1975, pp 3386-3392.

30. Silverman, B. A.; and Weinstein, A. I. "Fog," "Weather and Climate Modification," 1974, New York (edited by W. N. Hess), Wiley, pp 355-382.

31. Warner, J.; and Warne, W. G. "The Effect of Surface Films in Retarding Growth by Condensation of Cloud Nuclei and Their Use in Fog Suppression," J. APPL. METEOROL., Vol 9, No 4, 1970, pp 639-650.

UDC 551.5(092)

IN MEMORY OF THE 90TH BIRTHDAY OF SEMEN IVANOVICH TROITSKIY

Moscow METEOROLOGIYA I GIDROLOGIYA in Russian No 5, May 79 pp 113-115

[Article by V. M. Mikhel' and A. S. Korovchenko]

Abstract. Brief information is given about the scientific-pedagogical activity of S. I. Troitskiy and biographical data about the scientist.

[Text] One of the leading Soviet meteorologists of a broad profile, S. I. Troitskiy was born on 9 February 1889 (according to the New Style) in St. Petersburg in a professor's family. After graduating from the mathematical department of the physical and mathematical department of Petersburg University in 1912 he remained in the department of physics for training to be a professor, but in 1913 he was drafted into the army and was sent to the battalion of aeronautical officers school in St. Petersburg.

The scientific research activity of Semen Ivanovich in the field of meteorology began in the years of World War I where, being the senior officer of the aeronautical unit he conducted aerological observations during air reconnaissance. Troitskiy was at the front until the end of 1917, while from the first days of the formation of the revolutionary aeronautical details in 1918 he entered the Red Army in whose ranks as a military aeronaut he then took active part in the defense of Petrograd against the attack of Yudenich. After finishing aeronautical school he remained in it as a teacher and head of the physics laboratory, then worked as the head of the training section, and finally, in 1918-1919 was the head of this school. The aeronautical school became the forefather of domestic aeronautics and aviation, and within its walls the air force glory of our Motherland was born. Here M. M. Pomortsev and N. N. Kalitin worked in various years as teachers and used the training flights of the aerostats for atmospheric research; they then became major scientists of our country. Here Semen Ivanovich also continued to be involved in scientific work.

In 1920 at the invitation of the head of the aerological observatory he began to work as a physicist of the observatory in Pavlovsk, then--in the department of the network of aerological stations of the geophysical observatory. At the same time he also worked in the field of military meteorology where he wasalso a major specialist, while up to 1927, being continuously in active military service in the Red Army, he conducted research in the field of military aeronautics.

Having an extensive knowledge of the needs of aeronautics S. I. Troitskiy on the basis of even more combat experience of military aeronautics wrote and published the following works on using the resources of aeronautics: "O glubokoy razvedke s aerostata" [Deep Reconnaissance from an Aerostat] (1917) and "Boyevaya sluzhba privyaznogo aerostata" [Combat Service of the Captive Aerostat] (1919). In the latter he paid a lot of attention to studying the meteorological conditions of the aerostat operation. His works on studying the atmosphere are associated with activity in the field of aeronautics. In one of the works on atmospheric physics that Semen Ivanovich considered "his first serious independent work," in the article "Question of the Structure of an Air Wave" (1920), based on theoretical studies then confirmed experimentally with the help of special apparatus he came to an important conclusion about the asymmetry of an air wave that consisted of the fact that " in an air wave there is a general striving observed towards a sharp rise in the wind with strong gusts in the anterior section of the wave (frontal impact) and comparatively slow drop with small gusts to the rear section." S. M. Troitskiy returned many times to this trend of research that he developed, but already in terms of studying the change in gustiness of wind with altitude under different meteorological conditions, using the captive aerostat for this.

Semen Ivanovich viewed the air waves not as a purely local phenomenon, but considered that they "...encompass a fairly considerable mass of the atmosphere."

S. I. Troitskiy paid a lot of attention also to questions of cloud physics and he made many flights to study them. One of these flights was his five-hour flight jointly with the pilot Ye. D. Karamyshev and two auditors of the aeronautical school that was made from Luga on 21 July 1923, the day when the cloud cover bore a thunderstorm nature. The aerostat entered a thick cumulus, and then was between three thunderstorm clouds from which thunder was heard. During the descent of the aerostat under thunderstorm conditions, as a result of the severe training, as Semen Ivanovich noted in this article, some of the aeronauts suffered. In this flight the experimental studies were accompanied by sketches, a description of the clouds, and observations of the movement of the storm foci.

The works of Semen Ivanovich on aeroclimatology linked to the services of air transport are very valuable. He developed a method for aeroclimatological processing of the wind that later became widespread as the "Troitskiy method." He provided the aeroclimatic characteristics not only for a number of individual points, but also for entire routes.

Jointly with S. K. Ivitskiy in 1924-1929 S. I. Troitskiy organized the network of pilot-balloon stations whose wind sounding data then served as the foundation for a study of the wind pattern in the free atmosphere in

Figure 1. Teachers and Auditors of State Courses of Observers of Meteorological Stations of the A. I. Voyeykov Main Geophysical Observatory, Graduating Class of 1930. Second row from left to right: Shillegodskiy, N. K., Ivitskiy, S. K., Parskiy, N. D., Kedrolivanskiy, V. N., Nachinkin, V. I., Nezdyurov, D. F., Troitskiy, S. I., Berezkin, V. A. and Sapozhnikov, A. A.

aeroclimatic and aerosynoptic respects. Semen Ivanovich at this time also wrote the first instructions for observations of pilot-balloons. For the theory of the method of pilot-balloons whose application especially in aerosynoptics and aeroclimatology was the focus of a lot of attention on the part of S. I. Troitskiy, the laboratory studies on the peculiarities of the distribution of resistance experienced by the balloon in calm and turbulent flows (1922) that he conducted jointly with P. A. Molchanov are very valuable. These experimental data made it possible to explain more strictly the nature of the vertical movement of the pilot-balloons in the atmosphere.

The services of S. I. Troitskiy are especially great in the area of using aerological data for weather forecasting. He developed the theory of wind change with altitude depending on the direction and the size of the horizontal temperature gradient that consequently received the title of the Troitskiy theory. In the operational practice of synoptics the "rule of the drive flow" is widely used that was empirically formulated for the first time from the data of pilot-balloon observations of S. I. Troitskiy and V. M. Mikhel' (1932).

Semen Ivanovich then developed a whole system for forecasting the synoptic position based mainly on the data on wind change with altitude. Already in the very first years of the development of aerology the results of aerological observations were useful for forecasting even in the presence of these limited data.

S. I. Troitskiy, an actual member of the scientific council of the Main Geophysical Observatory since 1926 worked in the observatory until the end of his life (he died 28 April 1934).

Semen Ivanovich was also known as an experienced and talented pedagogue. He taught in the Higher Military Aeronautical School meteorology, physics and the theory of aeronautics, and in the Institute of Engineers of Means of Communication--applied aerodynamics. He was a lecturer of Leningrad State University and the head of the department of aerology at Moscow Hydrometeorological Institute; he worked as a teacher in the Air Force and Naval Academies, in the Agronomical Institute and the Agronomical Technical School, and for a long time taught aerology at state courses for observer-meteorologists in the Main Geophysical Observatory.

S. I. Troitskiy as a scientist had a surprising combination of the fine researcher-theoretician and experimenter. He was not bent by any work in the field, at the test site, or in flight, and often participated in the manufacture of apparatus as a mechanic. This was a man of exceptional modesty, responsiveness and great personal charm.

Undoubtedly he would have done more than what we know, but his life was cut short too soon. Much of what he succeeded in doing has firmly entered Soviet meteorological science and continues to be successfully developed.

UDC 551.508(092)

IN COMMEMORATION OF VIKTOR NIKOLAYEVICH KEDROLIVANSKIY'S 90TH BIRTHDAY

Moscow METEOROLOGIYA I GIDROLOGIYA in Russian No 5, May 79, pp 115-117

[Article by A. S. Korovchenko, N. P.Rusin, and M. S. Sternzat]

Abstract. A brief biography is given and certain information is presented on the scientific, pedagogical and administrative activity of the leading Soviet scientist and meteorologist V. N. Kedrolivanskiy.

[Text] The modern generation of meteorologists remembers Viktor Nikolayevich Kedrolivanskiy mainly as a pedagogue and the author of courses on meteorological courses and methods of meteorological measurements. Many of us heard in different educational institutions the lectures of Professor Kedrolivanskiy, and studied the meteorological instruments in the textbooks written by him.

Viktor Nikolayevich was born on 31 March (12 April) 1889 in St. Petersburg in the family of a minor employee. After finishing the gymnasium he entered Petersburg University in the physical-mathematical department. A year before graduating from the university, 1915, he was accepted in the Main Physical (later Geophysical) Observatory (GFO) in the department of observations and instruments as an adjunct. At this time Academician B. B. Golitsyn was the director of the observatory and he attracted young physicists in order to give the GFO research a greater physical direction. From this moment to the end of his life (4 April 1952) the scientific activity of Viktor Nikolayevich was linked to the observatory.

In the first years he was entrusted with work to verify instruments and develop methods of observations. These were important works and in their time such famous scientists as A. M. Shenrok, G. F. Abel's, S. I. Savinov and D. S. Smirnov were involved in them. The following testimonial about the work of their young colleague has been preserved: "Relating to his work very thoughtfully and quite conscientiously, interesting himself in it Viktor Nikolayevich took direct participation in all types of current work of the department. The indicated circumstances permitted him to acquire rich experience and knowledge both on questions of the actual meteorological instruments, and on technique and verification"; and further: "work was done to perfect the technique of verifying the anemometers in an aerodynamic tunnel whose results made it possible to put into practice more efficient verification methods." The aerodynamic tunnel then had just started to be used in verification.

In 1918 Viktor Nikolayevich was selected a physicist (scientific colleague of the first class) of the verification department.

V. N. Kedrolivanskiy was an active participant of the research of the North. In 1921 the observatory sent him to the Kara. expedition in the oceanographic team led by V. Yu. Vize to conduct hydrological, meteorological and magnetic measurements. These measurements were made by him at Novaya Zemlya and on the ship "Taymyr." Thus, in the ship's log of the meteorological observations it is noted that the "meteorological observations on the ship 'Taymir' were made alternately by three individuals: V. Yu. Vize, V. N. Kedrolivanskiy and N. O. Yakobi." In the joint work of V. Yu. Vize and V. N. Kedrolivanskiy that was published from the results of this expedition "Novyye dannyye po gidrologii Karskogo morya" [New Data on the Hydrology of the Kara Sea] (ZAPISKI PO GIDROGRAFII, Vol 47, 1923, pp 81-130) it is indicated that "the relatively high temperature and salinity of this water leaves no doubt as to its Atlantic origin." Redommendations are also given there for the measurement technique on ships, and it is indicated that the"technique of observations of the air temperature on ships still awaits further study. It is possible that the observations with the help of the Assman psychrometer are better made from the nose of the ship than from the captain's bridge as is usually done." It is appropriate to note that the technique of measuring air temperature even in our time, when research is conducted with the help of marine scientific research ships with modern measuring resources still requires improvement.

Viktor Nikolayevich participated in many other scientific expeditions associated to a considerable measure with the development of a meteorological network; they were made in the regions of difficult access of Siberia, Transbaykal region, Yakutsk, Altay, the Arctic, on the islands of the north and in the mountains of the Caucasus. On the expeditions V. N. Kedrolivanskiy carried out scientific work and at the same time fulfilled the commitments of the senior inspector of the Main Geophyiscal Observatory meteorological station network, a position he was appointed to in 1923. The inspections of Viktor Nikolayevich bore a broad nature. His detailed reports, besides the materials on the results of the inspection, contained notes of an ethnographic and historical nature, and other important information. He always noted new and useful seedlings that appeared in the deep regions of the country during the years of Soviet power.

In 1929 V. N. Kedrolivanskiy participated in organizing the Yakutsk Geophysical Observatory, selected the site for its construction, and inspected the meteorological stations of Tommot, Nezametnyy, Chul'man, Nagornyy, and B. Never. The modern works that cover the climate peculiarities of the BAM (Baykal-Amur Trunk Line) route according to the data of these stations contain also a percentage of the work of Viktor Nikolayevich.

V. N. Kedrolivanskiy wrote (as a coauthor) the first "Rukovodstvo po inspektsii stantsiy" [Handbook on Inspection of Stations] that was published in 1932. In 1948 it became the foundation for the instructions on inspection of stations and was used to a considerable measure in preparing the subsequent editions.

In 1925 Viktor Nikolayevich was sent to Persia (Iran) to help in organizing there a meteorological network. He organized six stations that started the Iranian network. For this successfully implemented work the USSR Geographical Society awarded Viktor Nikolayevich a medal.

The articles of V. N. Kedrolivanskiy on the results of expeditions and inspections, and the travel notes, for example, "Altayskaya ekspeditsiya," [Altay Expedition], "Tri mesyatsa v Persii," [Three Months in Persia], "Po Lene i Aldanu," [Along the Lena and Aldan], "Po reke Yeniseyu do ostrova Dikson," [Along the Yenisey River to Dikson Island], "Na lednikakh Bogosskogo khrebta" [On the Glaciers of the Bogosskiy Crest] that were published in METEOROLOGICHESKIY VESTNIK, ISVESTIYA GFO, the journal KLIMAT I POGODA and TRUDY SOVETA PO IZUCHENIYU PROIZVODITEL'NYKH SIL are still read now with great interest.

In 1931 in the period of preparation of the second International Polar Year (IPY) Viktor Nikolayevich was appointed the head of the sector of polar and high-mountain stations. With his participation a plan was worked out for conducting geophysical and meteorological works whose fulfillment for the organization of new polar stations, inspections of the extant, and training of meteorologist-polar research workers to a considerable measure was the responsibility of Viktor Nikolayevich. The meteorological observations of the second IPY were processed under the supervision of Viktor Nikolayevich and were published with his editorship. He was mentioned by the Central Administration of the YeGMS [United Hydrometeorological Service] and the Presidium of the Committee of the Second IPY for the successful fulfillment of a broad front of work on the IPY.

Viktor Nikolayevich continued to focus a lot of attention to the organization of instrument verification. In 1937-1938 he headed the section of instrument verification of the Main Geophysical Observatory, and in 1940 he wrote (as a coauthor) "Instruktsiya po poverke meteorologicheskikh i aerologicheskikh priborov" [Instructions on Verification of Meteorological and Aerological Instruments].

Viktor Nikolayevich began his pedagogical activity in 1917 in the courses of Professor P. I. Brounov.* Starting in 1924 he conducted studies on instruments and methods of meteorological observations in courses of observers of meteorological stations under the Main Geophysical Observatory that in 1929 were converted into state. Starting in 1930 for a number of years he lectured on meteorology at Leningrad State University, and in 1938 occupied

*"Higher Courses on Training of Scientists in Agricultural Meteorology," that were conducted by Professor P. I. Brounov.

the position of professor at Leningrad State University in the department of atmospheric physics where he lectured on instruments and methods of meteorological observations. The heads of the department of climatology Professor A. A. Kaminskiy and the department of atmospheric physics Professor N. P. Tverskoy highly evaluated his lectures and noted that they "enjoy great success with the audiences..."

In 1937 the book of V. N. Kedrolivanskiy was published "Meteorologicheskiye pribory" [Meteorological Instruments]. This was the first, and for a long time the only manual on instrument meteorology in Russian. For the first time it stated the physical bases of meteorological instruments and the technique of their verification. Viktor Nikolayevich worked all his life on the creation and perfection of such a course corresponding tothe needs of the time.

In 1938 the Main Administration of the Northern Sea Route invited Viktor Nikolayevich to the Hydrographic Institute (today the Admiral S. O. Makarov Leningrad Higher Engineering Nautical School). He organized there a department of meteorology which he supervised for 10 years; many meteorologists associated with the north were trained in this department.

At the same time Viktor Nikolayevich continued his activity in the Main Geophysical Observatory. He was one of the leaders of the Method Commission of the Main Geophysical Observatory and participated in the preparation of handbooks, the improvement in measurements and in solving other questions of the scientific and method supervision of the network.

During the Great Patriotic War Viktor Nikolayevich worked in the observatory (in Leningrad and Sverdlovsk), then in the Central Design Office of the Main Administration of the Hydrometeorological Service of the Red Army (Sverdlovsk, Moscow). During these years he prepared a new monograph on meteorological instruments that was published in 1947. The materials of this book were a component part of his doctoral dissertation that he successfully defended in 1947.

For exemplary fulfillment of the assignments of the command Viktor Nikolayevich was awarded the Order of the Red Banner of Labor in 1943.

Starting in 1944 and then in the postwar years V. N. Kedrolivanskiy headed the meteorological department of the Main Geophysical Observatory (in Leningrad). He joined the editorial commission of the Main Administration of the Hydrometeorological Service for the publication of new instructions for stations and their inspection, and took active part in the planning and efficient placement of hydrometeorological stations and posts. He was elected a deputy of the Vyborg rayon Soviet of Workers' Deputies of Leningrad. He often met with his electors and was interested in their needs.

Because of the condition of this health Viktor Nikolayevich was forced to stop his extensive scientific and pedagogical activity in the Main Geophysical Observatory and Higher School of Aeromechanics. In the last year of his life he finished work (as a coauthor) on the textbook for higher institutes of learning on meteorological instruments and measurement methods. This book was published in 1953 after the death of Viktor Nikolayevich. It is still used now.

The scientific and pedagogical activity of V. N. Kedrolivanskiy was broad and multifaceted. He created a school of meteorologist-instrument workers, inspectors, verifiers, and participated in the conducting of many important scientific expeditions, wrote a number of books and set up courses on meteorological instruments and measurement methods that guaranteed the training of specialists who played an important role in the technical equipping of the meteorological service. Throughout his entire life Viktor Nikolayevich played a great role in the scientific supervision of the meteorological network. He was a reliable guardian of the high requirements for meteorological instruments and observations.

REVIEW OF MONOGRAPH BY I. N. DAVIDAN, L. I. LOPATUKHIN AND V. A. ROZHKOV ENTITLED " VETROVOYE VOLNENIYE KAK VEROYATNOSTNYY GIDRODINAMICHESKIY PROTSESS" (WIND-INDUCED WAVES AS A RANDOM HYDRODYNAMIC PROCESS), LENINGRAD, GIDROMETEOIZDAT, 1978, 287 PAGES

Moscow METEOROLOGIYA I GIDROLOGIYA in Russian No 5, May 79 pp 118

[Article by Candidate of Technical Sciences A. B. Menzin, and Candidate of Geographical Sciences M. M. Zubova]

[Text] In the last 10-15 years wind-induced waves have been primarily viewed as a random process. Here in many cases the problem is merely reduced to a mathematical description of the agitated surface without involvement of the physical pattern of the phenomenon. Often such a statement of the theme is completely substantiated, making it possible to obtain general ideas about the characteristics of the wind field.

Despite the fairly great number of works on the given problem, the authors have found new aspects of this complex natural phenomenon that deserves investigation both from the scientific and the practical viewpoint.

The authors of the book have set themselves the task of generalizing not only their own research, but also the results of other researchers published in different scientific journals. The authors were quite successful in coping with this task, and they used extensive observational materials to verify the different theories and models.

The contents of the book have been divided into three parts, closely linked among themselves by the unified method of approach to the studied phenomenon.

The first part gives a detailed characterization of the random properties of the sea surface. It is based on many years of study, both theoretical and full-scale of the authors themselves. The use of the latter and their thorough analysis gives special value to this section, and by the way, to the entire book as well.

The technique of analyzing the observational data consists of establishing the affiliation of the empirical distributions to the Weibull asymptotic distribution. Analysis of the results made it possible to draw the conclusion that in a quasistationary process for wave heights the Rayleigh distribution is correct that is a particular case of the Weibull distribution and coincides with that previously obtained by Ya. G. Vilenskiy, B. Kh. Glukhovskiy, et al. The laws governing the distribution of periods, lengths, curvature and the two-dimensional distributions differ from those previously obtained.

For the sake of fairness to the authors of the book one should nevertheless note that the distribution of wave periods that they obtained coincides with the analogous distribution obtained by L. F. Titov, based on the law of dispersion distribution (L. F. Titov, "Vetrovyye volny" [Wind-Induced Waves], Gidrometeoizdat, 1969).

Since the book is intended not only for specialists, but is also recommended as a textbook, then it seems that this section would be more understandable if its presentation was started from chapter 5.

The second part of the monograph covers the spectral theory of the development, spread, and damping of waves. It gives a detailed analysis of energy transfer from the air stream to waves, and the peculiarities of the nonlinear interactions and dissipation of energy. In analyzing the equation of the wave energy balance in the spectral form and in evaluating its components, the authors show that a number of the spectral components require further refinement and specification.

A comparison of the results of full-scale observations with spectral calculations based on the correlations obtained from the united theory of Phillips-Miles brings the authors to the extremely important conclusion that underestimated evaluations of the amount of energy transmitted from the air stream to waves is probably explained by the fact that a mechanism of energy transfer exists that is linked to the action of the tangential wind stresses. The role of the tangential stresses rises due to the emergence on the main system of waves of secondary overtones.

Chapter 8 presents methods for calculating the random characteristics of wave action. The presented results from calculations according to the refined method of Barnett demonstrate the expediency of using spectral methods, and once again indicate the need for refining certain components in the equation of the wave energy balance.

The third part of the book is of an applied nature. That circumstance that in addition to the multiple-year functions of wave distribution the functions of wind distribution are examined makes this part especially valuable, since despite the intensive study of seas and oceans, the observational data of the wind and wave-action are quite insufficient to obtain the pattern characteristics. Therefore the detection of the laws or refinement of the already available laws is of undoubted scientific importance and has great applied value. As a result of these studies the authors have compiled a manual on the pattern of wind and wave action in the seas and oceans.

The book which is an integral generalization of the theoretical, experimental and full-scale studies of wind-induced wave action as a random process is of definite scientific and applied value and is very timely.

REVIEW OF MONOGRAPH EDITED BY YU. P. DORONIN ENTITLED "FIZIKA OKEANA" (PHYSICS OF THE OCEAN), LENINGRAD, GIDROMETEOIZDAT, 1978, 294 PAGES

Moscow METEOROLOGIYA I GIDROLOGIYA in Russian No 5, May 79 pp 119-120

[Text] In the last decade the scales and intensity of development of seas and oceans have been considerably altered. Complex problems of a global nature have arisen and been acknowledged as the most important problems that can be solved by methods of mathematical modeling. As a consequence of this there has been increasing interest in the monographic and educational literature that generalizes the theoretical foundations for the oceanographic science at the modern stage of their development. Therefore the book "Fizika okeana" that has been published by Gidrometeoizdat under the editorship of Yu. P. Doronin as a textbook for students of higher institutes of learning that are studying the specialty of "oceanology" deserves the most intent attention.

In this textbook, written by a group of major specialists (V. V. Bogorodskiy, A. V. Gusev, Yu. P. Doronin, L. N. Kuznetsova, K. S. Shifrin) the most important questions are covered of ocean thermodynamics, turbulence, formation and properties of ice, optics, acoustics, electromagnetic phenomena. In its structure it is closest to the basic work of V. V. Shuleykin "Fizika morya" [Physics of the Sea] which the authors say they often referred to.

The textbook is not large in size, which complicated the task of the compilers to state such extensive material with the required completeness and strictness. We will examine its contents in more detail from this viewpoint.

The textbook consists of an introduction and eight chapters.

The introduction formulates the main tasks of the course, the state of studying the physical properties of sea water and the processes occurring in the ocean, as well as indicates the method for solving them based on the use of mathematical apparatus.

It further examines the modern ideas about the molecular nature of water and about the effect of the intermolecular bonds on the macroscopic properties of water, ice and vapor.

The first chapter presents the fundamentals of ocean thermodynamics. The ocean is viewed as an equilibrium macroscopic system whose condition is characterized by the set of interrelated physical parameters (temperature, salinity, pressure) and functions (inner energy and entropy).

In isolating the fundamental role of entropy the authors introduce this concept from two viewpoints: statistical and thermodynamic, and show its use in the derivation and application of the main equation of thermodynamics, in particular, to determine the thermophysical characteristics of sea water, as well as the areas of existence of its phases and the transition conditions between them.

The chapter ends with an examination of the questions of thermodynamic stability in the example of an analysis of the adiabatic process and conditions of vertical stability that is evaluated according to the numerical values of the Weisel frequency and the Hesselberg-Sverdrup criterion.

The second chapter is a continuation of the first and covers problems of the evolution of the system. Based on the general equations of sea water movement and the equations of preservation of mass and diffusion of salts the author studies the energy condition of the system during its change in time, and obtains one of the forms of the first principle of thermodynamics--the equation that expresses the change in the internal energy through the parameters of the system and the amount of exchange with the environment.

The change in time of the second function of the state of the system--entropy is revealed from the position of an examination of the conditions for its transfer and generation. An approach is shown for finding the water temperature according to the change in entropy that results in the derivation of the equation of heat conductivity.

Thus, in the first two chapters the theoretical foundations are given for determining the condition and dynamics of the ocean.

The third chapter presents the main ideas about turbulence as the phenomenon inherent to the majority of types of water movement in the ocean.

The author successively examines the criteria for the transition from the laminar pattern to the turbulent, lists all the main mechanisms for the generation of turbulence and shows the multiple-scale nature of the spatial-temporal structure of turbulent movements. The characteristics of the ocean mass of water is given according to the type of formation and manifestation of turbulence in it.

The main portion of the chapter covers the technique of detecting the turbulent effect in the equations of hydrothermodynamics, study of the statistical laws governing turbulence, and presentation of the semi-empirical theories of turbulent exchange. With respect to the latter, especial attention is paid to the methods for determining the coefficients of turbulent exchange, as well as the derivation and analysis of the equation for the balance of turbulent energy that is widely used in the practice of oceanological calculations.

The fourth chapter uses the theoretical developments of the previous sections to solve problems of the distribution of heat and salts in the ocean.

The author traces the logically completed chain of operations to study the thermocline fields in the ocean in the following order:

1. Analysis of equations of heat conductivity and transfer of salts in order to reveal the role of individual components of equations in the description of the physical processes depending on the scale of the phenomenon;

2. Obtaining of the balance equations of heat and salts, and establishment of a relationship with the atmospheric parameters;

3. Compilation of simplified models and obtaining of analytical solutions that make it possible to evaluate the heat-salt exchange processes on the boundary ocean-atmosphere, and in the mass of sea water. In addition, this chapter has certain important sections that cover questions of the structure of the active ocean layer, and the dependence of the profiles of temperature and salinity on the nature of change in the coefficients of turbulent mixing.

The fifth chapter treats the laws governing the formation and breakdown of sea ice depending on its physical-mechanical properties. Here also, as in the fourth chapter, the results of the research of their author, Yu. P. Doronin are widely used that are presented in the monographs "Teplovoye vzaimodeystviye atmosfery i gidrosfery v Arktike" [Thermal Interaction of the Atmosphere and Hydrosphere in the Arctic] and "Morskoy led" [Sea Ice] (the latter was coauthored with D. Ye. Kheysin).

The sixth chapter contains the main information about the electromagnetic properties of the sea medium, sources, structure and mechanism for the formation of magnetic and electrical fields. Processes of formation of telluric and natural electrical currents are especially isolated due to their close interrelationship with the dynamics of sea water and the distribution of microorganisms.

The seventh chapter examines successively the processes of absorption and scattering of solar radiation in sea water (practically without description of their nature), the laws governing the reflection and refraction of the light stream falling on the sea surface, as well as the optical characteristics of the light field governed by them: brightness, irradiance, color.

A central place with respect to its importance and information content is occupied by the treatment of absorption and scattering processes in sea water expressed in a detailed summary of the parameters of the sizes and spectra of absorption and scattering both for pure water, and for the substances dissolved and suspended in it.

The eighth chapter covers the spread in the ocean of acoustic waves. After brief information about the nature of sound oscillations and the links of their parameters to the characteristics of the media the authors (V. V. Bogorodskiy, and A. V. Gusev) advance a derivation of the wave equation and study its application to a description of the spread of flat, spherical and cylindrical waves in an unlimited, ideal liquid. Further presentation covers the effect of a heterogeneous aqueous medium and the surface "water-bottom," "water-air" on the formation of sound fields in the ocean. Here such phenomena are examined as reflection and refraction of acoustic waves, their absorption and scattering, ways to distribute sound in stratified-heterogenous media, and in particular, in the zone of underwater sound channel.

At the end of the chapter there is a brief report about the interesting process called "sea reverberation" and about the sources of generation of sea noises.

From the given brief survey of the book contents it is clear that the authors have attained the set goal--demonstrating the fundamentals of the subject. They succeeded in a concise form of stating extensive material on all sections of the theory of ocean physics, and here maintain (which is very important for a textbook and complicated with collective writing of it) a single technique of examination. Each chapter looks as follows in the structural respect: formulation of the initial definitions, derivation of the main equations, study on their basis of the physical processes of the examined phenomena. In its scientific ideology and employed information the textbook is quite modern, although mention of such a phenomenon (discovered about 10 years ago) as the fine structure, and its effect on the development of turbulence, apparently, would be pertinent in the appropriate sections.

Despite the isolated misprints that are found in the text the textbook leaves a very good impression, and due to the urgency of the questions it states that are associated to a certain degree with the fact that the studies of the authors themselves are used in the book, one can hope that the circle of its readers will not be limited only to the student audience to whom it is addressed.

COMMEMORATION OF 70TH BIRTHDAY OF GEORGIY MIKHAYLOVICH TAUBER

Moscow METEOROLOGIYA I GIDROLOGIYA in Russian No 5, May 79 p 121

[Article by comrades from work]

[Text] On 26 May 1979 the prominent Soviet scientist, doctor of geographical sciences, Professor Georgiy Mikhaylovich Tauber celebrates his 70th birthday. His name is linked to the development of research of Antarctic

climate and the most important branch of modern oceanology--study of the interaction of the "ocean-atmosphere" system. Working in the State Oceanographic Institute as the head of the laboratory of marine meteorology, Georgiy Mikhaylovich conducts extensive scientific studies on the climate of Antarctica and its sea water areas, and is involved in problems of the interaction of the "ocean-atmosphere" system.

A result of the many years of research work of G. M. Tauber is the monograph "Antarktika, ch.I. Osnovnyy cherty klimata i pogody" [Antarctica, Part One. Main Features of Climate and Weather] that played a considerable role in the studies of the Antarctic and in the organization of further work during the International Geophysical Year. On the problems of "ocean-atmosphere" interaction and the climate of the Antarctic G. M. Tauber wrote about 80 scientific works. For many years Georgiy Mikhaylovich participated in the works of WMO on the Commission of Marine Meteorology, and fulfilled great public work in the institute.

For his fruitful and irreproachable scientific and public activity G. M. Tauber was awarded the Order of the Red Banner of Labor, medals, and honorary certificates.

The characteristic features of Georgiy Mikhaylovich, the scientist, communist and citizen are high scientific principles, modesty, exactingness towards himself, and great humanity.

Georgiy Mikhaylovich continues the great work of a scientist.

We wish him good health and further success in his fruitful activity.*

---

*More detailed information about the biography of G. M. Tauber is given in issue No 5 of METEOROLOGIYA I GIDROLOGIYA, 1969.

COMMEMORATION OF 90th BIRTHDAY OF IVAN NIKOLAYEVICH YAROSLAVTSEV

Moscow METEOROLOGIYA I GIDROLOGIYA in Russian No 5, May 79 pp 121-122

[Text] 1 May was the 90th birthday of the honored worker of science and technology of the Uzbek SSR, doctor of geographical sciences, Professor Ivan Nikolayevich Yaroslavtsev.

From 1947 to 1959 Ivan Nikolayevich headed in Tashkent the department of physics in the Polytechnical Institute and worked in the geophysical observatory.

In 1959 Ivan Nikolayevich retired and moved to Ryazan'. Enormous industriousness, superior capabilities, eruditeness in many areas of geophysics, a well-meaning attitude towards people, and a readiness to help them--all of this brought I. N. Yaroslavtsev to the department of physics of the Ryazan' agricultural institute. During his work (to October 1970) he succeeded also in Ryazan' of earning the respect of his colleagues and students of the institute. He is an active public worker and an active propagandist. Ivan Nikolayevich visits the classes of the teachers in the department, and gives them valuable advice about the methods of teaching.

Of great theoretical and practical importance are the scientific studies of I. N. Yaroslavtsev in meteorology, in particular, in the field of actinometry. He has published over 70 scientific works.

At present Ivan Nikolayevich has returned to his research on the effect of aerosol on solar radiation that he started in 1949. Now he is ending calculations of the aerosol component in attenuation of solar radiation over the globe.

We wish Ivan Nikolayevich strong health and further creat've successes.*

*Biographical information about I. N. Yaroslavtsev is given in METEOROLOGIYA I GIDROLOGIYA No 12, 1964 and No 6, 1969.

PRIZES OF EXHIBITION OF THE ACHIEVEMENTS OF THE NATIONAL ECONOMY OF THE USSR

Moscow METEOROLOGIYA I GIDROLOGIYA in Russian No 5, May 79 pp 122-124

[Article by M. M. Kuznetsova]

[Text] The main committee of the Exhibition of Achievements of the National Economy of the USSR has awarded additional prizes to the participants in the thematic exhibition "Water Resources of the USSR and Hydrological Provision for the National Economy of the Country" and the examination of works of inventors and efficiency experts in the pavilion "Hydrometeorological Service."

Diplomas of honor:

A. A. Sokolov, director of State Hydrological Institute, for development of the theory of global and continental hydrologic cycle as the fundamentals for evaluating the water resources in different natural conditions, methods of evaluating the water resources in their natural condition, and transformed as a result of economic activity at present and in the distant future, and evaluation of the water resources on global and continental scales.

S. M. Novikov, head of the section of the State Hydrological Institute, for development of the theory of hydrology of swamps as the foundation for the hydrological substantiation of plans for development of regions of West Siberia, methods of determining the water pattern and water balance of rivers, lakes and swamps, plans for complete dessication of swamps that makes it possible to most economically and rapidly develop the oil fields of West Siberia.

Diplomas of the first degree:

State Order of the Red Banner of Labor Hydrological Institute--for conducting research and scientific generalization of the materials of many years of observations that made it possible to evaluate the water resources of the country, develop methods for their evaluation and calculations, to evaluate the water supply of economic oblasts, union republics, and the anthropogenic effects on the water resources.

Order of Lenin Hydrometeorological Scientific Research Center of the USSR for development and introduction into practice of new methods of hydrologic forecasts, rapid supplying of the national economy of the country with forecasts and information.

Omsk Administration of the Hydrometeorological Service for conducting hydrologic and aerohydrometric work to investigate the channel deformations on the Ob' and Irtysh at the sites of laying underwater passages of the main gas and oil pipelines. The economic effect from introducing the recommendations only for one branch of the gas pipeline passage built through the Ob' River was 150,000 R.

Central Aerological Observatory for developing and creating the apparatus "Osadki" that provides measurement of intensity distribution and quantity of atmospheric precipitation; radio-transparent concealment of the ship radar station "Meteorit," that yields an economic effect of about 10,000 R per year; method of remote determination of moisture content.

Diplomas of the second degree:

Transcaucasus Scientific Research Hydrometeorological Institute for the monograph "Matematicheskoye modelirovaniye gidrologicheskikh ryadov" [Mathematical Modeling of Hydrological Layers]. The developed methods of modeling are designed for hydropower and hydroeconomic calculations in regulating the river flow with the help of reservoirs, GES, water supply systems, and others.

Institute of Experimental Meteorology for the creation of an instrument for separate sampling of precipitation and dry precipitate that is a world innovation and was acknowledged to be the best at an international comparison of instruments and methods of atmospheric pollution control, as well as the creation of a soft bathometer for taking sea water samples.

Central Design Office of Hydrometeorological Instrument Making for the development of a device for measuring the wind parameters, and instrument for controlling thermal patterns, and indicator for verifying the logical devices and an impulse regulator of medium power.

Scientific Research Institute of Hydrometeorological Instrument Making for the development of methods of electrical modeling of channel flow movement, introduction of the quasianalog machine PR-49 for calculations of flow rate and levels of water of natural and regulated flows.

Ukrainian Scientific Research Hydrometeorological Institute for developing and manufacturing on-board apparatus for remote contactless determination of the nature of the earth's mantle.

Belorussian Territorial Hydrometeorological Center for the development of an electronic integrator of radiation designed to obtain hourly sums of different flows of solar radiation with their recording on diagram tape of a potentiometer. The use of an integrator reduces the time for processing the recording material on the average by 70%.

West Siberian Administration of the Hydrometeorological Service for the improvement in the current meter GR-98, the calculating-impulse mechanism for current meters of any type, and modernization of the anemometer with arrow reset to zero.

Upper Volga Administration of the Hydrometeorological Service for the development and introduction into the network of aerological stations of the technique and practical use in the system of sounding of the meteorite "RKZ-Oka-3" of a small-sized UHF 6250 amplifier.

Diplomas of the third degree:

Administration of the Hydrometeorological Service of the Lithuanian SSR for the development of a test stand to verify the M-63m instrument designed for rapid troubleshooting in the M-63m sensor.

Kirov Zonal Hydrometeorological Observatory of the Upper Volga Administration of the Hydrometeorological Service for introduction into the system of radio sounding of a small-sized UHF 6250 amplifier that makes it possible to obtain high indices in sounding.

Administration of Hydrometeorological Service of Far East for the development of a loading device for repairing L1-3 lamps that makes it possible to verify the scales of the instrument and control the correctness of its operation, the checking device for the ARS program with verification of the addressing distributor and the bathometer for taking water samples for chemical analysis.

A number of workers of the USSR State Committee on Hydrometeorology and Environmental Control were awarded medals of the VDNKh [Exhibition of Achievements of the National Economy of the USSR].

Gold medal:

V. N. Parshin, V. A. fisenko, A. A. Chernikov, I. A. Shiklomanov.

Silver medal:

G. G. Belov, N. A. Bochin, E. V. Buryak, A. D. Volkov, A. N. Volosevich, K. P. Voskresenskiy, N. F. Dement'yev, F. L. Dul'yaninov, I. F. Karasev, A. B. Klaven, R. A. Kruglov, V. A. Levitskiy, A. I. Leytus, A. N. Mal'tsev, I. I. Matveyenko, A. I. Mekhovich, Yu. V. Mel'nichuk, V. A. Mikhaylov, Yu. P. Moskvin, Ye. G. Popov, G. G. Svavidze, V. P. Sklavinskiy, V. P. Tyukhlyayev.

Bronze medal:

B. I. Aksamentov, V. I. Babkin, N. A. Barabanova, G. P. Beryulev, Yu. A. Boytsov, V. P. Brivkin, V. G. Budilin, A. G. Voronovskiy, V. V. Voskanyan, Ye. B. Geyz, V. V. Goncharov, Yu. V. Gorbunov, O. P. Guznishchev, Ye. N. Davydov, V. I. Den'gin, A. V. Yelfimov, V. M. Yermakov, V. V. Yerokhin, I. A. Zheleznyak, A. P. Zhidikov, Ye. I. Zhukovskiy, G. V. Zaklinskiy, I. V. Zelenov, A. A. Ioanesyan, A. V. Karaushev, V. Ye. Karpusha, N. L. Kochutovskiy, A. P. Kopylov, V. I. Koren', Ye. A. Leonov, A. N. Mel'kher, P. I. Merem'yanina, S. A. Milovidova, V. V. Milkov, L. A. Mirmovich, A. N. Myslitskiy, V. A. Nesterenko, V. G. Noskov, G. M. Osipenko, V. B. Osis, L. V. Pen'kova, G. A. Plitkin, V. N. Polyakov, G. P. Popov, M. G. Pupishskaya, V. N. Pupkov, G. V. Ragozina, A. V. Savel'yeva, Ye. I. Savchenkova, S. N. Samusev, V. I. Sapozhnikov, B. G. Skakal'skiy, L. Ye. Smirnova, T. I. Starovaytova, M. S. Sternzad, V. I. Timofeyev, G. P. Ugol'kov, Yu. V. Uryvayev, K. M. Uskov, Sh. D. Fridman, I. M. Chernov, Z. M. Chuvakina, M. V. Zhaginyan, I. M. Shenderovich, G. N. Shepilov, Ye. P. Shurupa.

Diplomas of the Main Exhibition Committee of the USSR VDNKh

have been awarded to the director of the pavilion "Hydrometeorological Service" Ye. V. Dzyubenko and the senior engineer of the Institute of Electromechanics V. V. Sudakova.

The total number of participants according to Goskomgidromet was 347 people. Besides the workers of the State Committee of the USSR on Hydrometeorology and Environmental Control, the Main Exhibition Committee of the USSR VDNKh for the pavilion "Hydrometeorological Service" awarded prizes to the outside organizations that took direct part in the development of a number of themes.

COOPERATION CONTINUES TO EXPAND

Moscow METEOROLOGIYA I GIDROLOGIYA in Russian No 5, May 79 pp 124-126

[Article by Yu. V. Olyunin]

[Text] On 26 December 1978 the regular meeting took place in Ulan-Bator of the representatives of the USSR State Committee on Hydrometeorology and Environmental Control and the Main Administration of the Hydrometeorological Service of the Council of Ministers of the Mongolian People's Republic (MNR) at which questions were discussed in a business-like and constructive atmosphere of the scientific and technical cooperation between the USSR and the Mongolian People's Republic in the feild of hydrometeorology of mutual interest. The Soviet delegation was headed by the first deputy chairman of the USSR State Committee on Hydrometeorology and Environmental Control Professor Yu. S. Sedunov, while the delegation of the Mongolian People's Republic Hydrometeorological Service--the head of the Main Administration of the Hydrometeorological Service of the Council of Ministers of the Mongolian People's Repbulic Doctor D. Tuvdendorzh.

During the meeting the results of cooperation in 1977-1978 were summed up and the specific plans were examined for the development and deepening of cooperation in future years.

Cooperation in the field of hydrometeorology between the USSR and the Mongolian People's Republic has a renowned history. The first agreement in this field was signed back in 1935, and since then cooperation has developed and been strengthened on the basis of agreements, each of which has marked a new page in the development of scientific and technical cooperation and improvement in its effectiveness. The successful realization of these agreements has had a significant effect on the setting up and the evolution of the Mongolian People's Republic Hydrometeorological Service. Currently, scientific and technical cooperation in the field of hydrometeorology is implemented on the basis of the extant basic bilateral agreement that is laid in the protocol on direct cooperation in the field of hydrometeorology of 2 September 1972 and the intergovernmental agreement on studying the upper atmospheric layers of 11 October 1977.

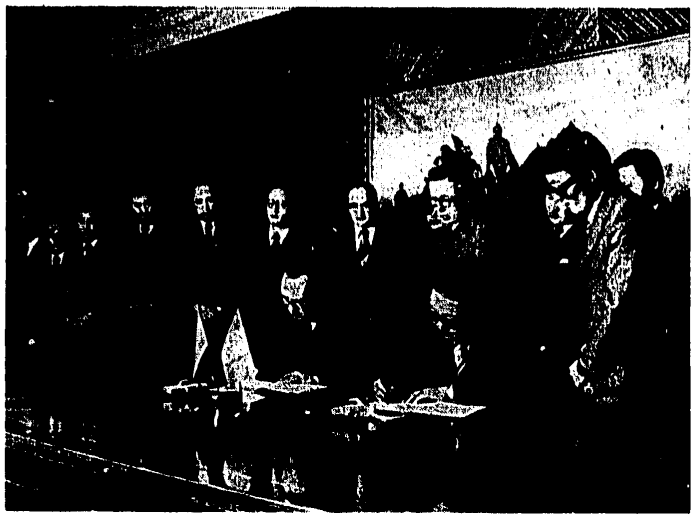

Signing of Protocol on Cooperation between the USSR and Mongolian People's Republic in the Field of Hydrometeorology.

From the left: First Deputy Chairman of the USSR State Committee on Hydrometeorology and Environmental Control Yu. S. Sedunov, from the right: head of the Main Administration of the Hydrometeorological Service of the Council of Ministers of the Mongolian People's Republic Doctor D. Tuvdendorzh.

At the opening of the meeting of the representatives of the sides the heads of the delegations noted with great satisfaction that the fraternal relationships between the Soviet and Mongolian peoples based on the principles of socialist internationalism continue to be developed dynamically and fruitfully in all directions of social activity, including the solution of the problems of modern hydrometeorology and environmental protection.

The sides stated that a whole series of sections of themes of great national economic importance have been completed or are at the stage of completion. In particular, the monograph "Gidrologicheskiy rezhim rek basseyna r. Selengi" [Hydrological Pattern of Selenga River Basin] has been published, a method has been formulated for calculating the rain floods on the rivers Selenga and Onona, and a plan has been set up for determining the most efficient placement of hydrological stations in the basin of these rivers.

A significant event in the scientific life of the Mongolian People's Republic will be the publication of the Hydrometeorological atlas of the country; work on its creation should be finished in 1979. The joint publication of this work will be a great contribution of the hydrometeorological specialists to the successful implementation of plans for national economic construction and improvement in the welfare of the workers of the Mongolian People's Republic adopted by the party and government.

The Mongolian People's Republic Hydrometeorological Service is focussing a lot of attention on the development and perfection of methods for weather forecasting of varying term. During the discussion of results of research within the framework of this theme it was noted that a lot has been done on the preparation of data and the development of a method for complex macrocirculation method of monthly temperature and precipitation forecasts over Central Asia. A physical-statistical method is being created for forecasting precipitation and temperature, and calculations are being made of statistical characteristics of temperature and precipitation at reference meteorological stations of the Mongolian People's Republic in order to prepare the predictants. The joint station of rocket sounding of the atmosphere that can be set up in the Mongolian People's Republic on the basis of the intergovernmental agreement will permit an even deeper investigation of the processes occurring in the upper atmospheric layers, while the data obtained with its help will help to create long-term forecasts of higher justifiability.

The computer center that has been created by the Mongolian People's Republic Hydrometeorological Service with the cooperation of the Soviet specialists in the near future will permit a rapid solution to the problems necessary for scientific research and guaranteeing the interests of the national economy.

The Mongolian side expressed especial interest in solutions and measures taken in the USSR for environmental protection and the use of space resources in the interest of the efficient use of natural resources (surface water, snow cover, plant cover, etc.). N. Zhagvaral, a member of the Politburo, secretary of the MNRP [Mongolian People's Revolutionary Party] Central Committee and academician, D. Maydar, a member of the Politburo of the MNRP Central Committee, first deputy chairman of the Council of Ministers of the Mongolian People's Republic, and doctor, and Doctor Zhadamba, head of the section of the MNRP Central Committee participated in the discussions of these questions. The head of the Soviet delegation Yu. S. Sedunov, and members of the delegation V. M. Voloshchuk and Ye. N. Mikhaylov answered the questions that interested the Mongolian comrades. During the conversations opinions were exchanged about measures for intensification of control over the condition of the environment. The successes achieved in this field in the USSR and Mongolian People's Republic were noted. In the Mongolian People's Republic with the help of Soviet specialists a laboratory for studying pollution of the atmospheric air, surface waters and soil has been set up, a network of points to observe the state of air pollution in the industrial centers of the Mongolian People's Republic has been created, and a plan has been compiled for the placement of observation points for water bodies of the Mongolian People's Republic.

Speaking of the use of remote sounding methods from space the members of the Soviet delegation informed the Mongolian side in detail about the technique of observation and exchange of information, and about the possibilities of using the observational data from space for the needs of the national economy, having especially stressed agriculture, pasture animal husbandry, i.e., the types of economic activity that are of especial interest for the Mongolian People's Republic.

During the meeting the Mongolian side repeatedly noted the contribution of the USSR to the development of the hydrometeorological service of their country and appraised the positive evolution of bilateral scientific and technical cooperation in this field as an important contribution to the strengthening and expansion of friendship between our countries. A detailed exchange exchange of opinions was also made on a number of urgent international questions concerning the organization and carrying out of international programs and projects to be implemented by the WMO, UNESCO and other international organizations.

Members of the Soviet delegation were given the opportunity to become acquainted with a number of scientific research institutions of the Mongolian People's Republic, and with historical and cultural monuments.

The negotiations, conversations and consultations that were made in an atmosphere of traditional friendship and warmth demonstrated the unity of viewpoints of the sides on the problems touched upon, their mutual striving to secure fraternal friendship and to steadily develop comprehensive cooperation between our countries.

As a result of the negotiations a joint protocol was signed with specific plans for further cooperation. After the signing of the protocol a meeting took place between the first secretary of the MNRP Central Committee, Chairman of the Great People's Khural Yu. Tsedenbal and the first deputy chairman of the USSR State Committee on Hydrometeorology and Environmental Control, Professor Yu. S. Sedunov. On the Soviet side Yu. V. Olyunin participated in the conversation.

In the name of the Soviet delegation Yu. S. Seduncv expressed deep gratitude for the reception and attention, and noted the high degree of effectiveness of the cooperation between the USSR and the Mongolian People's Republic in the field of hydrometeorology and environmental protection, and the exceptionally favorable conditions based on fraternal friendship between our people for its further development and deepening.

Yu. Tsedenbal dwelt on certain questions of international cooperation and especially noted the importance of the strengthening of cooperation between our countries, having stressed here the need to increase the effectiveness of scientific research.

CONFERENCES, MEETINGS AND SEMINARS

Moscow METEOLROLOGIYA I GIDROLOGIYA in Russian No 5, May 79 pp 126-127

[Article by R. G. Reytenbakh, Yu. G. Slatinskiy and A. P. Zhilyayev]

[Text] On 23-27 October in Obninsk in the All-Union Scientific Research Institute of Hydrometeorological Information--World Data Center an all-union seminar was conducted "Creation of Hydrometeorological Data Banks." The need for the organization of such a seminar was elicited by the rising problems of collecting and accumulating data on the environment, and an increase in the scales of use of computers to solve scientific and practical problems of studying the environment, forecasting its condition, putting out manuals and atlases on the hydrometeorological pattern. Representatives participated in the seminar from the leading scientific research institutes of the USSR State Committee on Hydrometeorology and Environmental Control, VSEGINGEO [All-Union Scientific Research Institute of Hydrogeology and Engineering Geology], TsNIIKIVR and BelNIIMiVKh [Belorussian Scientific Research Institute of Reclamation and Water Management]. Thirty-six reports were heard and discussed on problems of developing automated systems for processing and storing hydrometeorological data, method and program provision, technology and plans for creating funds of hydrometeorological data on technical carriers, their control, organization and use for serving the consumers.

A large group of reports covered the presentation of questions of method and program analysis. The report of V. M. Veselov and R. G. Reytenbakh (VNIIGMI-MTsD) "Zadachi, struktura i funktsional'nyye vozmozhnosti Avtomatizirovannoy informatsionnoy sistemy obrabotki rezhimnoy informatsii (AISORI)" [Tasks, Structure and Functional Potentialities of the Automated Informational System for Processing Systems Information (AISORI)] gave the brief characteristics of hydrometeorological information, characteristics of the accumulated files of hydrometeorological data and the problems of processing them, analyzed the modern technical and method potentialities of data processing in hydrometeorology, and presented the structure of the processing system developed in VNIIGMI-MTsD. V. M. Veselov in his report

"Sredstva upravleniya dannymi v AISORI" [Means of Data Control in AISORI] presented the main functions of control of hydrometeorological data in the processing programs, illuminated the possibilities for the developed language resources, and gave information about the methods of program realization.

The reports of Yu. P. Churakov, V. M. Pan'kov and V. P. Platonov (VNIIGMI-MTsD) stated the program and language resources for working with the hydrometeorological punched card files prepared in the SPM [punched-card computer] code and for exchange of data on magnetic tapes of the M-222 computer, Minsk-32 and YeS computer.

V. A. Semenov, V. G. Litvin et al. (VNIIGMI-MTsD) stated the main tasks and principles of developing an automated informational system of state accounting of water and water cadaster that will include three subsystems: "Surface Water," "Underground Water," "Use of Water."

In a number of reports of the colleagues of the VNIIGMI-MTsD [All-Union Scientific Research Institute of Hydrometeorological Information-World Data Center] and the GGO [A. I. Voyeykov Main Geophysical Observatory] the content was presented for the data bases on meteorology, aerology and oceanology for the systems to be set up on the basis of the YeS computer, with substantiation of the sequence of preparation of the different files.

The functional potentialities and peculiarities of program analysis of the automated informational-reference system Katalog designed to provide the users of hydrometeorological information with information about the data files, the site of their storage, information carriers, periods and means of observations were presented in the reports of V. M. Veselov, I. R. Danilova, et al. (VNIIGMI-MTsD).

A whole number of reports of the colleagues of TsAO [Central Aerological Observatory], GGO, GGI [State Hydrological Institute], VNIIMGI-MTsD, and IEM [Institute of Electromechanics] covered the experimental work with specific files of archive hydrometeorological data. Questions of control of information were presented by colleagues of the GGI, LGMI [Leningrad Hydrometeorological Institute], GGO, VNIIGMI-MTsD, and GKhI [State Scientific and Technical Publishing House of Chemical Literature]. The potentialities for increasing the reliability of information storage by interference-killing coding were shown in the reports of L. P. Afinogenov (GGO) and Ye. P. Ryzhiye (VNIIGMI-MTsD).

Representatives of the Belorussian Scientific Research Institute of Reclamation and Water Management in their report familiarized the seminar participants with the experimental automatic processing and accumulation of data obtained at a number of test bodies. The features of the technique of constructing the base for rapid information exchange were stated in the report of V. D. Zhupanov and N. L. Shestakova (GMTs SSSR).

On the whole the seminar demonstrated that in the institutions of the USSR State Committee on Hydrometeorology and Environmental Control there has been a considerable increase in the number of data files designed for processing on computers, and the volume and potentialities for program analysis of data processing. The experience that has been accumulated by now is a good foundation for developing data banks based on third generation computers.

R. G. Reytenbakh

On 31 October in Kiev a meeting took place of the scientific and technical council of YGMS [Administration of Hydrometeorological Service] of the Ukrainian SSR that covered the work of the marine network. G. V. Yatsevich and A. P. Zhilyayev gave reports on the results of work of the marine and estuarine subdivisions of the UGMS and the tasks for 1979-1980.

It was noted in the reports and speeches that in recent years in the Ukrainian SSR UGMS extensive work has been done to improve the efficiency of the marine network and types of observations, improve the quality of information entering for the service of the national economic organizations and the forecasting organs of the USSR State Committee on Hydrometeorology and Environmental Control.

It was noted at the meeting that the Ukrainian SSR UGMS systematically works on the construction of new and the reconstruction of extant units in the marine network. In 1979 it is planned to examine the question of the possible construction of self-recorders for the level at a number of posts in the estuarine region of the Dnepr and the South Bug.

In order to provide information to the continuously increasing transportation and passenger trips there are 12 wavemeter posts operating in the UGMS. In the near future it is planned to add to them another two-three seasonal posts on the routes of the most dense hydrofoil traffic.

Ice observations play an important role in the activity of the marine network of the Ukrainian SSR UGMS.

Annually the marine network of the Ukrainian SSR UGMS carries out a large volume of expedition work. In 1978 alone about 4,500 series of hydrologic observations were made in the Black and Azov Seas.

The participants of the meeting noted that in developing the annual plans of expedition work for the marine network the Ukrainian SSR UGMS and the SO GOIN [Siberian Department of the State Institute of Oceanography] in accordance with the decisions of the Scientific Council on the Problem of Studying Oceans and Seas of the USSR State Committee on Hydrometeorology and Environmental Control are constantly reaching increases in the sailing duration of expedition ships of all types by reducing the between-voyage stops, winter settling period, and other unproductive losses of work time.

The experience of operating the best crews of the Dunay GMO demonstrates that for ships of the SChS type [Black Sea medium seiner] under conditions of the Azov-Black Sea basin the practically continuous operation in the sea for the entire navigation period is quite possible.

In the development of plans for expedition work the UGMS and SO GOIN focus a lot of attention on the organization of complex research with simultaneous participation of all or the majority of scientific research ships. Such work makes it possible to solve immediately several problems on one trip, whereby observations are made synchronously in one or several regions of the sea.

The meeting examined in detail the question of the operation of the ship network. It was noted that in 1978 within the Ukrainian SSR UGMS there were 316 ship hydrometeorological stations with navigator's crew. In 1977-1978 about 150,000 hydrometeorological observations were made in different regions of the World Ocean, the number of meteorological reports coming to the shore forecasting agencies rose by more than 15%. The ship inspectors of the UGMS did a lot of work to improve the regularity of report transmissions and increase in the quality of observations.

The adopted decision formulated a number of primary tasks for the further improvement in activity of the marine network of the Ukrainian SSR UGMS, intensification in coordinated activities for supervision of the network between the UGMS of the Ukrainian SSR and the SO GOIN, and improvement in the responsibility of all links in the UGMS apparatus for the fulfillment of the approved plan assignments.

Yu. G. Slatinskiy and A. P. Zhilyayev

NOTES FROM ABROAD

Moscow METEOROLOGIYA I GIDROLOGIYA in Russian No 5, May 79 pp 127-128

[Article by B. I. Silkin]

[Text] As reported in ENVIRONMENTAL DATA SERVICE, January 1978, p 5, a group of American scientists headed by U. L. Gates that is participating in the international project CLIMAP (Climate: Long-Range Investigation, Mapping and Prediction) has created a numerical model demonstrating the condition of the earth's atmosphere in the period of maximum development of the last ice age, that is roughly 18,000 years ago.

The initial material was the set of paleosynoptic charts gathered for the first time that reflect the meteorological conditions on the entire surface of the planet 18,000 years ago; they include data on the extent and thickness of the ice cover on dry land and on the sea, the temperature of the sea surface, and the albedo (reflecting ability) of the dry land in this period.

Then computations were made of the temperature of the near-surface air layer and other characteristics of the epoch. After averaging with respect to the entire globe and comparison with the temperatures inherent to our modern climate, it was established that a drop in the mean air temperature with the onset of the ice period is only 5°C. This conclusion is extremely important both for an explanation of the problem of the paleoclimate, and for an answer to the questions of the super long-term climatological forecast.

In SCIENCE NEWS, 1978, Vol 113, No 8, p 118 it is reported that a group of astrophysicists from Kitt-Pikski National Observatory (Tucson, Arizona) led by U. Livingston have recorded a drop in the solar temperature by 6 K in 1977. Such a fluctuation, which in the opinion of the researchers, could be cyclic, was noted for the first time in 1975 when systematic observations were started.

The observed drop is 0.1% of the normal solar temperature (5700 K), it also means a reduction by 0.5% in the solar constant, that is the quantity of energy released by the star.

The tendency towards a drop in temperature was noted for the first time in January 1977 during one of the six monthly measurements of this parameter. At this time the spot-forming activity of the sun passed the minimum and began to grow, and further observation of both parameters demonstrated their correlation.

The observed temperature oscillations are small, but, in the opinion of certain climatologists, a 2% reduction in it in the space of several centuries is sufficient to assume the beginning of an epoch of glaciation.

In respect to the seasonal changes in the distance separating the earth from the sun, the quantity of energy obtained by our planet from it in a year is altered by 6%. An additional change by 0.5%, in the opinion of U. Livingston, can already have climatological consequences.

However, before drawing final conclusions it is necessary to have a longer series and greater diversity in the observational methods. Preliminary analysis of the data from the meteorological satellite "Nimbus-6" confirms the opinion of the Kitt-Pikskiy group of researchers.

In the journals ICARUS, Vol 34, 1978 p 28 and SCIENCE NEWS Vol 113, No 18, 1978, p 298 it is reported that several years ago it was established that clouds in the atmosphere of Venus contain a large quantity of sulfuric acid. However its precise amount there remained unknown.

James B. Pollak and colleagues (Ames Research Center of the United States National Aeronautics and Space Research Administration) came to the conclusion that sulfuric acid comprises more than five-sixths of the total weight of substance contained in these clouds.

The concentration of this acid in drops forming the cloud, according to these studies, is in the upper part of the clouds, at altitude from 68 to 80 km above the planet's surface 84% (±2). The observations that came to such a conclusion were made on a 91-centimeter telescope installed on board the Cooper airplane laboratory with whose help reflecting spectra were obtained in the frequency band 2.9-3.4 μm.

In the lower part of the clouds (about 49 km over the underlying surface), according to the measurements made by the Soviet researchers on board the automatic interplanetary station "Venera" the concentration of sulfuric acid is almost the same, 84% (±6).

The American researchers established that the existence of clouds saturated with sulfuric acid significantly reduces the already low water content in the atmosphere of Venus: in its layers below the clouds it is within the limits of 0.0006 and 0.01 (by volume), and above the clouds, only 0.000002.

With respect to the spectra in the short-wave section of the range it was established that the optic depth of clouds on Venus (that is the degree to which they prevent the penetration of light) is between 25 and 50. This is equivalent to the conditions of a strong cloud cover on the earth, and indicates that the surface of Venus is better illuminated than assumed up to now.

9035
CSO: 1864

END